Violacein-producing *Janthinobacterium* sp. HH01 – Genome analysis revealed a novel α-hydroxyketone-sensing reporter-strain

Dissertation

In fulfillment of the requirements for the degree
Doctor of Natural Sciences

Submitted to the Department of Biology, Faculty of Mathematics,
Informatics and Natural Sciences
University of Hamburg

by
Claudia Katharina Hornung
from Hamburg

Hamburg 2013

Genehmigt vom Fachbereich Biologie
der Fakultät für Mathematik, Informatik und Naturwissenschaften
an der Universität Hamburg
auf Antrag von Professor Dr. W. STREIT
Weiterer Gutachter der Dissertation:
Professor Dr. P. HEISIG
Tag der Disputation: 28. Juni 2013

Hamburg, den 14. Juni 2013

Professor Dr. C. Lohr
Vorsitzender des
Fach-Promotionsausschusses Biologie

Certification

To whom it may concern,

I hereby verify that I have proofread the dissertation of Claudia Hornung, also known by the title:

'Violacein-producing Janthinobacterium sp. HH01

- ***Genome analysis revealed a novel α-hydroxyketone-sensing reporter strain'***

Which is being submitted by Claudia Hornung as part of her doctoral dissertation for the University of Hamburg.

I confirm that the document has been checked thoroughly and to the best of my ability, that I have advised on potential corrections, and that I have found the level of English in the aforesaid work to be suitable. I also confirm that I am a native English speaker and have completed postgraduate university degrees in English, as well as having previously been employed in an editorial capacity in publishing work involving the English language.

Yours Sincerely,

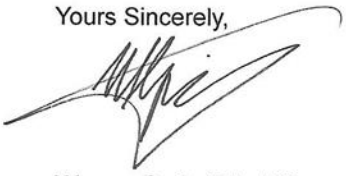

01.05.2013

Warren Greig MA, MSc
Research Psychologist

Main parts of this thesis were published as follows:

Claudia Hornung, Anja Poehlein, Frederike S. Haack, Martina Schmidt, Katja Dierking, Andrea Pohlen, Hinrich Schulenburg, Melanie Blokesch, Laure Plener, Kirsten Jung, Andreas Bonge, Ines Krohn-Molt, Christian Utpatel, Gabriele Timmermann, Eva Spieck, Andreas Pommerening-Röser, Edna Bode, Helge B. Bode, Rolf Daniel, Christel Schmeisser and Wolfgang R. Streit. **"The *Janthinobacterium* sp. HH01 Genome Encodes a Homologue of the *V. cholerae* CqsA and *L. pneumophila* LqsA Autoinducer Synthases".** PLoS ONE. 2013; **8**(2): e55045. doi:10.1371/journal.pone.0055045

http://www.plosone.org/article/info%3Adoi%2F10.1371%2Fjournal.pone.0055045

Table of contents

List of figures

List of tables

1 INTRODUCTION

Quorum sensing – a sophisticated way of communication or only a matter of "do lunch or be lunch"?

About forty years ago scientists observed a relationship between the number of cells of the marine bacterium *Vibrio fischeri* and the expression of bioluminescence (Nealson *et al.* 1970). This can be considered as the starting point of an ever growing division of microbial research, which is commonly referred to as quorum sensing (QS). In the meantime, the trigger for this gene regulation was attributed to endogenously synthesized chemical molecules. Moreover, the underlying signal transduction mechanisms, usually resulting in a positive feedback loop, were revealed. The progress that has been made within this field of research since 1970 is depicted in Figure 1.

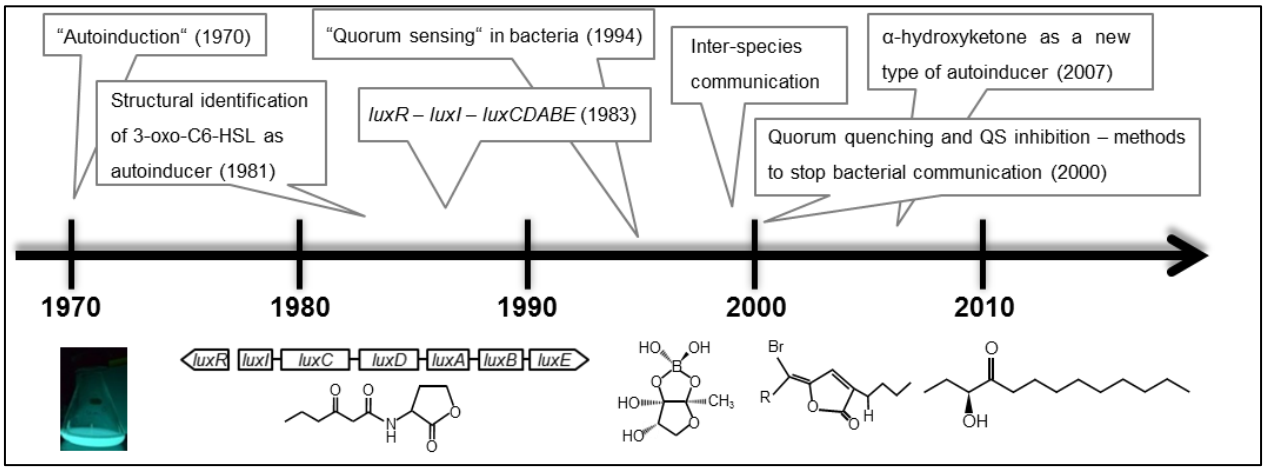

Figure 1. Some milestones of QS research from 1970 until today. From left to right, flask containing *Vibrio harveyi* cells showing bioluminescence, corresponding genes (*luxR*, *luxI*, *luxCDABE*; Engebrecht *et al.* 1984; 1983) and AI molecule (3-oxo-C6-HSL) (Eberhard *et al.* 1981), molecule structures of AI-2 (Chen *et al.* 2002), a halogenated furanone as QS inhibitor (Manefield *et al.* 2002) and CAI-1 (Higgins *et al.* 2007).

Their experiments regarding a cell density-dependent formation of the enzyme luciferase, led Nealson and his colleagues to term this phenomenon "autoinduction" in order to reflect the self-produced nature of the inducing cue (Nealson *et al.* 1970). A few years later both the chemical structure of the inducing compound (3-oxo-C6-homoserine lactone; Eberhard *et al.* 1981) and the corresponding genes (*luxI*, *luxR*, *luxCDABE;* Engebrecht *et al.* 1984; 1983) were identified. After this kind of gene regulation was

initially termed “autoinduction”, it was referred to as “quorum sensing” in 1994 (Fuqua *et al.* 1994), to emphasize its direct relation to cell density. In the course of time, QS-associated components, *i.e.*, signaling molecules, or autoinducer (AI), as well as their synthases and receptors were found in many organisms (Ng and Bassler 2009). Moreover, it turned out that this type of communication is not only a kind of self-talk within single species, but also a communication across species boundaries. Inter-species communication was detected *e.g.*, in mixed biofilms of phylogenetically distant bacteria (Riedel *et al.* 2001) as well as by the finding of the widespread AI synthase LuxS suggesting a new class of signaling molecules (AI-2) (Surette *et al.* 1999; Bassler *et al.* 1994; 1993).

Meanwhile about 100 organisms are known to communicate by QS and their listing reads like the who´s who of the microbial world: Starting with “A” as *Agrobacterium* (White and Winans 2007; Hwang *et al.* 1994), about *Burkholderia* (Eberl 2006), *Chromobacterium* (McClean *et al.* 1997), through to *Yersinia* (Atkinson *et al.* 1999). Nevertheless, the concept is not only limited to proteobacteria but was also found in cyanobacteria (Sharif *et al.* 2008), archaea (Tommonaro *et al.* 2012; Zhang *et al.* 2012; Paggi *et al.* 2003) and even fungi (Albuquerque and Casadevall 2012). Moreover, microbes thriving in extremophile environments like halophiles, acidophiles, thermophiles and psychrophiles use a signaling molecule-based communication (Montgomery *et al.* 2013). And even interplay between prokaryotes and eukaryotes was discovered (Rumbaugh and Kaufmann 2012; Lowery *et al.* 2008).

The focus of current research is aimed to elucidate more QS pathways and in particular the existence of molecules with an interspecies impact (Mangwani *et al.* 2012). Although AI-2 lost a bit of its universality and it seems to be merely a byproduct or metabolite rather than a true signal in some species (Diggle *et al*. 2006), there are certainly more such AI molecules (Shank and Kolter 2009). Another interesting branch of research was established by the discovery of AI-degrading enzymes known as quorum quenching (QQ) and the capability of certain chemical compounds to inhibit QS pathways so-called QS inhibitors (QSI). Since 2000, both an *N*-acyl-homoserine lactone-degrading enzyme AiiA in *Bacillus* sp. (Dong *et al.* 2000), and a halogenated furanone produced by the macroalga *Delisea pulchra* (Manefield *et al.* 2002; Rasmussen *et al.*

2000) were found to inhibit QS-regulated phenotypes, this opened new techniques for the inhibition of bacterial growth. In the meantime, several QSIs and QQ enzymes were identified, displaying a promising alternative to traditional antibiotics (LaSarre and Federle 2013; Hong *et al*. 2012).

1.1 Quorum sensing

The minimum set of QS circuits comprises an AI synthase producing the autoinducer signal and a cytoplasmic transcription factor that modulates gene expression upon binding of the signaling molecule (Bassler 1999). In addition, more complex QS networks are known. These include two-component and phosphorylation systems which detect, transmit and integrate multiple signals (Henke and Bassler 2004).

1.1.1 Autoinducer molecules – the vocabulary of bacterial language

After the first identified AI was grouped as *N*-acyl-L-homoserine lactone (AHL) (Fuqua and Greenberg 1998; Eberhard *et al.* 1981) in the meantime further classes of AIs were detected. Figure 2 gives an overview of several AI molecules, their corresponding synthases and the strains responsible.

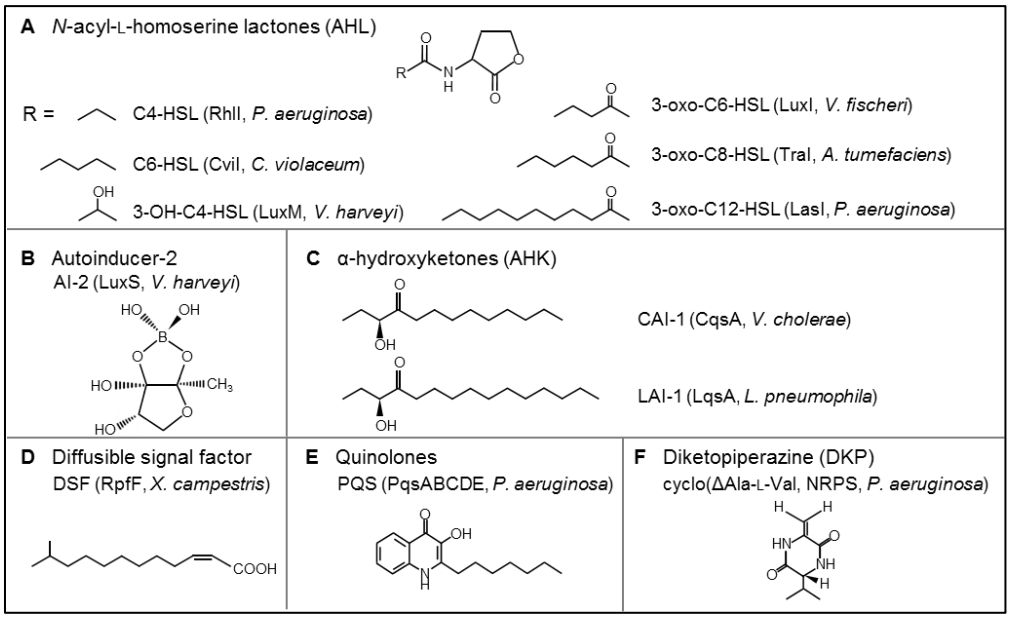

Figure 2. Examples for the structural diversity of bacterial QS signaling molecules. (A) *N*-acyl-L-homoserine lactones (AHLs), the R represents the specified side chain. **(B)** Autoinducer-2 (AI-2). **(C)** α-hydroxyketones (AHKs). **(D)** Diffusible signal factor (DSF). **(E)** Quinolones, *Pseudomonas* quinolone signal (PQS). **(F)** Diketopiperazine (DKP). (Deng *et al.* 2011; Ng and Bassler 2009; Camara *et al.* 2002a).

The well-studied *N*-AHLs are mainly synthesized by members of the LuxI protein family (Waters and Bassler 2005). The AHL structure consists of a conserved homoserine lactone (HSL) ring which is linked to a fatty acid chain of varying length (between 4 and 18 carbon atoms). Further variation of the AHL molecule structure is given by differing saturation state of the acyl chain as well as the oxidation state at position C3 (Churchill and Chen 2011). Meanwhile, AHL-family signals were found in more than 70 bacterial species (Williams *et al*. 2007) and given the many genomes that have been sequenced it is likely that this list has even increased over the last five years.

The afterwards identified group of signaling molecules was termed autoinducer 2 (AI-2) (Federle 2009; Federle and Bassler 2003). Due to the wide distribution of its synthase gene *luxS* in both Gram-negative and Gram-positive bacteria it was considered as a universal signal for inter-species communication (Surette *et al.* 1999; Bassler *et al.* 1994; 1993). The enzyme LuxS, S-ribosyl homocysteine lyase, catalyzes the last reaction step within the multistage AI-2 biosynthesis resulting in 4,5-dihydroxy-2,3-pentanedione (DPD), which undergoes spontaneous rearrangements to form a variety of interconvertible DPD derivates. Thus, DPD represents the precursor for various AI-2 molecules whose receptors were identified in several bacteria, *e.g.*, *V. harveyi*, *Salmonella enterica* spp. *enterica* serovar Typhimurium and *E. coli* (Pereira *et al.* 2013). Hence, different bacterial species can detect different forms of AI-2. *V. harveyi* for example detects a boric acid-complexed form of AI-2 (furanosyl borate diester, Figure 2B) (Chen *et al.* 2002).

Recently, a novel AI class, the α-hydroxyketones (AHKs), was discovered in the Gram-negative aquatic microorganisms *L. pneumophila* and *Vibrio* spp. The responsible AI synthase found in *V. cholerae*, was referred to as CqsA and its final product cholera autoinducer-1 (CAI-1; 3-hydroxytridecan-4-one; Wei *et al.* 2011; Higgins *et al.* 2007). This is somewhat simplified, since the substrates (*S*)-2-aminobutyrate and decanoyl coenzyme A (decanoyl-CoA) are actually linked by the enzyme to generate amino-CAI-1, which is subsequently converted to CAI-1 in a CqsA-independent reaction. However, the homologous enzyme, which was detected in *L. pneumophila,* was analogously termed LqsA and the product derived therefrom, *Legionella* autoinducer-1 (LAI-1; 3-hydroxypentadecan-4-one) (Jahan *et al.* 2009; Kelly *et al.* 2009; Spirig *et al.* 2008).

A QS signal originally identified in the Gram-negative plant pathogen *Xanthomonas campestris* pv. campestris (Wang *et al.* 2004; Barber *et al.* 1997) is the diffusible signal factor (DSF; *cis*-11-methyl-2-dodecenoic acid) (Deng *et al.* 2010). In *X. campestris*, DSF synthesis depends on the enzymes RpfF, a putative enoyl-CoA hydratase, and RpfB, a putative long-chain fatty acyl CoA ligase. Evidence mounts that DSF belongs to a widespread QS signal family (He and Zhang 2008; Wang *et al.* 2004; Barber *et al.* 1997) since similar molecules were detected in a variety of bacterial species including *Burkholderia cenocepacia*, *Xylella fastidiosa*, and *Stenotrophomonas maltophilia* (Deng *et al.* 2011). Another group of QS signaling molecules are the heterocyclic 4-quinolones (4Qs) whose first member is the *Pseudomonas* quinolone signal (PQS; 2-heptyl-3-hydroxy-4(1*H*)-quinolone). Its synthesis, catalyzed by the *pqsABCDE* operon, depends on the condensation of anthranilate and a β-keto-fatty acid (Heeb *et al.* 2011; Dubern and Diggle 2008; Diggle *et al.* 2006; Pesci *et al.* 1999).

A further group of chemical compounds that may represent a new AI class are the diketopiperazines (DKP) (de Carvalho and Abraham 2012; Campbell *et al.* 2009). It was found that DKPs can activate or antagonize LuxR-mediated QS systems (Camara *et al.* 2002a; Degrassi *et al.* 2002) presumably by competing for the AHL-binding site on LuxR-type regulator (Holden *et al.* 1999). Synthesis of this diverse group of cyclodipeptides which is widely distributed in bacteria, fungi, and even higher organisms, is catalyzed by nonribosomal peptide synthetases (NRPS) or the newly discovered cyclopeptides synthases (Belin *et al.* 2012, de Carvalho and Abraham 2012).

1.1.2 Different signal transduction pathways

The various patterns of AI integration within QS-regulated pathways are as diverse as the chemical structures within AIs themselves. Several QS systems were characterized, most notably those of opportunistic pathogens like *Pseudomonas aeruginosa*, *Legionella pneumophila* and *Vibrio cholerae* (Tiaden and Hilbi 2012; de Kievit and Iglewski 2000). Thereby, it was found, that some organisms are able to synthesize and respond to multiple QS signals (such as *P. aeruginosa*, *V. harveyi* or *V. cholerae*) (Lo Scrudato and Blokesch 2012; Rutherford and Bassler 2012; Defoirdt *et al.* 2008), while others have only one AI-based regulatory circuit. *C. violaceum* is an example of such a

microbe featuring only one QS pathway. Its CviI/R system can be regarded as a prototype for the LuxI/R-based mechanism. Here, the AI synthase CviI produces the signal C6-HSL, which exerts after binding to the receptor CviR a positive influence on violacein production (McClean *et al.* 1997) (Figure 3A).

In contrast, the QS system of *P. aeruginosa* provides an example of a hierarchically structured and complex network. It is comprised of at least three distinct signal/receptor pairs, thereof two LuxI/R homologous (LasI/R and RhlI/R) which function via the AHL signaling molecules 3-oxo-C12-HSL and C4-HSL (Venturi 2006). Beside the influence of LasR on *rhlR* both systems have a regulatory impact on the PQS circuit. Finally, there is another solo LuxR-type receptor protein (QscR) that binds 3-oxo-C12-HSL and subsequently inhibits both the *las* and *rhl* QS systems by multiple mechanisms (Jimenez *et al.* 2012) In *P. aeruginosa* expression of numerous virulence-related products is regulated by QS (Figure 3B; Lee *et al.* 2013; Antunes *et al.* 2010).

A similar complex QS circuit was identified in *Vibrio harveyi* and *Vibrio cholerae*. Here, different QS molecules assemble in the same signal transduction pathway: (i) the CAI-dependent CqsA/S system; (ii) the AI-2-dependent LuxS/PQ system and, (iii) in *V. harveyi* additionally the 3-OH-C4-HSL-dependent LuxM/N system. All are channeled onto the same phosphorelay cascade. Subsequently, expression of virulence-related genes proceeds via integrative means including LuxU, LuxO and further downstream regulatory components (Figure 3C; Henke and Bassler 2004; Camara *et al.* 2002b).

The simplified regulatory network of the plant pathogen *Xanthomonas campestris* (Figure 3D) is based on typical signaling components: an AI molecule (DSF), its corresponding synthase (RpfF), a sensor kinase (RpfC) and a downstream acting response regulator (RpfG). However, two previously uncommon characteristics have been unveiled. On the one hand it was found that RpfC and RpfF perform under certain conditions a protein-protein interaction, which affects the subsequent QS cascade (Deng *et al.* 2011). On the other hand, this QS system is one of the first examples in which a coupling via the second messenger cyclic di-GMP (c-di-GMP) and its effector Clp was detected (Srivastava and Waters 2012; Tao *et al.* 2010; Ryan *et al.* 2006).

This overview of some previously characterized QS systems reveals how differently these mechanisms are applied in the described bacterial strains. It also shows that mainly virulence-related phenotypes are controlled by QS pathways making it a promising target in fighting bacterial infections (Njoroge and Sperandio 2009).

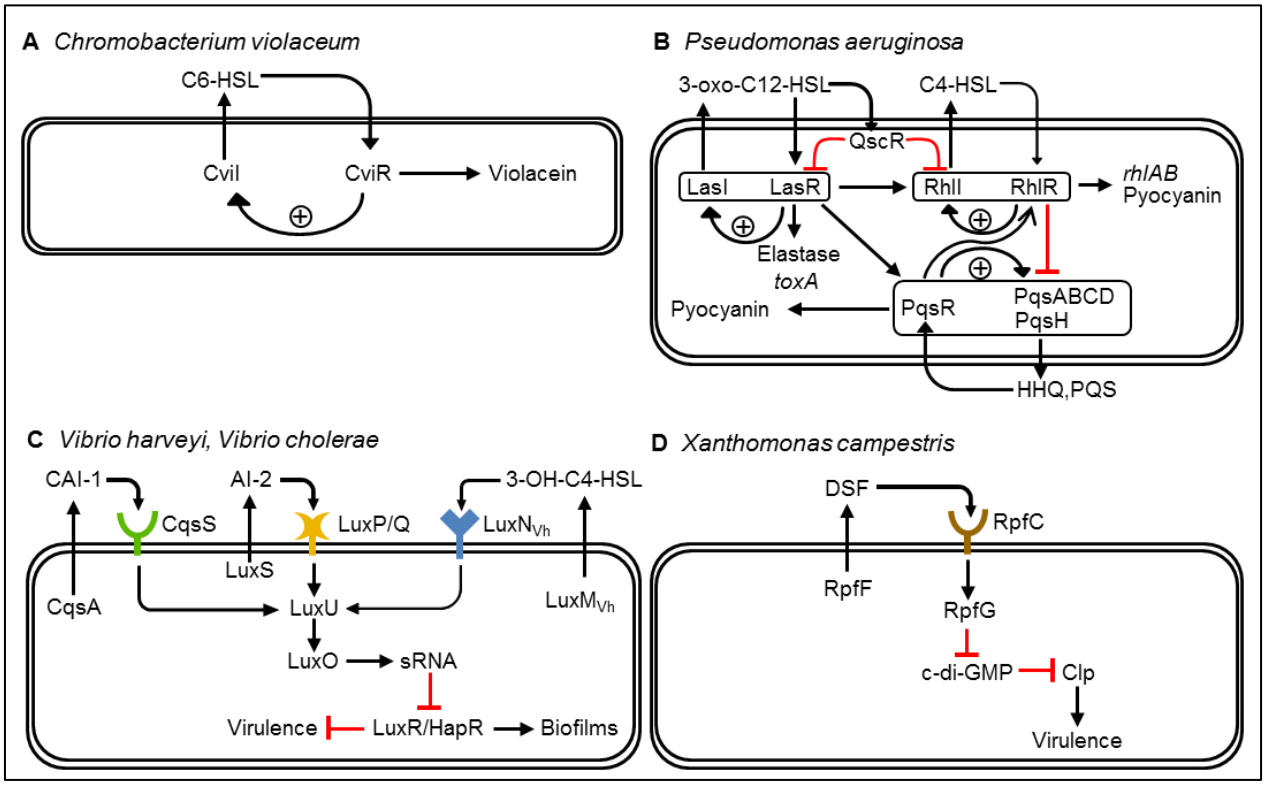

Figure 3. Quorum sensing in its various forms. (adapted from LaSarre and Federle 2013).

1.1.3 Violacein synthesis – an example of a QS-regulated phenotype

After bioluminescence, which was the first characteristic to be attributed to autoinduction, various QS regulated phenotypes have become known. These include among others biofilm formation (Li and Tian 2012), production of virulence factors (Kanamaru *et al.* 2000), swimming and swarming motility (Atkinson *et al.* 2006), sporulation (Steiner *et al.* 2012), nodulation (Yang *et al.* 2009), secretion (Sperandio *et al.* 1999), plasmid transfer (Haudecoeur and Faure 2010), production of antibiotics and other secondary metabolites (Thomson *et al.* 2000; Latifi *et al.* 1995). Another virulence-related phenotype, whose regulation is at least in some species known to be controlled by QS signaling molecules, is the violacein biosynthesis (Wang *et al.* 2008; McClean *et*

al. 1997). Violacein is a natural violet pigment with a wide range of biological effects including antibacterial, antiviral and antitumoral activity (Durán *et al.* 2007). In recent years both the CviI/R system controlling the transcriptional regulation of the violacein operon *vioABCDE* (Figure 4A) in *C. violaceum* (Morohoshi *et al.* 2010) and the function of the corresponding gene products, VioA to VioE (Hoshino 2011; Balibar and Walsh 2006), were described in detail. The latter unveiled that violacein biosynthesis depends on the initial condensation of two L-tryptophan molecules and results after several reaction steps in the pyrrolidone-containing scaffold of the final pigment (Figure 4C). Thus, violacein exhibits as chromophore-inherent property a typical absorption spectrum, which facilitates its quantification (Figure 4B).

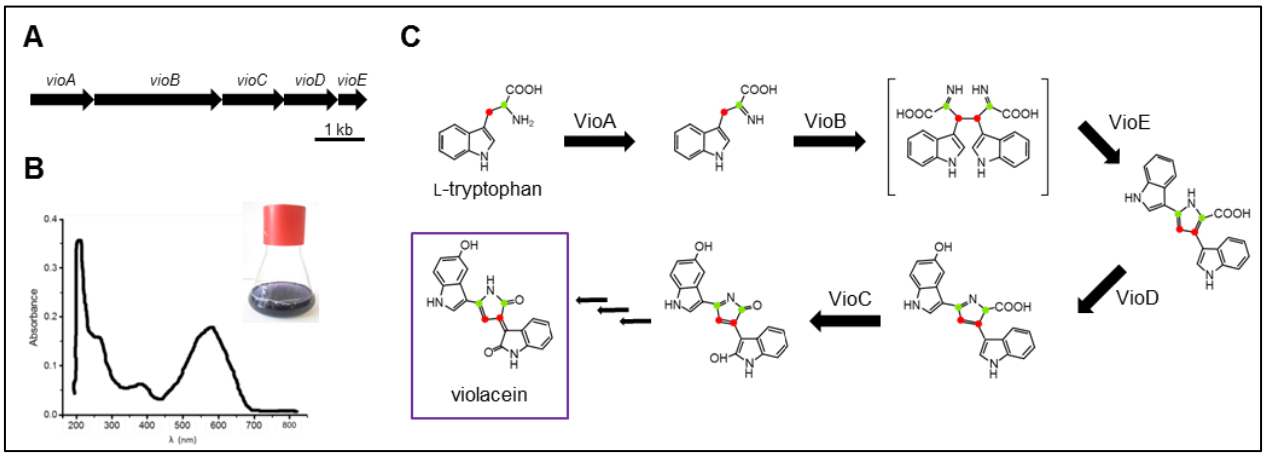

Figure 4. Violacein – from gene expression to a quantifiable phenotype. (A) The violacein operon consists of five genes (*vioA* to *vioE*) and has a size of about 7.4 kb. **(B)** UV-visible spectrum of violacein in ethanol (adapted from Dias Jr *et al.* 2002) and a flask showing a cultured violacein producing strain. **(C)** Diagram of the biosynthetic pathway of violacein (adapted from Hirano *et al*. 2008). Tryptophan oxidation and dimerization is catalyzed by tryptophan 2-monooxygenase VioA and polyketide synthase VioB. In the presence of the violacein biosynthesis enzyme VioE, the intermediate undergoes an indole rearrangement. The last two enzymes, tryptophan hydroxylase VioD and monooxygenase VioC, act on one of the two indole rings. To complete violacein formation the final step occurs non-enzymatically by autooxidation (Jiang *et al.* 2010; Balibar and Walsh 2006).

Beside *C. violaceum* (August *et al.* 2000) the violacein operon was found in various bacterial strains, such as *Collimonas* sp. (Hakvag *et al.* 2009), *Duganella* sp. (Aranda *et al.* 2011; Jiang *et al.* 2010), *Janthinobacterium lividum* (Pantanella *et al.* 2007), *Massilia* sp. (Agematu *et al.* 2011) and *Pseudoalteromonas* spp. (Thomas *et al.* 2008; Yang *et al.* 2007). In contrast to the detailed investigation of the regulatory

mechanisms in *C. violaceum*, only in *Pseudoalteromonas* an AHL-based violacein production was identified (Wang *et al.* 2008). Thus, it is certainly worthwhile to elucidate how the expression of the violacein operon is regulated in other bacteria. This is particularly the case since a strain with impaired violacein biosynthesis (CV026), which was found while investigating the violacein regulation mechanism in *C. violaceum*, has now been seen to have far-reaching relevance. In the meantime this biosensor strain CV026 was applied countless times when analyzing QS systems that are based on the autoinducer AHL (Biswa and Doble 2013; Gomes *et al.* 2013; Krysciak *et al.* 2011).

1.2 Autoinducer reporter systems

In order to detect the presence of QS molecules such as AHLs or furanosyl borate diesters strains producing a measurable phenotype like luminescence or pigment production were used (Rajamani *et al.* 2007; Steindler and Venturi 2007). Although these reporter strains or biosensors are (mostly) not able to produce AIs, they react very sensitively to exogenously added molecules. Until today, a variety of such strains has been established as a useful tool to study QS pathways (Table 1). One example of a widely used AHL biosensor is the abovementioned strain *C. violaceum* CV026, which produces the purple pigment violacein in response to an exogenous AHL stimulus (McClean *et al.* 1997). *C. violaceum* CV026 is a violacein and AHL-negative double miniTn5 mutant. One transposon is inserted into the *cviI* AHL synthase gene and the other one into a putative violacein repressor locus. Exposure of strain CV026 to exogenously added AHLs, which are able to interact with CviR, results in production of a visually purple pigmentation. Several other (AHL-detecting) biosensors rely on a plasmid construct containing a functional LuxR-family protein and a cognate target promoter fused to reporter genes such as *lacZ* or *luxCDABE*. Therefore, they easily can be quantified determining their β-galactosidase activity or bioluminescence. Nevertheless, most of them pose certain drawbacks like detection of only a narrow range of AIs (Zhu and Mekalanos 2003). Therefore it would be beneficial to increase their sensitivity and broaden the variety of detected AIs; not only in terms of the AHL-like AIs but also for other AI classes such as the AHKs.

Table 1. Common AI reporter systems.

Autoinducer reporter **strains** (sensor mutants)			
Host	**Designated strain**	**Sensed AI**	**Reference**
C. violaceum	*C. violaceum* **CV026** (Smg^{R}mini-Tn5 Hg^R *cvi*::Tn5xylE Km^R)	AHL	McClean *et al.* 1997
V. harveyi	*V. harveyi* **BB170** (*luxN*::Tn5)	VAI-2	Bassler *et al.* 1994; 1993
V. cholerae	*V. cholerae* **MM920** (Δ*cqsA* Δ*luxQ* pBB1 (*luxCDABE* from *V. harveyi*))	CAI-1	Miller *et al.* 2002
Autoinducer reporter **plasmids**			
Host	**Designated plasmids**	**Sensed AI**	**Reference**
A. tumefaciens	**NTL4** (pCF218)(pCF372) (*traR*) (*traI*::*lacZ*)	AHL	Zhu *et al.* 1998; Fuqua and Winans 1996
A. tumefaciens	**NT1** (pDCI41E33) (*traG*::*lacZ*; *traR*)	AHL	Shaw *et al.* 1997
E. coli	**pSB401** (*luxRI´*::*luxCDABE*)	AHL	Winson *et al.* 1998

1.3 The genus *Janthinobacterium*

Janthinobacterium is a genus of Gram-negative bacteria, typically isolated from soil and aquatic habitats (Sneath 1984). So far the best studied janthinobacterial strain is *J. lividum*. It has been found in various environments like on the skin of amphibians that resist fungus (Brucker *et al.* 2008) or in the gastrointestinal tract of certain salamanders (Wiggins *et al.* 2011), but it was also identified while investigating healthy human skin microbiota (Grice *et al.* 2008).

According to bacterial systematics Janthinobacteria are assigned to the family Oxalobacteraceae of the order Burkholderiales in the class β-proteobacteria. Currently at least three species are described: *J. lividum* (Eisenberg 1891) (Kämpfer *et al.* 2008; De Ley *et al.* 1978), *J. agaricidamnosum* sp. nov. (Lincoln *et al.* 1999) and the recently isolated strain *J. svalbardensis* sp. nov. (Ambrozic Avgustin *et al.* 2013). Moreover, the complete or partial genome sequences of four janthinobacterial strains have been published thus far. These include *J.* sp. Marseille (Audic *et al.* 2007), *J. lividum* PAMC 25724 (Kim *et al.* 2012), *J.* sp. GC3 (Franklin *et al.* 2012), and *J.* sp. HH01 (Poehlein *et al.* 2013). Besides the aforementioned whole genome sequences about 600 16S rRNA gene sequences, affiliated to the genus *Janthinobacterium* have also been published to date (NCBI, 2013-Jan. 1st).

Even though the term "*Janthinobacterium*" means "violet-colored rod" not all known species exhibit a violet phenotype. Nevertheless, it was shown that the genus *Janthinobacterium* is a promising source to isolate different pigments or compounds with antibiotic activity. Beside violacein (Becker *et al*. 2009; Pantanella *et al.* 2007), this also includes a so-called purple violet pigment (PVP; Mojib *et al.* 2010), bluish-purple pigments (Shirata *et al.* 2000) and prodigiosin (Schloss *et al.* 2010). In addition, certain antibiotics or antifungal metabolites (Brucker *et al.* 2008) were isolated, some of them particularly from janthinobacterial strains. These are jagaricin, an antifungal virulence factor (Graupner *et al.* 2012) and the peptide lactone antibiotics janthinocin A, B and C (Johnson *et al.* 1990). Also certain enzymes, some even with industrial reach, like chitinase (Gleave *et al.* 1995), chitosanase (Johnsen *et al.* 2010), polyvinyl alcohol-degrading enzyme (Du *et al.* 2007), agarase (Shi *et al.* 2008), alkaline β-propeller phytase (Zhang *et al.* 2011), and a metallo-β-lactamase (Docquier *et al.* 2004; Rossolini *et al.* 2001) were found and characterized. Despite these extensive studies so far no QS system has been elucidated in this organism.

1.4 Aim of the study

The aim of the present study was to investigate the recently isolated violacein-producer termed *Janthinobacterium* sp. HH01. Two aims were defined:

(1) Sequencing of the whole genome of HH01.

(2) Establishment of an applicable reporter system to screen for AI-active compounds.

(1) Janthinobacteria are known to produce several secondary metabolites and enzymes, which are biotechnologically applicable. Nevertheless there are only a few janthinobacterial genome sequences available. Therefore, analysis of its genome sequence is of particular importance. In addition, this knowledge should also serve as a basis for the examination of genetically and regulatory factors involved in the production of the purple phenotype of this microbe.

(2) So far only the regulation of the violacein biosynthesis in *C. violaceum* is well-studied. Therefore, it would be interesting (i) to analyze regulatory mechanisms controlling violacein production in HH01 and (ii) to establish a reporter-based screening system for the detection of AI-active compounds (and QS systems).

2 MATERIALS AND METHODS

2.1 Bacterial strains

Table 2. Bacterial strains used in this study.

Strain	Characteristics	Reference/Source
Agrobacterium tumefaciens NTL4 (pCF218)(pCF372)	Reporter strain used for AHL detection, Tc^R, Sp^R	Fuqua and Winans 1996; Fuqua and Winans 1994
Chromobacterium violaceum	Wildtype, DSM Nr. 30191, QS-induced violacein production	Kimmel and Maier 1969
Cupriavidus necator N-1	Type strain of the genus *Cupriavidus*	Poehlein *et al.* 2011
Duganella violaceinigra DSMZ #15887	Wildtype strain	DSMZ, Braunschweig, Germany
Escherichia coli DH5α	Cloning strain *recA1* Δ*lacZ*	Hanahan 1983
E. coli EPI100	Host strain for fosmid libraries	Epicentre, Madison, WI, USA
E. coli OP50	Derivative of *E. coli*(B) Berkeley strain, *ura*$^-$, str^R	Brenner 1974
E. coli S17-1 (λ pir)	Modified RP4 plasmid integrated into genome	Simon *et al.* 1983
Janthinobacterium sp. HH01	Wildtype isolate, Amp^R, Cm^R, Tc^R, Nal^R, Cyc^R, Gm^S, Km^S	This work
Janthinobacterium sp. HH02	Δ*jqsA* mutant of HH01, Gm^R	This work
Janthinobacterium sp. HH5-1	EZ-Tn5™ Km^R, *trpF* of HH01, *trp*$^-$, *vio*$^-$	This work
Pseudomonas aeruginosa PAO1	Non-mucoid wildtype strain, Amp^R	Holloway *et al*. 1979
Ralstonia eutropha H16	Wildtype strain	Pohlmann *et al.* 2006
Vibrio cholerae A1552	*Vibrio cholerae* O1 El Tor	Yildiz and Schoolnik 1998
Vibrio cholerae A1552Δ*cqsA*	A1552 Δ*VCA0523 (csqA)*	Suckow *et al.* 2011
Vibrio harveyi BB120	Wildtype strain	Bassler *et al.* 1997
Vibrio harveyi MR14	Δ*cqsA,* Δ*luxS* mutant of *V. harveyi* strain BB120 carrying the HH01 *jqsA* gene in pBBR1MCS-2	Research group K. Jung, Martinsried, Germany

2.2 Vectors and constructs

Table 3. Vectors used in this study.

Vector	Characteristics	Size (kb)	Reference/source
pBBR1MCS-2	Broad host-range vector, Km^R	5.14	Kovach *et al.* 1995
pBBR1MCS-5	Broad host range vector, Gm^R	4.77	Kovach *et al.* 1995
pCC1FOS™	Inducible fosmid vector, Cm^R	8.14	Epicentre, Madison, WI, USA
pCR®4-TOPO	TA cloning vector, Amp^R, Km^R	3.96	Invitrogen, Carlsbad, USA
pDrive	TA cloning vector, Amp^R, Km^R	3.85	QIAGEN, Hilden, Germany
pGEM-T	TA cloning vector, Amp^R	3.00	Promega, Mannheim, Germany
pNPTS138-R6KT	Suicide vector for knock outs	4.43	Lassak *et al.* 2010
SuperCos	Cosmid vector, Amp^R, Neo^R, *cos*	7.94	Stratage/Agilent Technologies (Santa Clara, CA, USA)

Table 4. Constructs used in this study.

Constructs	Characteristics	Reference/source
pBBR1MCS-2-$cqsA_{Vch}$	*cqsA* from *V. cholerae* A1552 integrated into plasmid pBBR1MCS-2	This work
pBBR1MCS-2-$cqsA_{Vh}$	pBBR1MCS-2 with *V. harveyi* BB120 *cqsA* under control of the arabinose promoter	This work
pBBR1MCS-2-*jqsA*	*jqsA* in pBBR1MCS-2	This work
pBBR1MCS-2-*lqsA*	*lqsA* in pBBR1MCS-2-in *Xho*I-*Bam*HI site	This work
pDrive-*vioABCDE*	pDrive encoding the *vioA-E* genes under the native promoter	This work
pBBR1MCS-2-*vioABCDE*	pBBR1MCS-2 encoding the *vioA-E* genes under the native promoter	This work
pBBR1MCS-5-*vioABCDE*	pBBR1MCS-5 encoding the *vioA-E* genes under the native promoter	This work
pTS21	*Legionella* sp. *lqsA* in pET28	Spirig *et al.* 2008

2.3 Primers

Table 5. Primers used in this study.

Primer	Sequence (`5-3´)[1)]	Reference
616V	AGAGTTTGATYMTGGCTCAG	Brosius *et al.* 1981
1492R	CGGYTACCTTGTTACGAC	Kane *et al.* 1993
KAN-2 FP-1	ACCTACAACAAAGCTCTCATCAACC	Epicentre, Madison, WI, USA
KAN-2 RP-1	GCAATGTAACATCAGAGATTTTGAG	Epicentre, Madison, WI, USA
Inv-1	ATGGCTCATAACACCCCTTGTATTA	Ducey and Dyer 2002
Inv-2	GAACTTTTGCTGAGTTGAAGGATCA	Ducey and Dyer 2002
vio_nst_18843	GCGCCACACCTGTTAATCGC	This work
vio_nst_27070	CGCCATGAAGTCGTAATCGG	This work
*jqsA*_cloning_for	TTGCCATGATCGCCTTAAAT	This work
*jqsA*_cloning_rev	ACCTCCATGATAGCGTACCG	This work
Gm^R_for_*Xba*I	GACATCTAGAGACGCACACCGTGGAAAC	This work
Gm^R_rev_*Xba*I	TAATCTAGACCGCGATCATCAAGGCCGTG	This work
*jqsA*_del_A1_*Bam*HI	CTTAGGATCCACCTCCATGATAGCGTACCG	This work
*jqsA*_del_A2_*Xba*I	CGATTCTAGATCAAGGGCTACTTCCTGTCC	This work
*jqsA*_del_B1_*Xba*I	GCTATCTAGATGTCCAGGTAGACCGGAATG	This work
*jqsA*_del_B2_*Eco*RI	GTCCGAATTCAAGTGCTGCCAGATCACGTA	This work
*jqsA*_del_control_outA	GTCTCGACGTTCTTCGCATACT	This work
*jqsA*_del_control_outB	GTGGTGTCGTGGAAGGTCTG	This work
*jqsA*_del_control_rev1	TGTCCAGGTAGACCGGAATG	This work
*jqsA*_del_control_rev2	GCACAACGACATCGAACATC	This work
*vioA*_del_A1_*Eco*RI	GAATTCTTAAGCGAGCTCAGCTTGAC	This work
*vioA*_del_A2_*Xba*I	TCTAGATTTTGGAAGTTCGGATGGAG	This work
*vioA*_del_B1_*Xba*I	CGATTCTAGACTACGAGCTTGCCTTCAACC	This work
*vioA*_del_B2_*Bam*HI	CTTAGGATCCCAAGGCTCTCAGGTGCTGAT	This work

[1)] Restriction sites are underlined. R, purine base A or G; Y, pyrimidine base C or T.

2.4 Antibiotics and other supplements

Antibiotics and other heat sensitive supplements such as Isopropyl-β-D-1-thiogalactopyranoside (IPTG) and 5-bromo-4-chloro-3-indolyl-β-D-galactopyranoside (X-Gal) were dissolved in the appropriate solvent, *i.e.*, water ($A._{bidest.}$), ethanol (EtOH) or dimethylformamide (DMF). Sterile filtered (Rotilabo® syringe filter (CME, sterile 0.22 µm), Roth Karlsruhe, Germany) aliquots were stored at -20 °C. The concentration of used antibiotics and other supplements for cultivation of bacterial strains are listed in Table 6.

Table 6. Antibiotics and other supplements used in this study.

Substance	Stock solution [mg/mL]	Final concentration [µg/mL]				Solvent
		A. tumefaciens	*E. coli*	*J.* sp.	*P. aeruginosa*	
Antibiotics						
Ampicillin	100		100	100	100	$A._{bidest.}$
Chloramphenicol	25		25			EtOH
Gentamicin	50		10	10		$A._{bidest.}$
Kanamycin	25		25	25		$A._{bidest.}$
Spectinomycin	50	50				$A._{bidest.}$
Tetracycline	5	4.5	5			$A._{bidest.}$
Supplements						
IPTG	100		100			$A._{bidest.}$
X-Gal	50	60	50		50	DMF

2.5 Microbiological methods

2.5.1 Cultivation of bacteria

Culture media and heat stable supplements were autoclaved at 121 °C for 20 min. Antibiotics and heat sensitive supplements were added sterile filtered after media cooled down to 56 °C. For solid culture media 1.5% (w/v) agar was added prior to autoclaving.

Liquid cultures were grown in Erlenmeyer flasks, test tubes or deep well plates at 140-200 rpm in rotary shakers (Infors HT, Minitron, Bottmingen, Switzerland). Cultures were either inoculated by single colonies from agar plates or by glycerol stocks. Liquid culture volumes above 30 mL (100-1,000 mL) were inoculated with a 1-5% aliquot of a 30 mL overnight grown pre-culture.

Agrobacterium tumefaciens NTL4 was inoculated from glycerol stocks in 5 mL liquid lysogenic broth (LB) medium (Sambrook 2001; 1% peptone, 0.5% yeast extract, 1% NaCl) and grown overnight at 30 °C. The following day 5 mL *Agrobacterium tumefaciens* (AT) medium (Tempe *et al.* 1977; 890 mL $A._{bidest.}$, 50 mL 20x AT salt solution (0.303 M $(NH_4)_2SO_4$, 0.013 M $MgSO_4$, 1.36 mM $CaCl_2$, 0.36 mM $FeSO_4$, 0.087 mM $MnSO_4$), 50 mL 20x AT buffer (1.57 M KH_2PO_4) and 10 mL glucose (50%, w/v) supplemented with appropriate antibiotics (spectinomycin, final conc. 50 µg/mL and tetracycline, final conc. 4.5 µg/mL) were inoculated with a 1-5% aliquot of the LB culture and incubated overnight at 30 °C. *Escherichia coli* (*E. coli*) strains were grown at 37 °C in LB medium supplemented with appropriate antibiotics. *E. coli* cosmid and fosmid clones were inoculated in deep well plates containing 1-1.2 mL LB medium supplemented with appropriate antibiotics and incubation at 37 °C on a rotary shaker at 350 rpm for 20 h. *Janthinobacterium* sp. HH01 was cultured in the presence of ampicillin (100 µg/mL) containing R2A medium (Reasoner and Geldreich 1985; 0.05% yeast extract, 0.05% tryptone, 0.05% casamino acids, 0.05% dextrose, 0.05% soluble starch, 0.03% sodium pyruvate, 1.7 mM K_2HPO_4, 0.2 mM $MgSO_4$, finally pH 7.2 adjusted with crystalline K_2HPO_4 or KH_2PO_4) at 22 °C for one or two days. *Pseudomonas aeruginosa* PAO1 was cultured overnight on solid or liquid LB medium supplemented with appropriate antibiotics at 37 °C.

2.5.2 Strain maintenance

For short-term storage strains were grown on agar plates. Sealed petri dishes were kept at 4 °C up to four weeks. For the long-term storage of bacterial strains, 87% sterile glycerol was added to liquid overnight cultures to a final volume of 33% (v/v). Glycerol stocks were stored at -70 °C.

2.5.3 Determination of cell density

The cell density of growing liquid cultures was monitored by measuring the optical density at a wavelength of 600 nm (OD_{600}) with a spectrophotometer (Eppendorf BioPhotometer; Eppendorf, Hamburg, Germany) using one-way cuvettes (10x4x45 mm, Sarstedt, Nuembrecht, Germany) with a path length of 1 cm. Pure medium was used as reference and for the dilution of cell cultures. Calculation of the corresponding cell number was performed based on the assumption that an OD_{600} of 0.1 corresponds to a cell number of $1*10^8$ *E. coli* cells/mL.

2.6 Molecular biological methods

2.6.1 Isolation of genomic DNA

For the isolation of genomic DNA, cells were harvested by centrifugation at 13,000 g and 4 °C for 5 min using centrifuge 5417R (Eppendorf, Hamburg, Germany). The obtained pellet was resuspended in 1 mL salt solution (800 mM NaCl, 100 mM EDTA, pH 8.0) and incubated for 1 h on ice. The suspension was centrifuged at 9,000 g and 4 °C for 5 min and the pellet resuspended in 250 µL TE-sucrose solution (10 mM Tris-HCl, 1 mM EDTA, 20% (w/v) sucrose, pH 8.0). After addition of 250 µL cell lysis buffer (10 mM Tris-HCl, 1 mM EDTA, 10 mg/mL lysozyme, 1 mg/mL RNaseA, pH 8.0) and subsequent mixing, the sample was incubated at 37 °C for 1 h. Then 150 µL Proteinase K-solution (1 mg/mL Proteinase K, 5% (w/v) sarcosyl) was added and the reaction mixture incubated at 37 °C for 1 h. After addition of 250 µL phenol/chloroform (1:1, v/v) the sample was mixed and centrifuged at 13,000 g for 15 min at 4 °C to achieve phase separation. The obtained supernatant was transferred into a new sterile reaction tube and addition of phenol/chloroform with subsequent mixing and centrifugation was repeated until no protein layer was visible as an interphase. Then 250 µL chloroform were added and the sample mixed. This was followed by another centrifugation step at 13,000 g and 4 °C for 5 min. The supernatant was transferred into a new sterile reaction tube. To precipitate DNA, 2.5 vol. EtOH (96%) and 0.1 vol. 3 M sodium acetate (pH 5.5) were added, the mixture inverted and incubated at -20 °C for at least 1 h. DNA precipitation was performed at 13,000 g and 4 °C for 20 min. After a careful supernatant removal, the pellet was washed twice with 300 µL EtOH (70%, v/v), and air-dried. To dissolve the isolated DNA an adequate volume of sterile 1x TE buffer (10 mM Tris-HCl, 1 mM EDTA, pH 8.0) or $A._{bidest.}$ was added. Finally the DNA integrity and

quantity was proofed by agarose gel electrophoresis (2.6.5) and spectrophotometric measurement (2.6.4).

2.6.2 Preparation of plasmid DNA

Plasmid isolation including spin column purification

Isolation and purification of plasmid DNA with the QIAprep® Spin Miniprep Kit (QIAGEN, Hilden, Germany) was performed following the instructions of the manufacturer.

Plasmid isolation without spin column purification

Otherwise, plasmid isolation and purification was performed according to the alkaline cell lysis method of Birnboim and Doly (1979). All centrifugation steps were performed at 13,000 g and RT using centrifuge 5415D (Eppendorf, Hamburg, Germany). 4 mL of an overnight culture were centrifuged for 30 sec and the pelleted cells resuspended in 100 µL buffer P1 (50 mM Tris-HCl, 10 mM EDTA, 1 mg/mL RNase A, pH 8.0). After addition of 200 µL buffer P2 (200 mM NaOH, 1% (w/v) SDS) the sample was inverted several times and incubated at RT until complete lysis of the cells. After a maximum of 5 min, 150 µL buffer P3 (3 M KAc, pH 5.5) were added to stop the lysis process. The sample was mixed and centrifuged for 5 min. The upper phase containing plasmid DNA was transferred into a new sterile reaction tube and mixed with 500 µL chloroform/isoamyl alcohol (24:1, v/v). The two phases were mixed by shaking and centrifuged for 5 min at 13,000 g. Then the upper phase was transferred into a new reaction tube and plasmid DNA precipitation performed by addition of the same volume cold 2-propanol. After inverting the sample it was incubated at -20 °C for 30 min followed by another centrifugation step at 4 °C for 20 min. After removing the supernatant, the pellet was washed twice with 500 µL 70% (v/v) EtOH. The air-dried pellet was resuspended in 50 µL sterile $A._{bidest.}$.

2.6.3 DNA purification and concentration

To purify DNA fragments with spin columns the PCR clean-up Gel Extraction Kit (Macherey-Nagel, Düren, Germany) was used according to the manufacturer's protocol. DNA was eluted twice with 15-20 µL $A._{bidest.}$ or the appropriate buffer.

To purify DNA fragments by ethanol precipitation 1/10 volume sodium acetate (3 M, pH 5.2) and 1 vol. chloroform/isoamylalcohol (24:1, v/v) were added, mixed and centrifuged for 5 min at 13,000 rpm and 4 °C. The upper layer was transferred into a fresh reaction tube and 2.5 volumes ethanol (96%) were added. After incubation at -20 °C for 20 min centrifugation was performed as described above for 20 min. The pellet was washed twice with 500 µL ethanol (70%), dried and resuspended with 20-50 µL $A._{bidest.}$.

To concentrate DNA solutions samples were centrifuged at 45 °C for up to 5 min in a vacuum concentrator (Concentrator 5301, Eppendorf, Hamburg, Germany).

2.6.4 Determination of DNA concentration and purity

The absorbance of DNA samples was measured spectrophotometrically at 260 nm in UV cuvettes (Brand, Wertheim, Germany) using Eppendorf BioPhotometer. It was assumed that 1 unit of absorbance corresponds to 50 µg/mL. The DNA purity was determined by the ratio of extinction at 260 nm/280 nm. A ratio of 1.8 to 2.0 counts for pure DNA. A lower ratio indicates a contamination with proteins or phenol, which are detected at 280 nm.

2.6.5 Agarose gel electrophoresis

For analysis or preparative purposes DNA samples were depending on the expected size loaded on 0.8-2.0% (w/v) agarose gels. Agarose was solved in 1x TAE buffer (40 mM Tris-Acetate, 2 mM EDTA, pH 8.0). After mixing with loading dye (60 mL glycerol (30%), 50 mM EDTA, 0.5 g bromphenol blue (0.25%), 0.5 g xylencyanol (0.25%), $A._{bidest.}$ ad 200 mL) samples were separated by gel electrophoresis in an electrophoresis gel chamber (Hoefer™ HE-33 mini horizontal submarine unit, Amersham Biosciences, Piscataway, NJ, USA). Electrophoresis was conducted in 1x TAE running buffer obtained by dilution of 50x TAE (2 M Tris-Acetate, 100 mM EDTA, pH 8.0) at 80 to 120 V clamping, provided by EPS 301 power supply (Amersham Biosciences, Piscataway, NJ, USA). To determine the size of the migrated fragments the molecular weight (MW) marker Gene Ruler™ 100 bp DNA Ladder (MBI Fermentas, St. Leon-Rot, Germany) or Gene Ruler™ 1 kb DNA Ladder (MBI Fermentas, St. Leon-Rot, Germany) were used. The gels were visualized after staining in ethidium bromide solution (10 µg/mL; 15 min) under ultraviolet light using the Universal Hood II system (BIO-RAD, Milan, Italy) and the supporting Quantity I 1-D-Analysis software (BIO-RAD, Philadelphia, PA, USA).

2.6.6 DNA gel extraction

In order to purify and isolate DNA fragments obtained by PCR or other enzymatic reactions they were extracted from the agarose gel using the QIAquick® Gel Extraction Kit (QIAGEN, Hilden, Germany) according to the instructions of the manufacturer. The cleaned up DNA was eluted in two consecutive aliquots of 15 µL sterile $A._{bidest.}$, or the appropriate elution buffer followed by spectrophotometrically determination of the DNA concentration (2.6.4).

2.6.7 Enzymatic DNA modification

Site specific digestion of DNA

Genomic DNA, plasmid DNA or PCR amplicons were digested with DNA restriction endonucleases from Fermentas (St. Leon-Rot, Germany) in the supplied buffers according to the instructions of the manufacturer. For double digest reactions the recommendations of the "DoubleDigest" program available by Thermo Scientific (http://www.thermoscientificbio.com/webtools/doubledigest/) were followed. The reaction mixture was incubated for 2-3 h or overnight at the recommended temperature. For analytical purposes 0.2 µg DNA was mixed with 1 µL 10x reaction buffer and 5 U enzyme in a final volume of 10 µL. For preparative DNA digestion between 0.5-5.0 µg DNA was incubated with 5 µL 10x reaction buffer and 10 U enzyme in a final volume of 50 µL. To avoid religation of the digested vector 1 µL enzyme (5 U/µL) Antarctic Phosphatase (New England Biolabs, Beverly, MA,USA) was added in 3 µL 10x reaction buffer, and 6 µL $A._{bidest.}$ to 50 µL digested vector DNA. After incubation for 1 h at 37 °C, heat inactivation was performed at 65 °C.

Ligation of DNA

After DNA digestion of vector and insert to generate fragments with fitting ends ligation of both was performed. Therefore DNAs of the insert and linearized and dephosphorylated vector (molar ratio insert:vector = 2:1 to 10:1) were incubated overnight at 22 °C in 10x ligation buffer (400 mM Tris-HCl, 100 mM $MgCl_2$, 100 mM DTT, 5 mM ATP, pH 7.8) and 0.5 µL T4 DNA ligase (Fermentas) in a total volume of 20 µL (diluted in $A._{bidest.}$).

Ligation into pDrive cloning vector

For a quick and simple ligation of PCR amplicons obtained by *Taq* polymerase the QIAGEN® PCR Cloning Kit (QIAGEN, Hilden, Germany) was used. The ligation reaction was set up as follows: 0.5-2.0 µL PCR product; 0.5 µL pDrive cloning vector (Table 3); 2.5 µL ligation master mix; $A._{bidest.}$ *ad* 5 µL. After incubation at 16 °C for 1-2 h or overnight, an aliquot of the reaction mixture was used for transformation into appropriate *E. coli* host strains (2.6.9.1).

Ligation into pGEM-T cloning vector

Ligation of PCR products into pGEM-T cloning vector was conducted using pGEM®-T Vector Systems Kit (Promega, Mannheim, Germany). The ligation reaction was set up as follows: 2.5 µL 2x rapid ligation buffer, 0.5 µL pGEM-T vector (Table 3), 1.5 µL PCR product, 0.5 µL T4 DNA ligase. Incubation was performed overnight at 4 °C.

2.6.8 Polymerase chain reaction (PCR)

2.6.8.1 Standard PCR reactions

For amplification of specific DNA fragments the polymerase chain reaction (PCR) was used. PCR primers were designed using the "Primer3 version 0.4.0" program, which is online available (http://frodo.wi.mit.edu/), and purchased from Eurofins MWG Operon (Ebersberg, Germany). Primers used in this study are listed in Table 5. The primer annealing temperature T_{ann} was calculated from the primer melting temperature T_m as follows: $T_{ann} = T_m - 5$ °C. For PCR reaction the lower T_{ann} of both primers was used in each case. PCR reactions were performed in a Mastercycler personal (Eppendorf Hamburg, Germany). The applied PCR program (Table 7) was adapted to the used polymerase and annealing temperatures of the primers. The elongation time was conformed to the length of the expected DNA fragment, whereby the synthesis rate was supposed to be 1 kb/min for *Taq* polymerase and 0.5 kb/min for *Pfu* polymerase. The amount of DNA template was between 20-40 ng for genomic or plasmid DNA.

Standard PCR reactions were performed in 100 µL-PCR tubes as follows: 1 µL template DNA; 2.5 µL 10 x *Taq* polymerase buffer (100 mM Tris, 25 mM $MgCl_2$, 500 mM KCl, pH 8.3); 2 µL dNTPs (2 mM); 1 µL forward primer (10 µM); 1 µL reverse primer (10 µM); 0.5 µL *Taq* polymerase; ad 25 µL $A._{bidest.}$.

Table 7. Standard PCR conditions.

PCR step	Temperature (°C)	Time	
Initial denaturation	95	2 min	
Denaturation	95	30 sec	30-35 cycles
Annealing	[$T_{ann} = T_m - 5$ °C]	30 sec	
Elongation	72	1 min/1 kb (*Taq*), 1 min/0.5 kb (*Pfu*)	
Final Elongation	72	up to 5 min	

2.6.8.2 Direct colony PCR

In order to obtain a straightforward result after transformation of ligation reactions (2.6.7) or transposon mutagenesis (2.6.11) the direct colony PCR method was used. Colonies of putative positive clones were suspended in 20 µL $A._{bidest.}$ and incubated for 10 min at 95 °C. 1 µL of this suspension was added to a prepared PCR reaction mixture as described for standard PCR reactions (2.6.8.1).

2.6.9 DNA transformation

2.6.9.1 Transformation of *E. coli* using heat shock

The standard procedure to transfer plasmid DNA or ligation reactions into *E. coli* host strains was carried out using the heat shock transformation method. For the preparation of chemically competent cells 100 mL LB medium was inoculated 1:100 with an appropriate overnight *E. coli* culture. The culture was incubated at 37 °C until an OD_{600} of 0.5. Following, cells were kept on ice for 5 min and centrifuged for 5 min at 4,000 g and 4 °C. Afterwards the cell pellet was gently resuspended in 30 mL ice-cold TFB1 buffer (100 mM RbCl, 50 mM $MnCl_2$, 30 mM potassium acetate, 10 mM $CaCl_2$, 15% glycerol, pH 5.8, sterile filtered) and kept on ice for additional 90 min. Following centrifugation was performed at 4,000 g at 4 °C for 5 min and after that cells were carefully resuspended in 4 mL ice-cold TFB2 buffer (10 mM MOPS, 10 mM RbCl, 75 mM $CaCl_2$, 15 % glycerol, pH 6.8 with KOH, sterile filtered). Aliquots of 100 µL were prepared and stored in sterile microcentrifuge tubes at -70 °C.

For the heat shock transformation 100 µL competent *E. coli* cells were thawed on ice and mixed with 5 µL ligation product or 2 µL plasmid DNA. The mixture was successively exposed to different temperatures: 30 min on ice, 90 sec at 42 °C, and again 5 min on ice. Following 800 µL LB medium were added, and the DNA-cell-mixture was incubated for about 1 h at 37 °C under gentle agitation. To obtain single clones, different aliquots were spread on agar plates containing the appropriate antibiotic and other supplements, if required. Agar plates were incubated overnight at 37 °C.

2.6.9.2 Transformation of *P. aeruginosa* PAO1 using heat shock

PAO1 competent cells were prepared as follows: Overnight grown cells were diluted 1:10 into fresh LB medium (50 mL) and incubated at 37 °C until mid exponential growth phase (OD_{600} = 0.6). The cells were incubated on ice for 20 min, transferred to sterile centrifuge tubes and centrifuged at 4,000 rpm for 5 min at 4 °C. The pellet was resuspended in 50 mL ice-cold 100 mM $MgCl_2$ and centrifuged again. Afterwards, the pellet was resuspended in 25 mL of ice-cold 100 mM $CaCl_2$ and incubated on ice for at least 60 min. After centrifugation the pellet was resuspended in 2 mL of ice-cold 100 mM $CaCl_2$. Finally, cells were aliquoted in a total volume of 100 µL and used directly for transformation.

For transformation 5 µL DNA was added and cells were kept on ice for 30 min. Heat shock was performed at 42 °C for 2 min, followed by incubation on ice for 20 min. Afterwards 1 mL LB medium was added and cells were incubated at 37 °C. Finally, cells were spinned down for

30 sec, resuspended in 100 µL LB medium and plated on selection plates containing the appropriate antibiotic. Incubation of inoculated plates was performed at 37 °C overnight.

2.6.9.3 Transformation of *Janthinobacterium* sp. HH01 by electroporation

Transformation of HH01 was conducted by electroporation. For this HH01 was grown overnight in R2A medium and then diluted in 100 mL sterile medium to an optical density (OD_{600}) of 0.1. Cells were subsequently grown to an OD_{600} of 0.6 at 22 °C. For the electroporation cells were kept on ice for 30 min prior to centrifugation at 4,000 g at 4 °C for 10 min. After this initial centrifugation step the cells were resuspended in 1 mL ice-cold sterile $A._{bidest.}$, transferred to a pre-chilled microcentrifuge tube, washed three times with 1 mL ice-cold $A._{bidest.}$ and resuspended in $A._{bidest.}$ to a final concentration of 10^{10} cells/mL. The cells were mixed with up to 1 µg of plasmid DNA and transferred to a pre-chilled 1 mm-electroporation cuvette (BIO-RAD, Gene Pulser Cuvette, *E. coli* Pulser Cuvette). The electroporation pulse was applied at 2.5 kV, 25 µF, 200 Ω using a Bio-Rad Gene PulserXcell, 165-2662 (Bio-Rad Laboratories GmbH, Munich, Germany). The electroporated cells were immediately mixed with 500 µL R2A medium, incubated for two hours at 22 °C and spread on selective R2A agar plates.

2.6.10 Sequencing analysis

2.6.10.1 Sequencing of vector constructs and PCR products

Sequencing was conducted in the working group of Prof. Schreiber at the “Institut für klinische Molekularbiologie” (Christian-Albrechts-Universität zu Kiel, Germany) using an ABI 3730XL DNA Analyzer (Applied Biosystems/Life Technologies, Darmstadt, Germany) based on the Sanger technique (Sanger *et al*. 1977). For analysis DNA was purified and adjusted to a concentration of 100 ng/µL. Each sequencing sample was composed of 3 µL template DNA and 1 µL primer (4.8 µM).

2.6.10.2 Whole genome sequencing of *Janthinobacterium* sp. HH01

DNA for 454 sequencing was isolated under standard conditions using the peqGOLD Bacterial DNA Kit (peqlab Biotechnology GmbH, Erlangen, Germany). The extracted DNA was used to generate 454-shotgun and paired-end libraries according to the manufacturer´s protocols (Roche 454, Branford, USA). Five and one, medium lane of a Titanium picotiter plate was used for sequencing of the libraries resulting in 1248653 total reads with 120,434 paired reads. The reads were *de novo* assembled using the Roche Newbler assembly software 2.3 (Roche 454). 7.3 Mbp non-redundant sequences on 1,957 contigs with a size of 50 nt to 127,075 nt were

created. Further a large insert-fosmid library was constructed according to the Copy Control fosmid library production kit manual (Epicentre Biotechnologies, Madison, WI, USA). A total of about 2,400 fosmid clones were generated. This equals a 3-fold coverage of the HH01 genome. Ends of 672 recombinant fosmids were sequenced using ABI 3730xl automated DNA sequencers (Life Technologies, Darmstadt, Germany), processed with Phred, and assembled using Phrap. PCR-based techniques were used to close the remaining gaps using both genomic DNA and fosmid clones as templates. In addition, DNA of selected fosmids was isolated using standard protocols and sheared for the construction of small insert plasmid libraries to close the gaps. These were constructed with the TOPO TA Cloning™ Kit (Invitrogen, Carlsbad, USA) using the pCR®4-TOPO® vector accodding to instructions of the manufacturer.

All manual editing steps were performed using the GAP4 software package v4.5 and v4.6 (Schiex *et al.* 2003). Coding sequences (CDS) and open reading frames (ORFs) were predicted with YACOP (Tech and Merkl 2003) using the ORF-finders Glimmer, Critica and Z-curve. All predicted genes were manually curated based on GC frame plot analysis, the presence of ribosome-binding sites, and comparison to known protein-encoding sequences employing the Sanger Artemis tool v13 (Carver *et al.* 2005). Functional annotation was initially performed with the ERGO software tool (Overbeek *et al.* 2003) and the IMG/ER (Integrated Microbial Genomes/Expert Review) system (Markowitz *et al.* 2012). All CDS were manually curated and verified by comparison with the publicly available databases SwissProt, EMBL (InterProScan) GenBank, COG and Prosite using the annotation software IMG/ER (https://img.jgi.doe.gov/cgi-bin/er/main.cgi). Gene products were classified into functional categories performing a BLAST search against the COG database (Tatusov *et al.* 1997). Comparative analyses of different organisms was done using a bidirectional BLAST algorithm, combined with a global sequence alignment based on the Needleman-Wunsch algorithm (Needleman and Wunsch 1970). ORFs were assumed to be orthologs at a similarity higher than 30% and a BLAST E-value lower than 10e-21. Visualization of the chromosome and other DNA sequences was done by using DNA Plotter (Carver *et al.* 2009).

2.6.11 Transposon mutagenesis

To generate a random transposon mutagenesis library the EZ-Tn5™ <KAN-2>Tnp Transposome™ Kit (Epicentre, Madison, Wisconsin, USA) was used. The EZ-Tn5™ <KAN-2>Tnp Transposome™ is a stable complex formed between the EZ-Tn5 Transposase enzyme and the EZ-Tn5 <KAN-2> Transposon. The EZ-Tn5 <KAN-2> Transposon contains the Tn903 kanamycin resistance gene flanked by hyperactive 19 bp Mosaic End (ME) EZ-Tn5 Transposase recognition sequences. The EZ-Tn5 Transposome was electroporated into *Janthinobacterium*

sp. HH01 following the manufacturer´s instructions. Electrocompetent host cells were prepared as described (2.6.9.3). The cells were mixed with 1 µL of the EZ-Tn5 <KAN-2>Tnp Transposome to achieve random insertion of the EZ-Tn5 Transposon into the genomic DNA. After electroporation (2.6.9.3) cells were immediately recovered by adding 500 µL R2A medium and incubation for 2 h under agitation. Aliquots of the recovered cells (50-200 µL) were spread on agar plates containing 25 µg/mL kanamycin. Incubation was performed at 28 °C for three days. A total of 8,500 mutants were generated. Thereof 50 white or cream colored mutants were selected and the insertion site of the transposon of 39 of these determined according to a modified protocol (Ducey and Dyer 2002). Forward and reverse transposon-specific primers (Inv1 or Inv2) were used for unidirectional PCR followed by direct sequencing (using primer KAN-2 RP1 or KAN-2 FP1) of the obtained PCR amplicons without cloning. PCR mixture was composed as described (2.6.8), but contained only one primer (Inv1 or Inv2). As DNA template either colony material directly taken from the agar plates or purified DNA was used. The PCR protocol was a three-step, single-primer PCR protocol. The first and third steps of the PCR program were performed at a stringent temperature (T_{ann} = 50 °C; step one: 20 cycles at 50 °C and 3 min elongation; step three: 30 cycles at 50 °C and 2 min elongation.) The second step was performed at 30 °C (30 cycles at 30 °C and 2 min elongation), allowing non-specific amplification of the single-stranded product generated in the first step. In the third step amplification of both the specific and non-specific products generated in the second step was achieved. The obtained PCR products were purified by ethanol precipitation (2.6.3) and sequenced (2.6.10.1) using primer KAN-2 FP-1 or KAN-2 RP-1. Thus mapping of the transposon insertion site within the HH01 genome was achieved.

2.6.12 Knockout mutant construction

To generate a *jqsA* gene knockout mutant, upstream and downstream regions (designated as fragment A and B) were amplified by PCR (2.6.8) and linked with a Gm^R cassette. Fragment A was amplified using primers *jqsA*_del_A1_*Bam*HI and *jqsA*_del_A2_*Xba*I (Table 5), resulting in a ~500 bp *Bam*HI-*Xba*I-fragment. Fragment B was amplified using primers *jqsA*_del_B1_*Xba*I and *jqsA*_del_B2_*Eco*RI, resulting in a ~800 bp *Xba*I-*Eco*RI-fragment. After ligation using the *Xba*I-restriction site the obtained ~1,300 bp *Bam*HI-*Eco*RI-fragment was cloned into the pGEM-T vector (2.6.7). The desired clone was subsequently linearized by *Xba*I and the achieved *Xba*I-flanked Gm^R-cassette (generated by PCR using primer Gm^R_for_*Xba*I and Gm^R_rev_*Xba*I and vector pBBR1MCS-5 as template; Table 5 and Table 3, respectively) inserted into the vector. After transformation in *E. coli* DH5α (2.6.9.1) and selection on agar plates containing 10 µg/mL gentamicine a positive clone bearing the ~2.3 kb gentamicin resistance cassette flanked by

fragment A and fragment B was obtained. The insert (A-Gm^R-B construct) was ligated into the suicide vector pNPTS138-R6KT (Table 3) using *Bam*HI and *Eco*RI restriction sites. After transformation in *E. coli* S17-1 λpir (Table 2) as host and selection on agar plates containing ampicillin (100 µg/mL) and gentamicin (10 µg/mL) the obtained construct (pNPTS138-*jqsA*::gm) was electroporated into HH01 (2.6.9.3). Single recombinant clones containing this construct were selected on R2A medium with gentamicin (10 µg/mL). To obtain double recombinant mutants bacteria were streaked on the same medium in the presence of 10% sucrose but lacking gentamicin. The correctness of the obtained *jqsA* mutant was verified by PCR using different primer pairs located inside (*jqsA*_del_control_rev1 and *jqsA*_del_control_rev2) or outside (*jqsA*_cloning_for, *jqsA*_cloning_rev, *jqsA*_del_control_outA and *jqsA*_del_control_outB) the *jqsA* gene. The presence of the introduced mutation was subsequently validated by sequencing.

In the same way a knockout of the gene *vioA* should be generated. Therefore primer pairs *vioA*_del_A1_*Eco*RI/*vioA*_del_A2_*Xba*I and *vioA*_del_B1_*Xba*I/*vioA*_del_B2_*Bam*HI (Table 5) were used to generate *vioA* flanking fragments A (~500 bp) and B (~800 bp). However, cloning failed of unknown reason.

2.7 Determination of the violacein amount

Quantification of the violacein amount was performed according to a previously published protocol with minor modifications (Blosser and Gray 2000). To measure the violacein amount of a freshly grown culture 2 mL were centrifuged for 2 min at 13,000 rpm and resuspended in 0.4 mL $A._{bidest.}$. After vortexing, the cells were lysed with 0.4 mL 10% sodium dodecyl sulfate and incubated at room temperature (RT) for 5 min. Violacein was quantitatively extracted from this cell lysate by addition of 0.9 mL water-saturated butanol, briefly mixing, and centrifugation at 13,000 rpm for 5 min in a microcentrifuge. 0.5 mL from the upper butanol phase containing the violacein were mixed with 0.5 mL water-saturated butanol, centrifuged again at 13,000 rpm for 5 min. The absorbance was measured at 585 nm in a SmartSpec^{TM}Plus spectrophotometer (Bio-Rad Laboratories GmbH, Munich, Germany). The relative violacein amount was calculated as the ratio of measured absorbance of the butanol extract versus the culture density (OD_{600}). To minimize variations in violacein assays, R2A culture media were prepared with nutrients from the same batch of chemicals.

2.8 *N*-AHL detection using *Agrobacterium tumefaciens* NTL4

NTL4 was used as an indicator strain for the detection of *N*-acyl-L-homoserine lactone (AHL) AI molecules. The biosensor NTL4 (Table 2) carries a *traI-lacZ* promoter fusion (under the control of the AHL-inducible *traI* promoter) on the vector pCF372 and extra copies of *traR* on vector pCF218. In the presence of AHLs, whereby NTL4 detects a wide range of AHL molecules (Steindler and Venturi 2007), the enzyme β-galactosidase is released and converts X-Gal present in the agar into a blue dye, whereas the medium remains white in the absence of AHLs. After growing NTL4 as abovementioned (2.5.1) AT soft screening agar was prepared as follows: The components of the AT medium were prepared separately whereby $A._{bidest.}$ contained 1% (w/v) Eiken agar (Eiken Chemical CO. LTD., Tokyo, Japan). After cooling down to 42 °C precultured *A. tumefaciens* NTL4 was added to a final cell density of 10^7 cells/mL. Medium was poured into Petri dishes and 10 µL culture supernatant was pipetted onto the solidified AT soft agar. Incubation was carried out at 30 °C overnight. 3-oxo-C8-HSL (10^{-8} M, diluted in liquid LB medium from an ethyl acetate stock solution) was used as a positive control.

2.9 Extraction of JAI-1 and CAI-1 autoinducer from bacterial cells

E. coli cells overexpressing either the *jqsA* or the *cqsA* gene in the vector pBBR1MCS-2 (Table 4) were induced by addition of 1 mM IPTG and grown overnight in 1 L LB medium. Cells were removed by centrifugation and the supernatant extracted using ethyl acetate (1:1). After concentration in a rotavapor (Buchi RE 111, Switzerland) the extract was resuspended in methanol. To test the effect of the autoinducer extract on violacein biosynthesis 10 µL extract of a dilution series was used to induce a 1% *Janthinobacterium* sp. HH01 culture. Violacein measurement was performed after 24-48 h. As control, an *E. coli* strain with an empty pBBR1MCS-2 vector was used.

2.10 Determination of the autoinducer amount

The quantitative determination of the AI (JAI-1) amount was performed in a two-step process. At first the samples were collected, frozen and stored at -20 °C until all samples were combined. The second step was to quantificate the AI (JAI-1) amount. Therefore, a freshly incubated HH02 culture was used. Of each sample to be measured an aliquot (100-500 µL) was added to a test tube containing the overnight grown strain HH02. After 24 h of incubation a quantitative measurement of the produced violacein amount was performed and corresponded to the originally existing JAI-1 quantity.

2.11 Complementation assays using *jqsA* deletion strain HH02

For complementation tests investigated strains were grown overnight in 5 mL LB media. 50-250 µL culture supernatant was added to 5 mL R2A media supplemented with ampicillin and 1% growing HH02 culture. Subsequent violacein quantification was performed after incubation at 22 °C for 24-48 h. The strains HH01 and HH02 served as positive and negative controls, respectively.

2.12 Complementation assay using *V. cholerae* Δ*cqsA*

To analyze the enhanced biofilm formation phenotype of *V. cholerae* Δ*cqsA* (Table 2) cells were incubated statically within 24-well plates and biofilm formation was scored after 24 h of growth using a standard crystal violet approach modified from Watnick *et al.* (2001). For analysis of the lowered hemagglutinin/protease (Hap) activity of *V. cholerae* Δ*cqsA* the strain was grown in LB medium until late exponential phase. At that time aliquots were taken from the culture and the Hap activity was measured using azocasein as a substrate (Syngkon *et al.* 2010). In order to determine natural-transformation frequencies in *V. cholerae* Δ*cqsA* cells were tested for chitin-induced natural transformation according to a previously published protocol (Suckow *et al.* 2011; Marvig and Blokesch 2010). Experiments using *V. cholerae* Δ*cqsA* and *V. cholerae* wildtype strain (O1 El Tor) A1552 were performed in the working group of Melanie Blokesch (Laboratory of Molecular Microbiology, Global Health Institute, Ecole Polytechnique Fédérale de Lausanne (EPFL), Lausanne, Switzerland).

2.13 Scanning and transmission electron microscopy

For scanning electron microscopy (SEM) cells were fixed in paraformaldehyde (1%) and glutaraldehyde (0.25%), dehydrated by ascending alcohol series and dried at the critical point with Balzers CPD 030 Critical Point Dryer (BAL-TEC, Schalksmühle, Germany). After coating of the samples with gold using a sputter coater SCD 050 (BAL-TEC), scanning electron microscopical pictures were taken with a LEO 1525 (Zeiss, Jena, Germany). For transmission electron microscopy (TEM) cells were fixed in 2% (v/v) glutaraldehyde for 2 h and 1% (w/v) osmium tetroxide overnight. The embedding was performed according to Spurr (Spurr 1969). Ultrathin sections were prepared with a diamond knife DiATOME ultra 45° (Diatome AG, Biel, Switzerland) on the ultramicrotome Ultracut E (Leica-Reichert-Jung, Nußloch, Germany) and were stained with 5% uranyl acetate and lead citrate. Analysis was performed with the transmission electron microscope Leo 906E (Zeiss, Jena, Germany) equipped with a CCD camera model 794.

2.14 *Caenorhabditis elegans* survival and developmental assays

For all experiments the *C. elegans* N2 strain was used. The nematodes were maintained on nematode growth media (NGM) at 20 °C and fed on the *E. coli* strain OP50 (Stiernagle 2006). Clean eggs and synchronized L4 larvae were obtained by bleaching as described by Stiernagle (2006). HH01 and the violacein-negative mutant HH5-1 (Table 2) were grown on R2A agar plates containing 25 µg/mL kanamycin at 23 °C. 500 µL of a bacterial overnight culture were spread onto 100-mm R2A agar plates and 90 µL onto 60-mm R2A agar plates. Plates were then incubated at 20 °C for three days before assays were performed. *E. coli* were grown overnight in LB medium at 37 °C and spread onto NGM plates. For the *C. elegans* developmental assay clean eggs were transferred onto 100-mm R2A agar plates with either HH01 or the violacein-impaired mutant (HH5-1) as a control onto NGM plates with *E. coli*, the standard laboratory food for *C. elegans*. 6 replicate plates were assayed per bacterial strain. Development was monitored for 4 days at 20 °C. Finally, for the *C. elegans* survival assay 30 L4 larvae were picked and transferred each onto 5 60-mm agar plates per bacterial strain and incubated at 20 °C. Worms were scored as dead or alive by gentle prodding with a platinum wire. Alive worms were transferred onto fresh plates every day. Data were analyzed using Kaplan-Meier statistics and survival curves were compared using the log-rank test. Due to multiple testing a Bonferroni correction of the *p*-value was made leading to a significance level of $p \leq 0.016$. *C. elegans* experiments were performed in the working group of Hinrich Schulenburg in Kiel (Department of Evolutionary Ecology and Genetics, CAU Kiel, Germany).

2.15 HPLC analysis

HPLC analyses were performed in order to elucidate the molecular structure of the proposed JAI-1 autoinducer molecule derived from AI synthase JqsA. High performance liquid chromatography-mass spectrometry-diode array detector (HPLC-ESI-MS) analyses were carried out in the research group of Stephanie Grond in Tübingen (Institute for Organic Chemistry, Eberhard Karls University Tübingen, Germany).

Sample preparation was performed as abovementioned (2.9) using either *E. coli* DH5α cells overexpressing AI synthase *jqsA* or *Janthinobacterium* strain HH01 (wildtype strain), which were both expected to produce the proposed AI molecule JAI-1. As control either *E. coli* DH5α carrying empty pBBR1MCS-2 vector or *jqsA* deletion strain HH02 were used. After the AI extraction using dichloromethane (DCM) samples were transferred to Tübingen, where the chemical analysis was carried out.

The mass spectrometric measurement was performed using ananytical HPLC combined with ESI-MS coupling (*Agilent* 1200 series with diode array detector (DAD), 10mm standard flow cell; mass detector (ESI-MS): *Agilent* LC/MSD Ultra Trap System XCT 6330. Software: *Agilent* LC/MSD ChemStation Rev. B.01.03; *Bruker Daltonik*, 6300 Series Trap Control Version 6.1), HPLC column (*Dr. Maisch* Nucleosil-100 C18, 100x2 mm, 3 µm, with precolumn, flow rate: 0.4 mL/min),gradient program (solvent A: 0.05% aqueous HCOOH; solvent B: 0.05% HCOOH in acetonitrile; gradient: 20% B to 100% B in solvent A in 20 min, 10 min 100% B, 100% B to 20% B in 2 min, 8 min 20% B). Following this, it was investigated whether signals were detected in the synthase samples, which could be assigned to known α-hydroxyketones and their biosynthetic precursors. This was done by extraction of the respective mass trace at positive ionization. The following most likely adducts were taken into account: $[M+H]^+$ = M + 1.0073; $[M+Na]^+$ = M + 22.9892; $[M+K]^+$ = M + 38.9632) as well as a water elimination for the α-hydroxyketone structure ($[M+H-H_2O]^+$ = M - 17.0033). A signal which met these conditions and occured in the synthase sample but was not detected in the negative control was regarded as preliminary finding. The corresponding signal (*m/z* = 242.3 for $[M+H]^+$) was subjected to further analytics applying a high-resolution mass spectrometer (HRMS). HPLC (Thermo Scientific Ultimate 3000 with DAD, analytical measuring cell; mass detector: *Bruker* Maxis 4G. Software: Chromeleon® Version 6.80.; DataAnalysis Version 4.0), HPLC column and program (as abovementioned).

2.16 Computational analysis

The analysis of sequence data was performed using the following software programs and databases:

2.16.1 Programs

Clone Manager Suite 7 (SciCentral Software)

ClustalW2 multiple alignment (http://www.ebi.ac.uk/Tools/msa/clustalw2/)

MEGA version 5.1 (Tamura *et al.* 2011; http://www.megasoftware.net/)

Quality One (Bio-Rad Laboratories, Munich, Germany)

SMART (Simple Modular Architecture Research Tool; Letunic *et al.* 2012; http://smart.embl.de/)

Staden Package (http://staden.sourceforge.net/)

2.16.2 Databases

BRENDA Enzyme database (http://brenda-enzymes.info/)

EMBL-EBI (http://www.ebi.ac.uk/ena/)

ExPASy Bioinformatics Resource Portal (http://expasy.org/)

IMG: the integrated microbial genomes database and comparative analysis system (Markowitz *et al.* 2012; https://img.jgi.doe.gov/cgi-bin/er/main.cgi)

KEGG: Kyoto Encyclopedia of Genes and Genomes (http://www.genome.jp/kegg/)

NCBI database (http://www.ncbi.nlm.nih.gov/)

Pfam (http://pfam.sanger.ac.uk/)

RCSB PDB (Protein Data Bank; http://www.rcsb.org/pdb/home/home.do)

UniProt (Swiss-Prot and TrEMBL; http://www.uniprot.org/)

3 RESULTS

The search for novel bacterial strains of biotechnological interest revealed a yet unknown violacein producing strain. Due to phylogenetic analysis it was named *Janthinobacterium* sp. HH01 (referred to as HH01). The actual habitat of this microbe was a watering pot at the Loki-Schmidt botanical garden of the University of Hamburg. Within this thesis HH01 has been studied particularly regarding its functionality in terms of AI detection systems.

First, analyses focused mainly on its ability to produce violacein. Therefore, one aim of the study was to investigate QS systems or other regulatory factors possibly involved in HH01 violacein production. This was performed primarily in order to exploit the violacein operon as an easily quantifiable feature of a potential AI-responsive reporter strain. Secondly, the strain HH01 was generally studied with respect to certain properties, such as its phylogenetic affiliation, morphology, growth behavior and genetic accessibility. Furthermore, the genome sequence of HH01 was deciphered and analyzed in detail. Finally, the third part of this study was addressed towards its putative defense and resistance mechanisms. Here, a number of remarkable features such as plenty of resistance-mediating genes and gene clusters as well as the presence of NRPS/PKS clusters were discovered. Additionally, the effect of violacein towards the nematode *C. elegans* was examined.

3.1 *Janthinobacterium* sp. HH01 – a potential AHK reporter strain

3.1.1 Investigation of HH01 violacein production

The purple pigmentation of HH01 is likely due to violacein. A dye typically found in purple-pigmented bacteria like *C. violaceum*. In order to verify the presence of violacein a spectrophotometric analysis was performed (2.7). In ethanolic solution the characteristic absorption maximum at 579 nm and minimum at 430 nm was found (Figure 4), indicating the actual presence of the purple pigment violacein.

Several factors influencing the HH01 violacein production such as a correlation between growth state and violacein biosynthesis were observed. Initially, increasing cell number was correlated with an increasing violacein amount until the late exponential growth phase. Despite a declining number of cells, subsequently no decrease but rather a continuous increase of the violacein quantity was observed (Figure 5A).

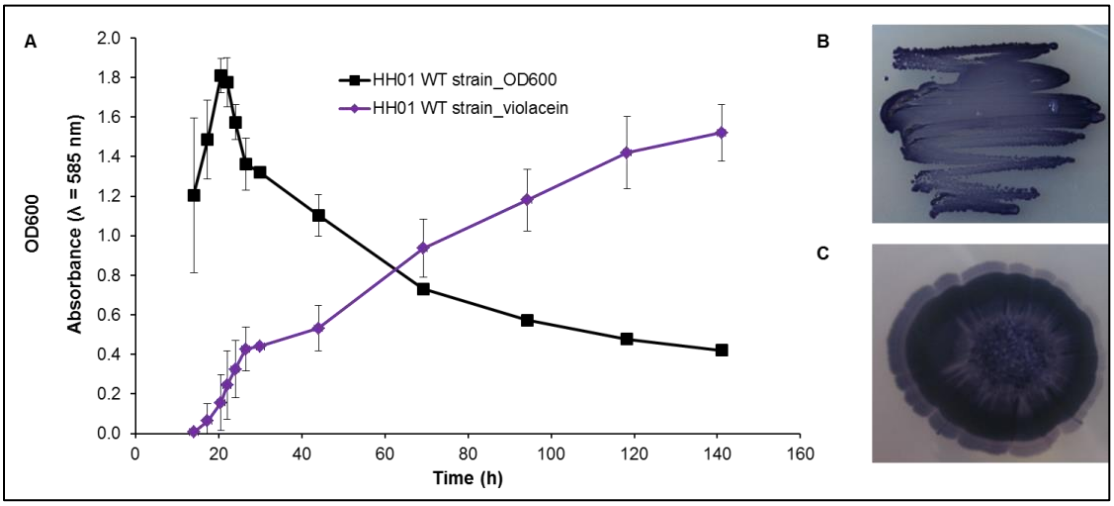

Figure 5. Violacein – growth-dependent synthesis and phenotype. (A) Time-dependent correlation between HH01 growth and violacein amount. The experiment was conducted in triplicate at an incubation temperature of 22 °C under agitation (200 rpm). **(B and C)** HH01 grown on agar plates shows its typical violet phenotype.

Furthermore, the violacein amount was influenced by the presence or absence of ampicillin in the culture medium. Addition of ampicillin led to an increased violacein production (data not shown). Also agitation and thus the amount of available oxygen positively influenced the violacein synthesis (data not shown). Moreover, a correlation between incubation temperature and violacein production was observed. At lower temperatures (between 4 and 10 °C) more violacein was produced (data not shown).

3.1.2 Cloning of the whole violacein operon *vioABCDE*

In order to use the violacein operon as a quantifiable system or to generate a reporter strain, the whole operon and additional sequence regions upstream and downstream (altogether 8,228 bp) were amplified by PCR using primer vio_nst_18843 and vio_nst_27070 (Table 5). By cloning and subcloning constructs pDrive-*vioABCDE* and pBBR1MCS-5-*vioABCDE* (Table 4) were obtained. With these constructs violacein

expression succeeded in the strains *E. coli* DH5α (Figure 6A) and *P. aeruginosa* PAO1 (Figure 6B). The clones were stable over multiple generations without impairment of violacein biosynthesis. This is worth mentioning, since it is known that violacein has an even if to a low extent antibacterial activity.

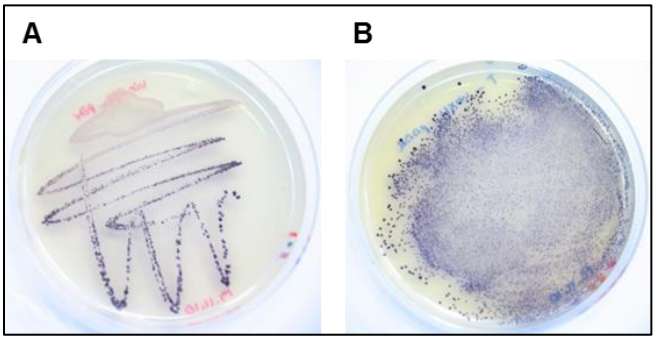

Figure 6. Violacein expression. Agar plates showing *E. coli* DH5α **(A)** and *P. aeruginosa* PAO1 **(B)** clones expressing the *vioABCDE* operon originated from HH01. Violacein production was induced by incubation at low temperatures.

3.1.3 Analysis of the HH01 violacein gene cluster

Since experiments revealed various factors influencing the violacein synthesis in HH01 investigations focused on the violacein gene cluster and surrounding sequence regions. Genes in vicinity to the violacein operon were analyzed by sequence comparison to investigate whether there are genes that may be involved in the regulation. Moreover, a detailed examination of the encoded protein domains was conducted.

The violacein biosynthetic gene cluster of HH01 encompasses about 7.4 kb and is composed of the five genes *vioABCDE* (Jab_2c08810-Jab_2c08850). Notably, upstream and downstream it is surrounded by several genes responsible for signaling and regulation. Sequence analysis and domain search revealed some interesting features (Figure 7, Table 8). Evaluation of the protein domains shown in Figure 7 illustrates the wealth of protein domains that are connected to these mechanisms. These include for instance the GGDEF domain, whose function is to synthesize the intracellular signaling molecule cyclic di-GMP and also receiver domains such as the PAS and Cache domains.

In Table 8 the predicted function of the analyzed genes is listed. The data suggest that among others ORF Jab_2c08730 may be of specific interest since it was annotated as an aerotaxis receptor. This putative function was indicated by blastp analysis and furthermore supported by the presence of corresponding domains such as PAS/PAC and MCP signaling domains and especially a HAMP linker domain. Also noteworthy is the similarity of Jab_2c08750 to the protein RpfG, a part of the *Xanthomonas'* RpfC/RpfG QS system, which depends on the AI DSF. This protein seems to function as a cyclic di-GMP phosphodiesterase response regulator. Moreover, just three ORFs downstream a putative RpfC protein (Jab_2c08780, a two-component sensor histidine kinase) was found.

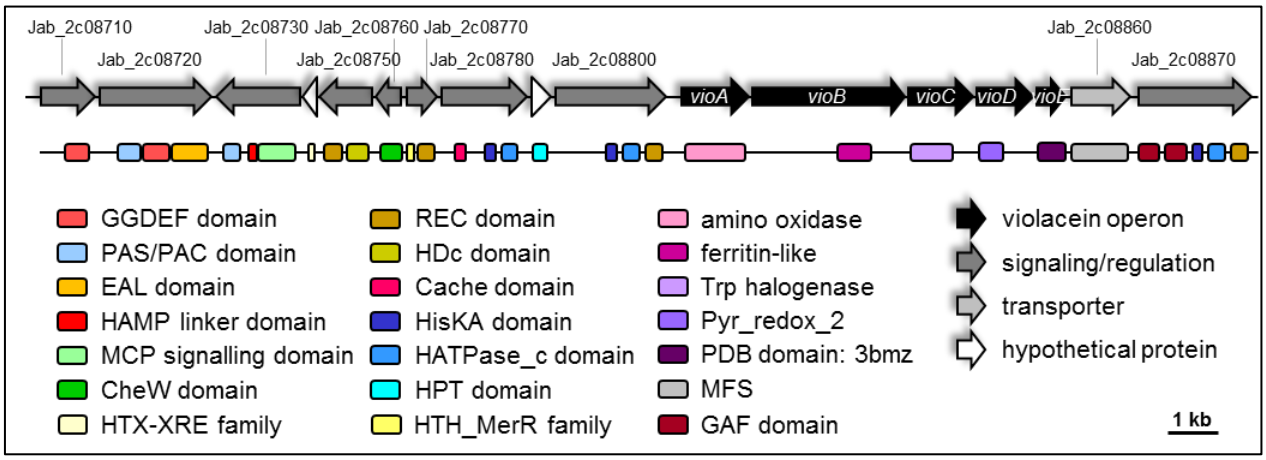

Figure 7. The HH01 violacein gene cluster and surrounding sequence regions. Domain search based on Simple Modular Architecture Research Tool (SMART) (Letunic *et al.* 2012) and InterProScan Sequence Search (http://www.ebi.ac.uk/Tools/pfa/iprscan/). Domain abbreviations: GGDEF domain, diguanylate cyclase domain; PAS, Per (period circadian protein)-Arnt (aryl hydrocarbon receptor nuclear translocator protein)-Sim (single-minded protein) homology region; PAC domain; PAS-associated, C-terminal; EAL domain, diguanylate phosphodiesterase domain; HAMP, Histidine kinases, Adenylyl cyclases, Methyl binding proteins, Phosphatases; MCP, methyl-accepting chemotaxis proteins; CheW, CheW proteins are part of the chemotaxis signaling mechanism in bacteria; HTX, Helix-Turn-Helix; XRE, xenobiotic responsive element; REC domain, receiver domain; HDc domain, phosphohydrolase domain; Cache, Calcium channel and chemotaxis receptor; HisKA domain, Histidine Kinase A domain; HATPase_c domain, Histidine kinase-like ATPases domain; HPT domain, Histidine Phospho Transfer domain; MerR, mercuric resistance operon regulatory protein; Trp, Tryptophan; Pyr_redox, Pyridine nucleotide-disulphide oxidoreductase; PDB domain: 3bmz, violacein biosynthetic enzyme *vioE*; MFS, Major Facilitator Superfamily; GAF domain,.cGMP phosphodiesterase, Adenylyl cyclases, and the bacterial transcription factor FhlA.

Table 8. ORFs upstream and downstream of the violacein operon.

Locus tag	Size (bp)	Putative protein function[1)2)]
ORFs upstream the violacein operon		
Jab_2c08710	1,056	diguanylate cyclase (*J.* sp. PAMC 25724, E 8e-71)[1)]
Jab_2c08720	2,208	diguanylate cyclase/phosphodiesterase with PAS/PAC sensor (*Sideroxydans lithotrophicus* ES-1, E 0.0)[1)]
Jab_2c08730	1,656	aerotaxis receptor Aer (*Herbaspirillium* sp. GW103, E 7e-156)[1)]
Jab_2c08740	273	hypothetical protein[1)]
Jab_2c08750	1,056	putative cyclic di-GMP phosphodiesterase response regulator, related to RpfG (*Xanthomonas campestris* pv. campestris str. 8004, E 2e-95)[2)]
Jab_2c08760	498	chemotaxis protein CheW (*J.* sp. PAMC 25724, E 2e-49)[1)]
Jab_2c08770	606	response regulator receiver protein (*Herbaspirillium frisingense* GSF30, E 5e-91)[1)]
Jab_2c08780	1,689	two-component sensor histidine kinase (*J.* sp. PAMC 25724, E 3e-174)[1)]; related to sensory/regulatory protein RpfC (*Xanthomonas campestris* pv. campestris, E 3e-34)[2)]
Jab_2c08790	363	hypothetical protein[1)]
Jab_2c08800	2,184	multi-sensor hybrid histidine kinase (*Oxalobacteraceae* bacterium IMCC9480, E 0.0)[1),3)]
ORFs downstream the violacein operon		
Jab_2c08860	1,161	putative sugar transporter (*J. lividum*, E 0.0)
Jab_2c08870	2,229	histidine kinase with GAF domain and response regulator receiver (*Herbaspirillium* sp. YR522, E 1e-129)[1),4)]

Remarks: Annotation based on **1)** NCBI blastp and **2)** Swiss-Prot, cited: 2012-12-24.; **3)** partly related to virulence sensor protein BvgS (*Bordetella pertussis*, 5e-64), sensory/regulatory protein RpfC (*Xanthomonas campestris*, E 1e-61), aerobic respiration control sensor protein ArcB (*Shigella flexneri*, E 3e-59), autoinducer 2 sensor kinase/phosphatase LuxQ (*Vibrio cholerae* O1, E 3e-58)**2)**, **4)** partly related to autoinducer 2 sensor kinase/phosphatase LuxQ (*Vibrio cholerae* serotype O1, E 8e-39), virulence sensor protein BvgS (*Bordetella pertussis*, 2e-36), sensory/regulatory protein RpfC (*Xanthomonas campestris*, E 9e-34)**2)**. E, E-value.

3.1.4 Generation of a transposon mutant library

After identification of several factors influencing violacein biosynthesis, this phenomenon was studied using mutant clones impaired in violacein production. Since it was shown that HH01 is genetically accessible via electroporation (2.6.9.3) a transposon mutagenesis library was constructed (2.6.11) to obtain violacein negative mutant clones of HH01. Finally, ~8,500 mutant clones were generated and of these about 50 white or cream colored clones were selected (Figure 8A). Of about 35 of these clones the transposon insertion site in the HH01 genome was determined by PCR (2.6.8) (Figure 8B) and following sequence analysis (2.6.10.1). To generate the PCR amplicons a special PCR approach was used, enabling a PCR with only one primer (2.6.11) (Ducey and Dyer 2002). The size of the obtained PCR amplicons ranged between 600 bp and 3 kb (Figure 8B). The fragments were sequenced and the insertion sites determined. Thus, the received transposon mutant clones with impaired violacein formation were classified into five groups: transposon insertion in regulatory genes; in tryptophan biosynthesis genes; in other structural genes; in RNA or RNA-related genes; and in hypothetical genes (Table 9). A detailed overview on the exact insertion sites of selected mutant clones is depicted in Figure 9.

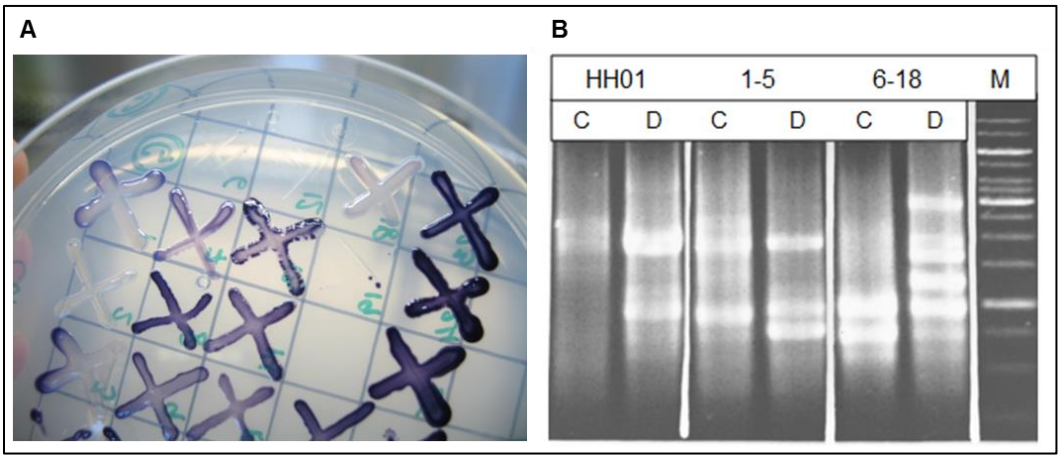

Figure 8. Clones obtained by transposon mutagenesis. (A) Transposon mutant strains on a representative R2A agar plate. The phenotype of the obtained mutant clones ranged from deep purple to colorless. **(B)** Representative agarose gel picture of *Janthinobacterium* sp. HH01 WT strain as control (HH01) and two selected transposon mutant strains (1-5; 6-18) after PCR analysis and DNA electrophoresis (2.6.8; 2.6.5). As template for PCR amplification either colony material directly taken from the agar plate (C) or DNA (D) was used. M, marker (Gene Ruler™ 1 kb DNA Ladder).

It turned out that concerning the group of regulatory genes, two independent sequence loci were affected by transposon insertion: Jab_1c01080 plus Jab_1c01090 and Jab_2c00660 plus Jab_2c00670 (Figure 9A). Three transposon mutants (✶[1], ✶[2], ✶[3]) were located in ORF Jab_1c01080 (a two-component transcriptional regulator) and two (✶[4], ✶[5]) in ORF Jab_1c01090 (a two-component sensor histidine kinase). Also in Jab_2c00660 (a signal transduction histidine kinase) two transposon mutants were located (✶[6], ✶[7]). While the first affected gene cluster (Jab_1c01080/Jab_1c01090) is adjacent to a conserved gene arrangement encoding, *i.a.*, enzymes for the synthesis of glutamate and histidine, the latter is located in a less conserved sequence region.

Moreover, in almost each gene known to be involved in the tryptophan biosynthesis a transposon insertion was found (Figure 9B). In HH01 the genes required for tryptophan biosynthesis are not organized in a single tryptophan operon, but are rather distributed as smaller clusters and single genes throughout the genome.

Among others, three transposon mutants were located in the tryptophan biosynthesis gene *trpB* (✶[8], ✶[9], ✶[10]) and two in *trpD* (✶[11], ✶[12]). The discovery of so many mutants in tryptophan synthesis genes can be explained by the fact that tryptophan is the essential substrate of the violacein biosynthesis. These mutants were in general white and did not turn purple after extended incubation time.

In addition, different structural genes were affected, whereby a large number was found particularly in a gene encoding the Lon protease. Also, transposon insertions in specific RNAs or RNA-related genes were found including 23S rRNA, ATP-dependent RNA helicase RhlE and ribonuclease E. Finally, at least four transposon insertions were discovered in genes with unclear function, these were grouped as hypothetical genes.

Surprisingly, no transposon mutant clone with an insertion in the violacein operon was detected. A detailed description of all mutants, that were either completely white or showed only a weak violet coloration is given in Table 9.

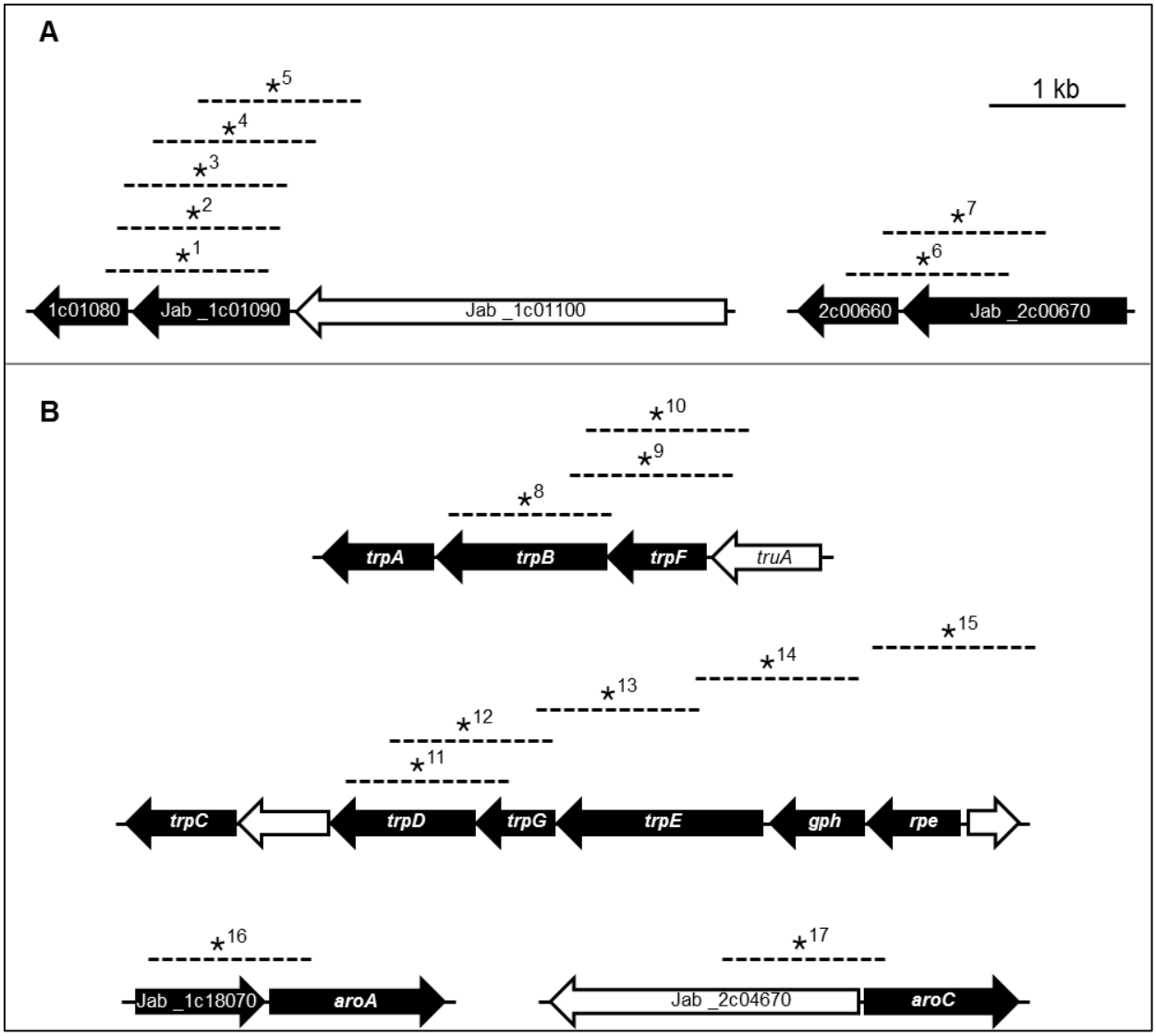

Figure 9. Schematic representation of the exact transposon insertion site of selected transposon mutants of HH01. (A) Transposon insertion in regulatory genes. Jab_1c01080, two-component transcriptional regulator; Jab_1c01090, two-component sensor histidine kinase; Jab_1c01100, SNF2/helicase domain-containing protein; Jab_2c00660, signal transduction histidine kinase; Jab_2c00670, sensor histidine kinase. **(B)** Transposon insertion in tryptophan biosynthesis genes. *trpA*, tryptophan synthase alpha subunit TrpA (Jab_2c21690); *trpB*, tryptophan synthase beta subunit TrpB (Jab_2c21700); *trpF*, N-(5'-phosphoribosyl) anthranilate isomerase TrpF (Jab_2c21710); *truA*, tRNA pseudouridine synthase A (Jab_2c21720); *trpC*, indole-3-glycerol phosphate synthase TrpC (Jab_1c10150); *trpD*, anthranilate phosphoribosyltransferase TrpD (Jab_1c10170); *trpG*, anthranilate synthase component II (Jab_1c10180); *trpE*, anthranilate synthase component I (Jab_1c10190); *gph*, phosphoglycolate phosphatase (Jab_1c10200); *rpe*, ribulose-phosphate 3-epimerase Rpe (Jab_1c10210); Jab_1c18070, prephenate dehydrogenase; *aroA*, 3-phosphoshikimate 1-carboxyvinyltransferase AroA (Jab_1c18080), Jab_2c04670, hypothetical protein; *aroC*, chorismate synthase AroC (Jab_2c04680). Asterisks and dashed lines indicate the transposon position. ✶[1] to ✶[17] are explained in detail in Table 9.

Table 9. Transposon mutants obtained in genes and pathways associated with the violacein biosynthesis pathway in the strain HH01.

Tagging in Figure 9	Locus Tag	Gene	Function assigned	Mutant designation	Phenotype[1)]
Group 1: Transposon insertion in regulatory genes					
✶[1], ✶[2], ✶[3]	Jab_1c01080	-	two-component transcriptional regulator	3-4, 2-20, G1-9	b
✶[4], ✶[5]	Jab_1c01090	-	two-component sensor histidine kinase	2-15, 2-17	b
✶[6], ✶[7]	Jab_2c00660	-	signal transduction histidine kinase	3-6, 3-15	d
Group 2: Transposon insertion in tryptophan biosynthesis genes					
✶[8], ✶[9], ✶[10]	Jab_2c21700	*trpB*	tryptophan synthase beta subunit TrpB	G2-26, R5, 1-5	b
✶[11], ✶[12]	Jab_1c10170	*trpD*	anthranilate phosphoribosyl-transferase TrpD	G2-14, 3-12	b
✶[13]	Jab_1c10180	*trpG*	anthranilate synthase component II	G-16	b
✶[14]	Jab_1c10190	*trpE*	anthranilate synthase component I	3-5	b
✶[15]	Jab_1c10210	*rpe*	ribulose-phosphatate 3-epimerase Rpe	3-13	b
✶[16]	Jab_1c18080	*aroA*	3-phosphoshikimate 1-carboxyvinyltransferase AroA	G1-5	b
✶[17]	Jab_2c04680	*aroC*	chorismate synthase AroC	5-1	a
Group 3: Transposon insertion in other structural genes					
	Jab_2c19980	*mdh*	malate dehydrogenase Mdh	K-6	b
	Jab_2c31090	*sucC*	succinyl-CoA ligase, beta subunit	G-1	d
	Jab_1c11630	*def1*	peptide deformylase 1	G1-21	d
	Jab_2c05900	*lon*	lon protease Lon	5-2, G-2, G-3, G-5, G2-5, G2-13	b/d
Group 4: Transposon insertion in RNA or RNA-related genes					
	Jab_1c24130	*rhlE*	ATP-dependent RNA helicase RhlE	2-16	b
	Jab_2c24230	*rne*	ribonuclease E	G1-16, K-1	b
	Jab_2c33810	*rrlE*	23S rRNA	3-24	b
Group 5: Transposon insertion in hypothetical genes					
	Jab_2c22730	-	hypothetical protein	2-26, 3-11	d
	Jab_2c24980	-	hypothetical protein	1-16	
	Jab_1c04320	-	hypothetical protein	2-3	
	Jab_2c34540	-	hypothetical protein	5-6	a

[1)] **a**, white colonies that were weakly purple after 4-5 days; **b**, white no purple visible after several days; **c**, slightly purple after 2 days; **d**, white but purple halo.

3.1.5 Analysis of HH01 regarding quorum sensing-related genes

Analysis of the HH01 genome sequence showed no common AHL-based QS system of Gram-negative bacteria. Using blastp analysis neither AI-1 synthase nor receptor proteins, which are known from *V. fischeri* (LuxI/R), *P. aeruginosa* (LasI/R, RhlI/R) or *C. violaceum* (CviI/R), were detected. This result was also confirmed by experiments using the AHL-reporter strain *A. tumefaciens* NTL4 enabling the detection of AI molecules such as 3-oxo-C8-HSL (2.8). These tests did not indicate the presence of any AHL molecules in the range of detectable amounts.

Furthermore, no LuxS-like synthase belonging to the AI-2 QS system was found. Also the search for LuxQ-like proteins, the cognate sensor, revealed no corresponding homologue. Nevertheless, this analysis revealed numerous signal transduction histidine kinases and related proteins because of their characteristic protein domains; although no real LuxQ homologue was found. However, some regulatory proteins with a more or less evident similarity to LuxQ were detected (*Vibrio* autoinducer-2 sensor kinase/phosphatase LuxQ), RpfC (*Xanthomonas* sensory/regulatory protein RpfC) and BvgS (*Bordetella* virulence sensor protein BvgS).

Particularly, one gene arrangement in the HH01 genome sequence showed a pronounced similarity to a corresponding region in *Xanthomonas campestris* pv. campestris (strain 8004). In HH01 these are the ORFs Jab_2c30820 (ZP_21466292), a multi-sensor hybrid histidine kinase and Jab_2c30830 (ZP_21466293), the adjacent response regulator. The first mentioned revealed a similarity to *Xanthomonas'* RpfC and the latter to *Xanthomonas'* RpfG. About 24 genes upstream another notable gene arrangement (Jab_2c30520 - Jab_2c30560) was identified. In this region two response regulators and putative signal transduction histidine kinases are located around a gene that was annotated as 7-keto-8-aminopelargonate synthetase. Such enzymes are known to be involved in the synthesis of a special class of AIs that are found, *i.a.*, in *Vibrio cholerae* and *Legionella pneumophila*. Although no respective similarity was discovered, this kind of putative AI synthase was found in the HH01 genome at least once in the sequence region from locus tag Jab_2c24330 to Jab_2c24350. The here identified QS system revealed similarity to corresponding *V. cholerae* and *L. pneumophila* systems.

Table 10. Evaluation of possible QS systems in HH01, further *Janthinobacterium* strains and *C. violaceum*.

QS system, with corresponding AI synthase and receptor	*J.* sp. HH01	*J.* sp. GC3	*J. lividum* PAMC 25724	*J.* sp. Marseille	*C. violaceum* ATCC 12472
***N*-AHL**	**-**	**(+)**	**-**	**-**	**+**
LuxI/LasI/RhlI/TraI	-	(+)[1)]	-	-	-
LuxR/LasR/RhlR/TraR	-	(+)[1)]	-	-	+
CviI	-	((+))[2)]	-	-	+
CviR	-	((+))[2)]	-	-	+
LuxM	-	-	-	-	-
LuxN	~[3)]	~[3)]	~[3)]	~[3)]	~[3)]
AI-2	**-**	**-**	**-**	**-**	**-**
LuxS	-	-	-	-	-
LuxQ	~[4)]	~[4)]	~[4)]	~[4)]	~[4)]
LuxP	-	-	-	-	-
α-HK (CAI-1, JAI-1, LAI-1)	**+**	**+**	**+**	**-**	**-**
CqsA/JqsA/LqsA	+	+	+	-	-
CqsS/JqsS/LqsS	~[5)]/+/~[5)]	~[5)]/+/~[5)]	~[5)]/+/~[5)]	~[5)]/-/~[5)]	~[5)]/-/~[5)]
JqsR/LqsR	+	+	+	-	-

-, no similar protein detected; +, similar protein detected; (+), weak similarity observed; ((+)), very weak similarity observed. [1)] Weak or [2)] very weak similarity to an AI-1 synthase (AHL synthase) and LuxR family transcriptional regulator, found (*e.g.*, among others in *Burkholderia* sp.); [3)] very weak similarity (<E-30); [4)] weak similarity (up to E-67); [5)] very weak similarity (<E-30). Proteins used for blastp analysis: **LuxI** (*Allivibrio fischeri*, GenBank: AAP22376.1), **LasI** (*Pseudomonas aeruginosa* PAO1, NCBI Ref. Seq.: NP_250123.1), **RhlI** (*P. aeruginosa* PAO1, AAC44037.1), **TraI** (*Agrobacterium tumefaciens*, AAZ50473.1), **LuxR** (*Allivibrio fischeri*, AAQ90222.1), **LasR** (*P. aeruginosa* PAO1, AAA25874.1), **RhlR** (*P. aeruginosa* PAO1, AAC44036.1), **TraR** (*A. tumefaciens*, AAZ50597.1), **CviI** (*C. violaceum* ATCC 12472, AAQ61751.1), **CviR** (*C. violaceum* ATCC 12472, AAQ61750.1), **LuxM** (*Allivibrio fischeri*, BAF43686.1; *Vibrio harveyi* AAC36807.1), **LuxN** (*Allivibrio fischeri*, BAF43687.1), **LuxS** (*E. coli* str. K-12 substr. MG1655, AAC75734.1; *Salmonella enterica*, AAR88507.1; *V. cholerae* INDRE 91/1, EEY49941.1; *V. harveyi*, ZP_06175640.1), **LuxQ** (*V. harveyi*, AAA20838.1; *V. cholerae* INDRE 91/1, EEY49480.1), **LuxP** (*V. harveyi*, AAA20837.1; *V. cholerae*, INDRE 91/1, EEY49479.1), **CqsA** (*V. cholerae*, NCBI Ref. Seq. ZP_18028386.1; *V. harveyi*, ZP_01984783.1), **JqsA** (*J.* sp. HH01, ELX10346.1), **LqsA** (*L. pneumophila*, YP_096734.1), **CqsS** (*V. cholerae*, NCBI Ref. Seq. ZP_18028385.1), **JqsS** (*J.* sp. HH01, ELX10347.1), **LqsS** (*L. pneumophila*, YP_096737.1), **JqsR** (*J.* sp. HH01, ELX10348.1), **LqsR** (*L. pneumophila*, YP_096735.1).

Perhaps the most interesting AI synthase gene of HH01, its adjacent sensor kinase/phosphatase and receptor protein are homologous to the AI systems *of V. cholerae* and *L. pneumophila*. In *V. cholerae* the genes are named *cqsA*/*cqsS* and in *L. pneumophila lqsA*/*lqsS*/*lqsR*. Following, the HH01 system was termed *jqsA*/*jqsS*/*jqsR*. JqsA (Jab_2c24330), which displayed 63% similarity (45% aa identity) over the entire protein length to the homologous synthase CqsA of *V. cholerae* O1 biovar El Tor strain N16961 (accession no. NP_232914) and 62% similarity (41% identity) to the homologous LqsA of *L. pneumophila* subsp. *pneumophila* (YP_006506863). However, despite this sequence similarity Figure 10 represents a divergent gene order whereby the AI synthase (*jqsA*/*lqsA*/*cqsA*) and the sensor kinase/phosphatase genes (*jqsS*/*lqsS*/*cqsS*) are located in a varying orientation. Another difference concerns the gene encoding receptor protein JqsR/LqsR. This exists as individual gene only in HH01 and *L. pneumophila* (*jqsR* and *lqsR*). In contrast, in *V. cholerae* the corresponding sequence information is assembled in the gene *cqsS*, and the resulting protein comprises respective functional domains.

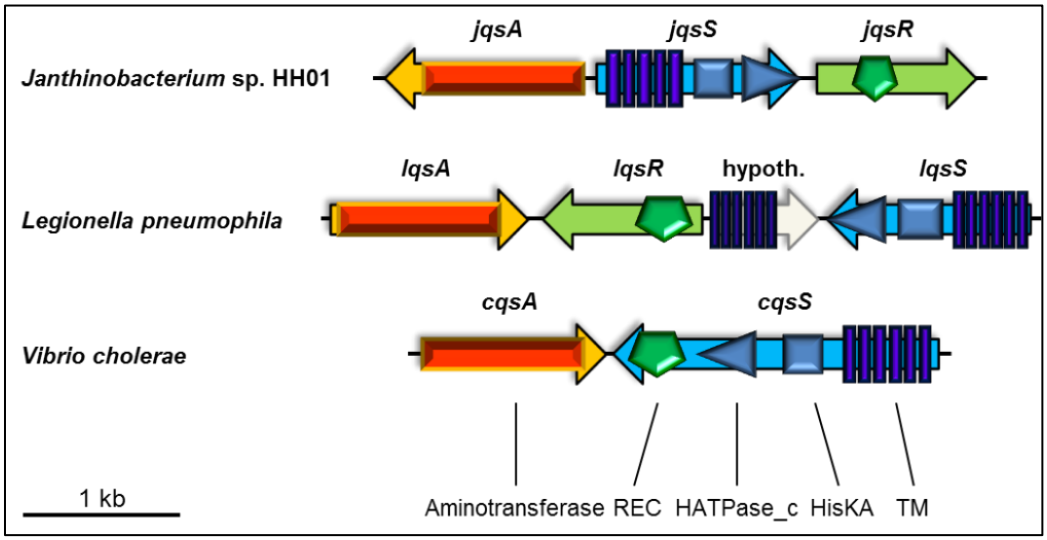

Figure 10. Alignment of homologous gene clusters of HH01 (*jqs*), *L. pneumophila* (*lqs*) and *V. cholerae* (*cqs*). Domain search based on SMART Sequence Search (Letunic *et al.* 2012). Analyzed proteins: autoinducer synthase JqsA, ZP_21465658; autoinducer sensor kinase/phosphatase JqsS, ZP_21465659; response regulator JqsR, ZP_21465660; LqsA, YP_006506863; LqsR, YP_006506864; LqsS, YP_006506866; CqsA, NP_232914; CqsS, NP_232913. Abbreviations: aminotransferase, aminotransferase class I and II (pyridoxal phosphate binding); REC, response regulator receiver domain; HATPase_c, Histidine kinase-like ATPases; HisKA, Histidine Kinase A (phosphoacceptor) domain; TM, transmembrane domains.

The mentioned *cqsA*/*jqsA*/*lqsA*-dependent QS system that is well-known in *Vibrio* and *Legionella* strains (Tiaden and Hilbi 2012; Ng *et al.* 2011) can also be found in other organisms including the recently sequenced *Janthinobacterium* strains GC3 and PAMC 25724. In both an identical gene order was detected and also in less related strains such as *Duganella zoogloeoides* ATCC 25935, *Cupriavidus taiwanensis* LMG19424 and *Collimonas fungivorans* Ter331. A graphical overview of various bacterial strains with a similar QS system is depicted in Figure 11.

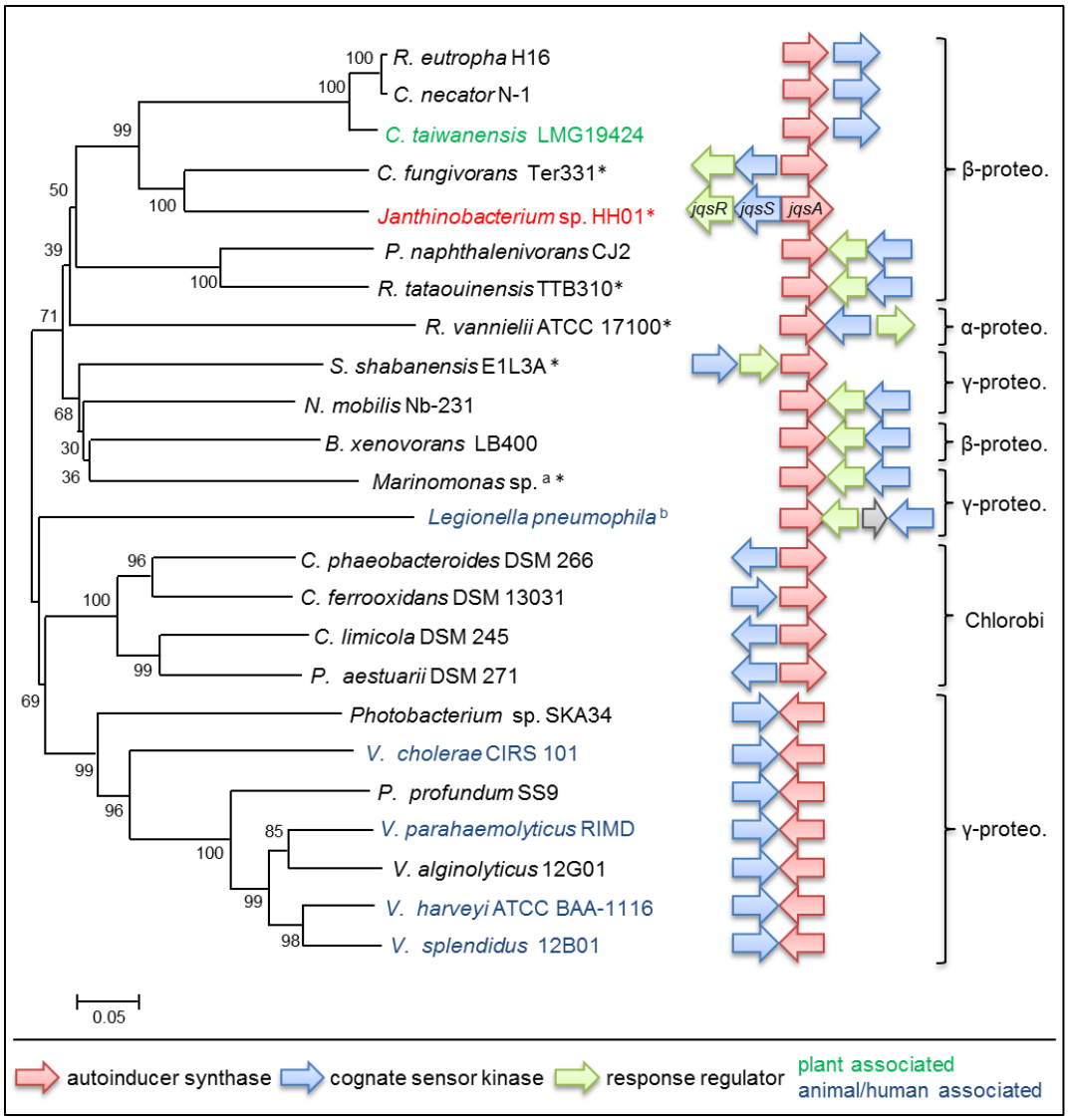

Figure 11. Phylogenetic analysis of *jqs*-like AI systems. The neighbor-joining phylogenetic analysis was performed using MEGA5 (Tamura *et al*. 2011) and was based on search for homologous amino acid sequences (cited: September 2012) in the IMG genome database (Markowitz *et al.* 2012) comparing JqsA-like AI synthases. Accession number of included aa sequences of the corresponding AI synthase are listed in Table 16.

3.1.6 Influence of *jqsA*, *cqsA*, and *lqsA* on violacein biosynthesis

The *jqs* system was not yet described in the genus *Janthinobacterium*. Therefore, it was analyzed which gene(s) might be regulated by this QS system. To investigate this, the HH01 AI synthase gene *jqsA* was cloned into the vector pBBR1MCS-2 (Table 4) and transformed in HH01 (2.6.9.3). As a control empty pBBR1MCS-2 vector (also electroporated in HH01) was used. After incubation at 22 °C for two days, the violacein amount of both samples was measured. Here, the *jqsA* sample yielded 60% more violacein compared to control (Figure 12B). Thus, it can be concluded that overexpression of *jqsA* resulted in an increased violacein amount, suggesting that the violacein biosynthesis of HH01 is somehow regulated by the identified *jqs* system.

To confirm this result the *jqsA* gene and the homologous *V. cholerae* AI synthase gene $cqsA_{Vch}$, were exogenously added after heterologous expression in *E. coli* and extraction with ethyl acetate (2.9). For this *E. coli jqsA* (pBBR1MCS-2-*jqsA*) and $cqsA_{Vch}$ (pBBR1MCS-2-$cqsA_{Vch}$) expression strains were grown overnight and supernatants containing the respective AI synthase (JAI-1 and CAI-1) were extracted. Diluted JAI-1 and CAI-1-extracts were added to freshly growing HH01 cultures. The violacein amount was measured after two days (2.7). As a negative control the empty pBBR1MCS-2 vector was used. Here, no increase of the violacein production was induced (Figure 12A, control). In contrast, in the presence of JAI-1 and CAI-1 the violacein amount was ~3-fold and ~1.5-fold higher than control, respectively (Figure 12A).

According to the *jqsA* overexpression in HH01 (Figure 12B) the related *V. cholerae* ($cqsA_{Vch}$), *V. harveyi* ($cqsA_{Vh}$) and *L. pneumophila* (*lqsA*) AI synthase genes were likewise overexpressed in HH01. Subsequent violacein measurement revealed a ~40-50% higher violacein amount in HH01 cultures overexpressing these AI synthase genes than in the control strain (Figure 12B). This observation suggests that the genes resembling to the HH01 AI synthase *jqsA* (*i.e.*, $cqsA_{Vch}$, $cqsA_{Vh}$, *lqsA*) had a similar effect on violacein production in HH01.

To make sure that this effect was reproducible, entire tests were repeated at least three to five times. All tests gave a similar result.

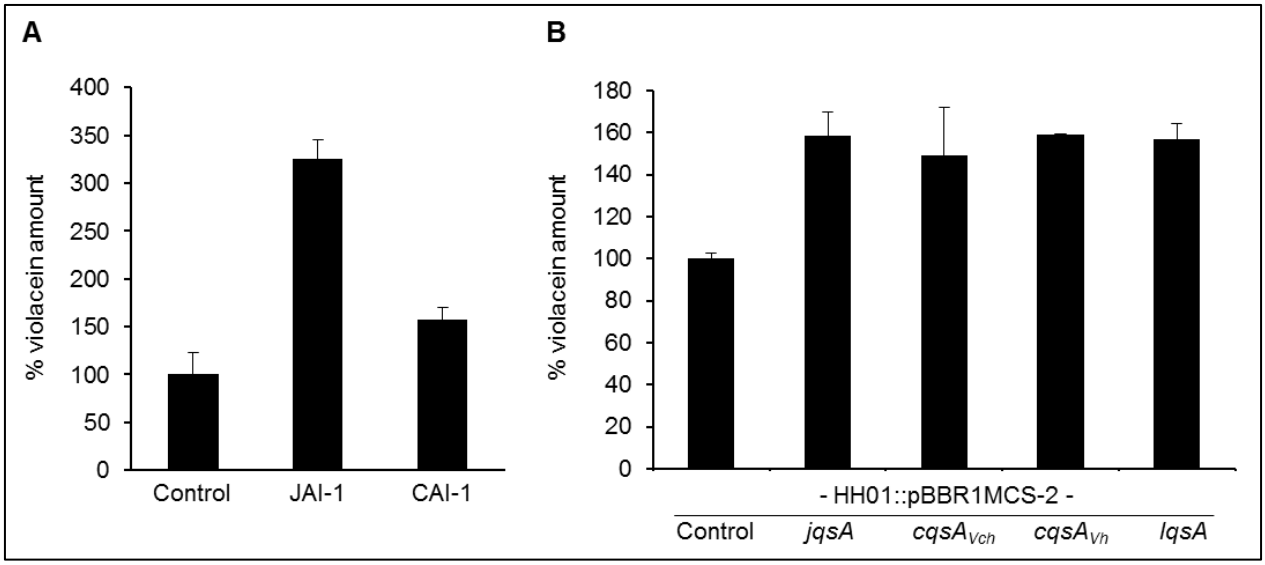

Figure 12. Effect of exogenously added or internally expressed AIs on the violacein production of HH01. (A) Determination of the HH01 violacein amount (expressed as %) after addition of supernatants of *E. coli-jqsA* (= JAI-1) and *cqsA* (= CAI-1) expression strains to freshly growing HH01 cultures. As a control the empty pBBR1MCS-2 vector was used. **(B)** Correlation between the overexpressed autoinducer synthase genes *jqsA*, $cqsA_{Vch}$, $cqsA_{Vh}$ and *lqsA* (on the vector pBBR1MCS-2) and the HH01 violacein production. As a control an empty pBBR1MCS-2 vector grown in HH01 was used. All values are shown relative to control. Bars represent the mean±SD. The number of samples was n=3.

3.1.7 Generation of a *jqsA* deletion strain

In order to confirm the correlation between the HH01 AI synthase gene *jqsA* and its influence on the violacein biosynthesis, a *jqsA* deletion strain, named HH02 (Table 2), was constructed using a homologous recombination approach (2.6.12) as shown in Figure 13A. For the construction upstream and downstream regions of the *jqsA* gene were amplified by PCR (designated as A and B) and linked with a Gm^R cassette. After selection and reselection all promising white or pale rose clones were analyzed by PCR. To confirm correct deletion of the *jqsA* gene three PCRs using different primer pairs were performed (PCR 1, PCR 2, PCR 3; Figure 13B).

To verify insertion of the A-Gm^R-B-cassette primers were located up- and down-stream of *jqsA* (PCR 1; Figure 13B). Here, in the WT sample (C1) the expected PCR amplicon of 2,200 bp was obtained and in samples bearing the A-Gm^R-B-cassette a

band shift was achieved (2,900 bp; S1 and S2). As negative controls PCR 2 and 3 were conducted. For PCR 2 primers (rev1 and outB) were located in a non-affected sequence region. Thus, WT and mutant samples revealed a similar band of 2,019 bp (PCR 2; Figure 13B). For PCR 3 one primer (rev2) was complementary to the affected region, whereas the other one (outA) was located upstream. Hereby, only in the WT sample (C1) as expected a band of 1,859 bp was detected (PCR 3; Figure 13B). In conclusion, the correctness of the *jqsA* deletion strain HH02 was verified by PCR. Additionally, this was also confirmed by sequencing (data not shown). Moreover, both HH01 WT and *jqsA* deletion strain HH02 showed significant differences concerning violacein production. In comparison to the HH01 WT samples HH02 flasks presented a reduced violacein phenotype, confirming the effect of the *jqsA* gene on violacein production (Figure 13C).

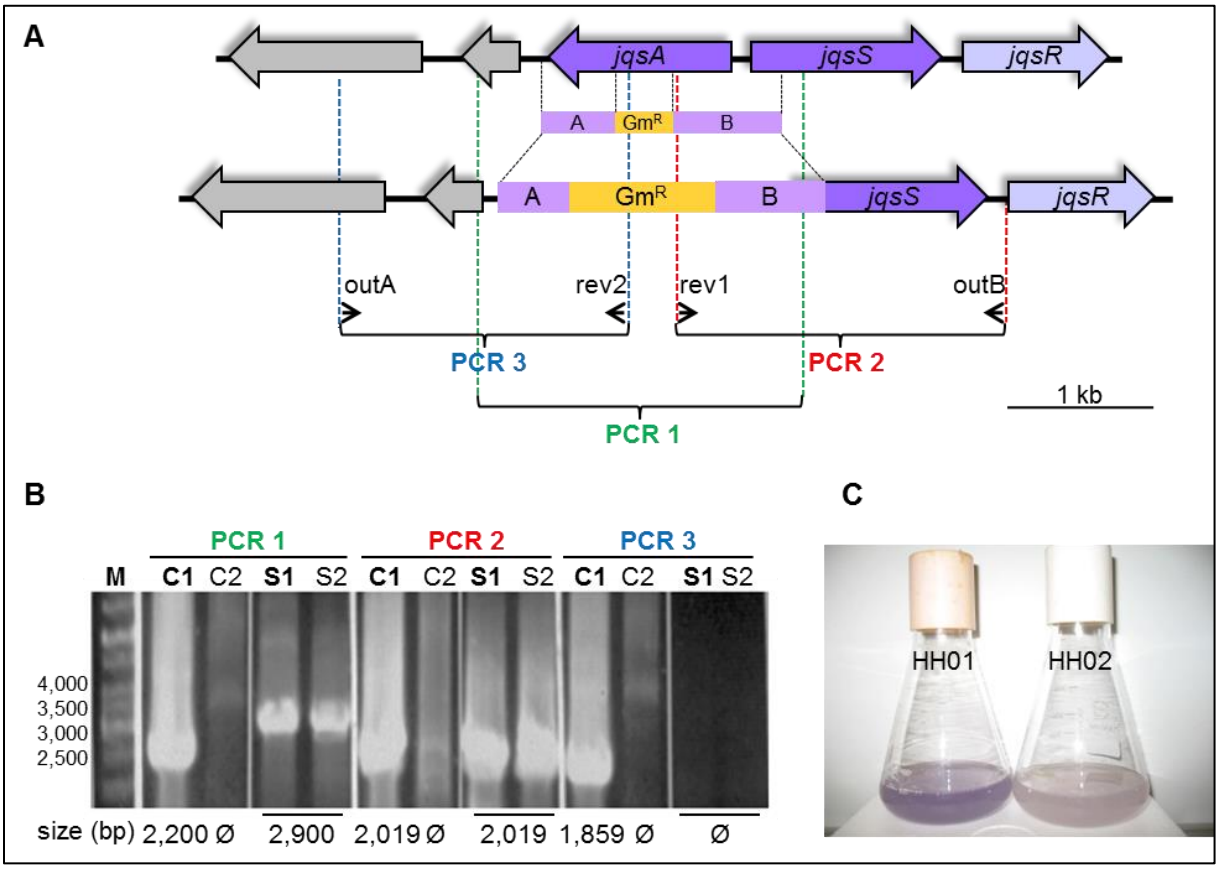

Figure 13. Design and validation of *jqsA* deletion strain HH02. (A) Schematic representation of the cloning procedure and location of the primers used for PCR verification. **(B)** PCR analysis confirming gene deletion of the obtained clones. C1, control 1 (HH01); C2, control 2 (negative PCR control); S1, later designated clone HH02; S2, another violacein-impaired clone; M, marker (Gene Ruler™ 1 kb DNA Ladder). **(C)** Flasks containing cultured violacein producing WT strain HH01 and violacein-impaired *jqsA* deletion strain HH02. Gm^R, gentamicin resistance.

Evaluation of time-dependent *jqsA* synthesis

For proof-of-concept *jqsA* deletion strain HH02 was generated (i) as a reporter strain to quantify autoinducer amount and (ii) to show a cell density-dependent *jqsA* expression in WT HH01. For this purpose, samples of a freshly growing HH01 culture were taken at four time points and each added to a growing culture of reporter strain HH02. After two-days of incubation the violacein amount was measured. It turned out that proceeding incubation time and accordingly an increased number of cells correlated with an increased quantity of the proposed AI JAI-1 (Figure 14). This suggests on one side, that the gene *jqsA* functions as AI synthase since a time-dependent increase in quantity is a typical characteristic of AI molecules. On the other side, it confirms that the *jqsA* deletion strain HH02 used herein as reporter system is an applicable tool for AI quantification.

In summary, experiments confirmed *jqsA* expression in a cell density-dependent manner. Time-dependent increase of the cell number over time resulted in accumulation of the proposed HH01 AI JAI-1.

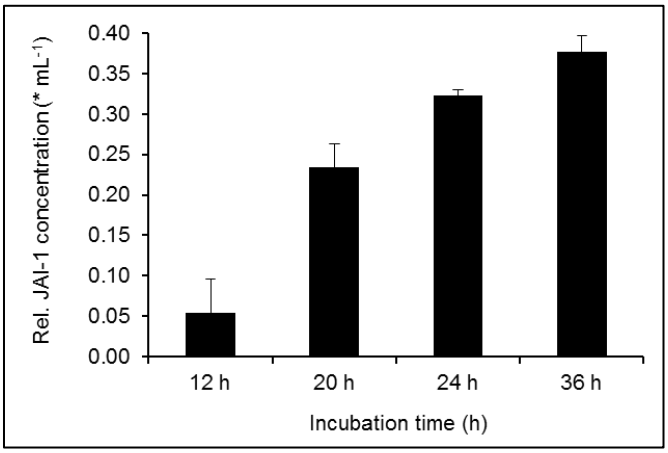

Figure 14. Time-dependent evaluation of *jqsA* synthesis. JAI-1quantity was determined by measurement of the violacein amount at four consecutive time points - after 12 h, 20 h, 24 h and 36 h. For this measurement the *jqsA* deletion strain HH02 was used as reporter strain. Bars represent the mean±SD. The number of samples for each experiment was n=3.

3.1.8 Evaluation of HH01 and HH02 regarding growth behavior and violacein production

To further analyze the effect of the *jqsA* deletion strain HH02, additional experiments were performed. Therefore, HH01 and HH02 were grown in liquid culture media for 24 h under permanent agitation at 22 °C. Samples were taken at various time points (*i.e.*, 12 h, 16h, 20 h, 22 h, 24 h; Figure 15A). Subsequent measurements of the produced AI molecule JAI-1 (2.10) and the violacein amount (2.7) revealed a lower JAI-1 production rate (Figure 15B) and a strongly decreased violacein expression (Figure 15C) for HH02 in comparison to HH01.

Although, a *jqsA* deletion strain was not expected to produce AI, JAI-1 quantification in HH02 showed over the entire analysis marginal measured values, suggesting a certain background concentration (HH02; Figure 15B). In contrast, the JAI-1 amount in HH01 WT cells increased after 20 h suggesting that AI production probably starts at this point in time (HH01; Figure 15B). However, regarding the violacein quantification for HH02 no violacein was detectable within an incubation period of 24 h. In contrast, for HH01 significant violacein production was observed with a continuous increase starting at about 20 h after inoculation (Figure 15C). This suggests a direct correlation between AI concentration and thereupon produced violacein in HH01 WT cells.

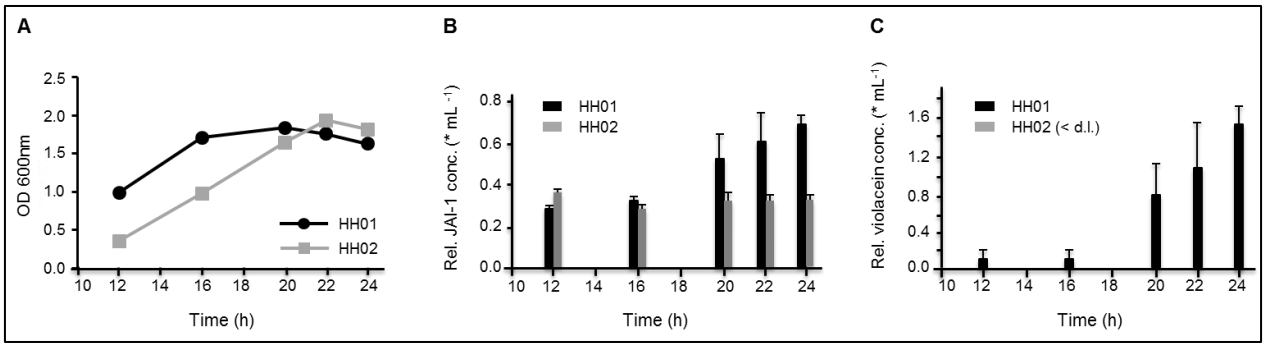

Figure 15. Effect of strain HH02 on the JAI-1 synthesis and violacein production. (A) Growth curves of HH01 and HH02 recorded over a period of 24 hours. Black curve, HH01 WT strain; grey curve, *jqsA* deletion strain HH02. **(B)** Determination of synthesized JAI-1 by HH01 (black) and HH02 (grey). **(C)** Determination of the violacein amount produced by HH01 (black) and HH02 (under detection limit). For HH02 no violacein was detectable during the time measured. Bars represent the mean±SD. The number of samples for each experiment was n≥3. <d.l., below detection limit.

In order to analyze growth and violacein production over a longer period (*i.e.*, 140 h), HH01 and HH02 were grown in liquid R2A culture media. Samples were taken at different time points and the violacein amount was quantified (Figure 16). Both strains grew well over a time period of 20-30 h and reached stationary phase after about 24 h. The cell numbers decreased after about 30 h sharply. During exponential growth phase both strains had doubling times of approximately 1.1 h. Whereas for both (HH01 and HH02) a similar growth curve was obtained (Figure 16A) the violacein amount strongly increased for HH01 and was barely detectable in HH02 (Figure 16B).

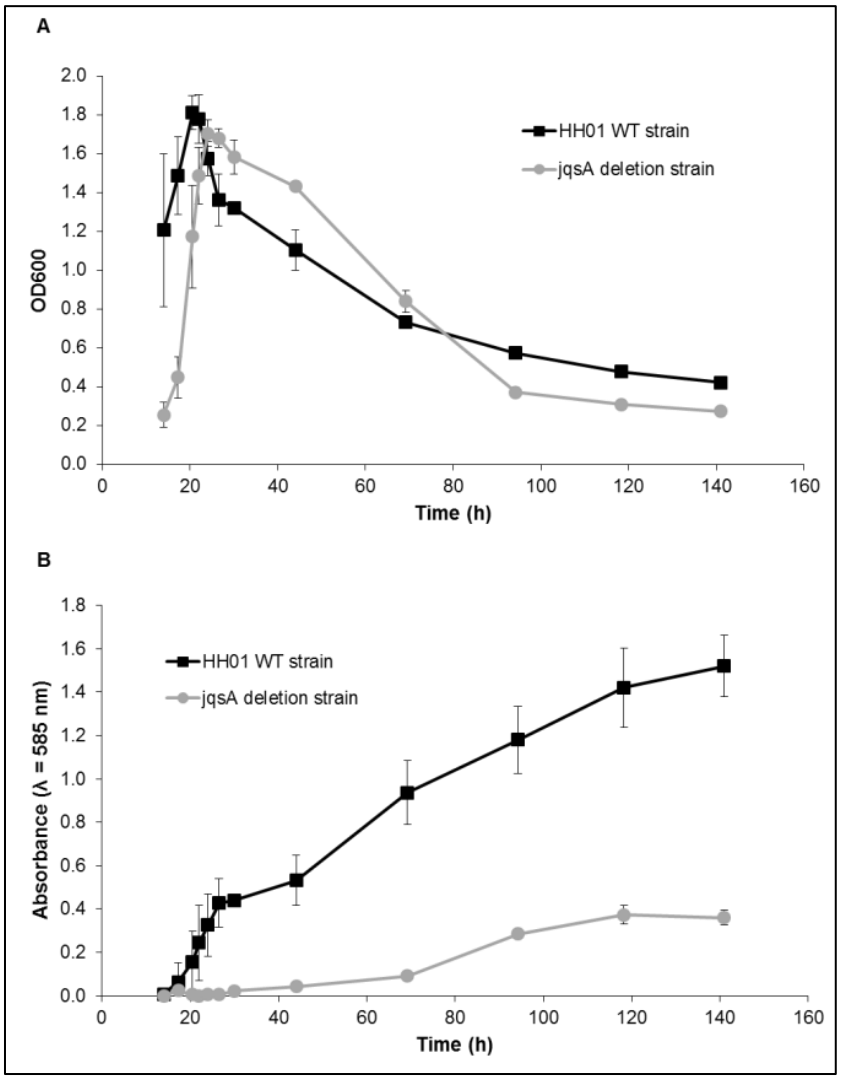

Figure 16. Growth and violacein production in HH01 and HH02 grown on R2A medium. (A) Growth curves of HH01 WT and *jqsA* deletion strain HH02 recorded at 22 °C under permanent agitation for a period of 140 h. **(B)** Measurement of the violacein amount in HH01 and HH02. Bars represent the mean±SD. The number of samples for each experiment was n=3.

Interestingly, but for an unknown reason a continuous increase of the violacein amount was observed in HH01 WT cells - during observation beyond a period > 24 h - despite a clearly decreasing cell number. In addition, it should be noted that in spite of the immense effect on both AI production (Figure 15B) and violacein biosynthesis (Figure 15C and Figure 16B) no impact on growth rate was observed. In conclusion, this indicates that QS is not an essential process within the cell, and QS mutants or deletion strains such as HH02 did not display growth defects in general.

3.1.9 Analysis of *jqsA* deletion strain HH02 concerning AI sensitivity

To verify the function of the *jqsA* gene complementation test were performed. For this the *jqsA* deletion strain HH02 was complemented with the AI synthase genes *jqsA*, *cqsA* and *lqsA* cloned into the vector pBBR1MCS-2 and each construct was transferred in HH02 cells as host (Figure 17A).

In these tests HH02 produced in general less than 80% violacein compared to the HH01 WT strain (Figure 17A). In contrast, HH02 carrying extra copies of the *jqsA*, *cqsA* and *lqsA* genes partly restored violacein production. However, in these test no HH01 WT levels were reached with respect to violacein production (Figure 17A). After two days of incubation, measurement of the violacein amount of each construct (gene *jqsA*, *cqsA* and *lqsA*; each on pBBR1MCS-2) revealed a ~30% - 70% rescue of the phenotype compared to HH01. These findings suggest that the observed phenotype of a decreased violacein amount of the the *jqsA* deletion strain HH02 was partially restored upon expression of the *jqsA* gene under the control of its native promoter and by expression of the homologous genes *cqsA* and *lqsA.* However, it may not be excluded that other effects are involved in the violacein biosynthesis as well as that the presence of multiple copies of the *cqsA*, *jqsA* and *lqsA* genes in the used pBBR1MCS-2 vector influenced the levels of violacein production.

In addition, partial complementation was achieved with assumed orthologous genes of other microorganisms, *i.e.*, the related *Ralstonia eutropha* H16 and *Cupriavidus necator* N-1 (Figure 17B). In contrast to Figure 17A no cloning was performed, but supernatants of the appropriate cultures were added. Again, for each sample an increased violacein amount was detected in comparison to deletion strain HH02. This

indicates complementation. Interestingly, the violacein amount of *R. eutropha* H16 did not differ from HH01 WT suggesting a complete rescue of the analyzed phenotype.

Based on these results it can be concluded, that *jqsA* is a functional homologue of *Vibrio cqsA* and the *Legionella lqsA*. Furthermore, tests suggest that the sensor/regulator system appears to detect the AI produced by these bacteria and others tested in this study. In summary, these experiments suggest that the *jqsA* deletion mutant HH02 might serve as a reporter strain for such CAI- or LAI-like AI molecules.

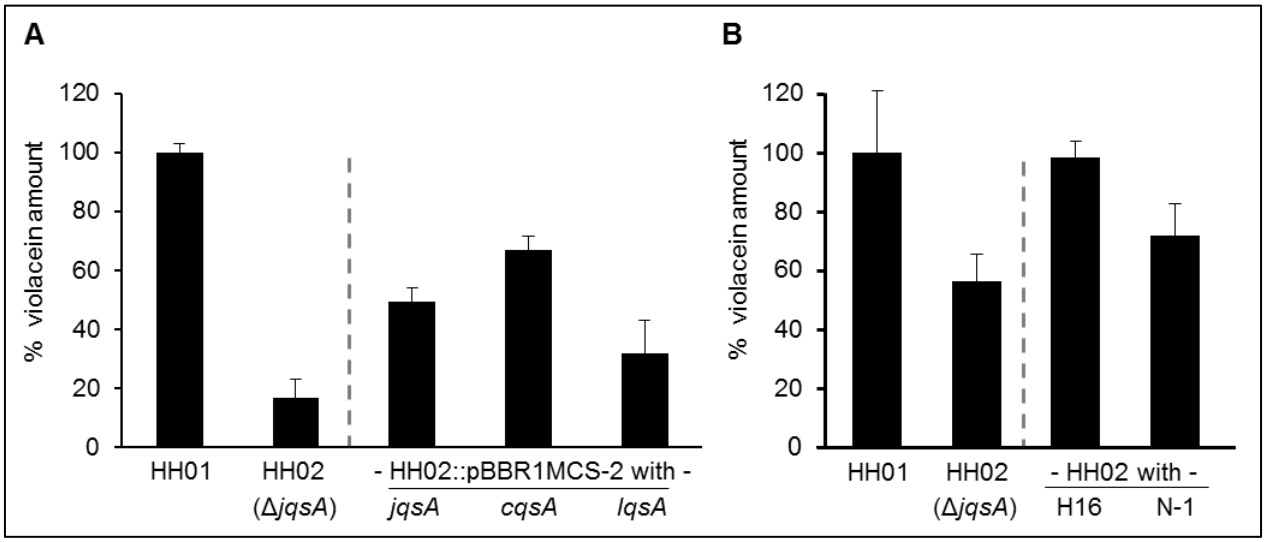

Figure 17. Complementation assays with HH02. (A) The violacein amount was determined in HH02 samples overexpressing AI synthase genes *jqsA*, *cqsA* and *lqsA*. HH01 or HH02 Δ*jqsA* served as controls. **(B)** Supernatants (100 µL) of bacterial cultures expressing a *jqsA*-homologous gene were added to growing cultures of HH02. The violacein amount was determined 48 h after addition. H16, *R. eutropha* H16 and N-1, *Cupriavidus necator* N-1. Bars represent the mean±SD. The number of samples was n=3.

3.1.10 Analysis of the *jqsA* effect on *V. cholerae* and *V. harveyi cqsA*-deficient mutants

Since it was shown that the deletion strain HH02 was restored by its own autoinducer synthase gene *jqsA* and homologous genes derived from other species, it was also investigated whether the gene *jqsA* can *vice versa* complement Δ*cqsA* mutant strains.

Therefore three different phenotypes of the *V. cholerae* O1 El Tor *cqsA* mutant (A1552Δ*cqsA*; Table 2) were investigated concerning biofilm formation,

hemagglutinin/protease (Hap) activity and natural transformation (Figure 18). This experiment was performed in cooperation with the working group of Melanie Blokesch (Laboratory of Molecular Microbiology, Global Health Institute, Ecole Polytechnique Fédérale de Lausanne (EPFL), Lausanne, Switzerland).

The *V. cholerae* Δ*cqsA* strain is characterized by an enhanced biofilm formation (2.12) that is due to a lack of repression in Δ*cqsA* (Figure 18A). While this lack was restored to WT level (*V. cholerae* A1552 WT strain) by the appropriate *cqsA* gene (lanes 7 and 8) it was not by the *jqsA* gene (lanes 5 and 6). As controls either *V. cholerae* A1552 WT cells expressing the empty vector pBBR1MCS-2 (A1552/pBBR1MCS-2; lanes 1 and 2) or Δ*cqsA* mutant cells expressing the pBBR1MCS-2 vector (Δ*cqsA*/pBBR1MCS-2; lanes 3 and 4) were used.

Similar results were obtained for the two other considered phenotypes, which are both positively regulated by the *V. cholerae* autoinducer CAI-1 in the tested strain. Whereas expression of the *V. cholerae*-inherent *cqsA* gene rescued lowered hemagglutinin/protease (Hap) activity (Figure 18B) and natural transformation (Figure 18C) of the *V. cholerae* Δ*cqsA* strain (lanes 7 plus 8 in Figure 18B and lane 8 in Figure 18C, respectively), no rescue was achieved by the *jqsA* gene (lanes 5 plus 6 in Figure 18B and lane 6 in Figure 18C, respectively). As controls served the *V. cholerae* A1552WT strain, which showed no lowered phenotype (lanes 1 plus 2 in Figure 18B and lane 2 in Figure 18C, respectively), and the Δ*cqsA* mutant strain expressing pBBR1MCS-2 vector representing a lowered phenotype that was not rescued (lanes 3 plus 4 in Figure 18B and lane 4 in Figure 18C, respectively).

To summarize the results, the HH01 *jqsA* gene was obviously not able to complement the *V. cholerae* O1 El Tor *cqsA* mutant (A1552Δ*cqsA*) with respect to any of the above described phenotypes.

Beside the test in *V. cholerae* a similar experiment was performed in a *cqsA*-deficient *V. harveyi* mutant (Table 2) by the working group of Kirsten Jung (Center for integrated Protein Science Munich (CiPSM) at the Department of Biology I, Microbiology, LMU Munich, Martinsried, Germany). They also showed that this mutant could not be rescued by *jqsA* gene expression (data not shown).

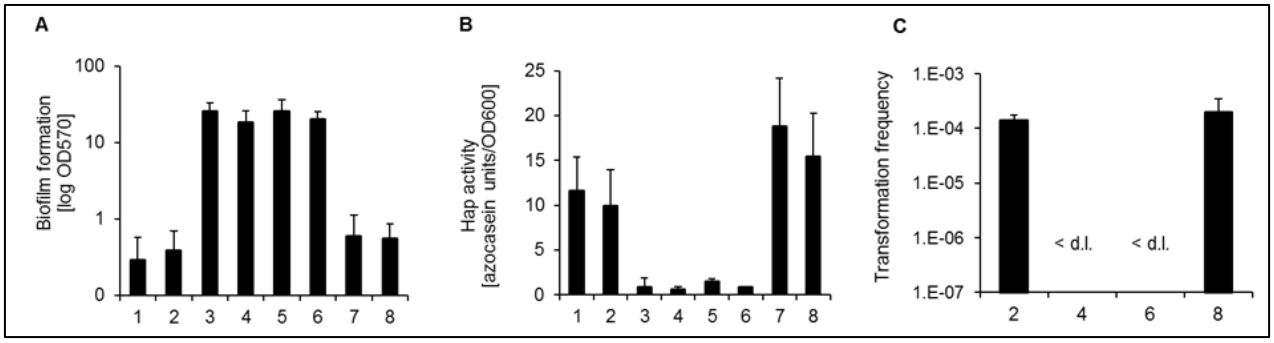

Figure 18. Complementation assay of HH01 *jqsA* in a *V. cholerae* Δ*cqsA* mutant. (A) Analysis of enhanced biofilm formation accomplished by a *V. cholerae* Δ*cqsA* strain. The average of two independent biological replicates with triplicate samples is shown. The error bar indicates the standard deviation. **(B)** Examination of a lowered hemagglutinin/protease (Hap) activity presented by the Δ*cqsA* strain. The haemagglutinin/protease (Hap) activity was measured using azocasein as a substrate. The average of two independent biological replicates with triplicate samples is shown. **(C)** Investigation of the natural transformation in a *V. cholerae* Δ*cqsA* mutant. Average transformation frequencies of two independent experiments are indicated on the Y-axis. <d.l., below detection limit.

V. cholerae strains tested in all panels: lanes 1 and 2, A1552/pBBR1MCS-2 (WT with vector as control); lanes 3 and 4, Δ*cqsA*/pBBR1MCS-2 (mutant with vector as control); lanes 5 and 6, Δ*cqsA*/pBBR1MCS2-*jqsA* (mutant with plasmid containing *jqsA* gene); lanes 7 and 8, Δ*cqsA*/pBBR1MCS2-*cqsA* (mutant with plasmid containing *cqsA* gene). Strains were grown in the absence (odd numbers) or presence (even numbers) of 1 mM IPTG.

3.1.11 Summary of chapter 3.1

The major findings of this chapter were:

- HH01 was identified as a further violacein-producing strain
- HH01 is genetically accessible
- Transposon mutagenesis succeeded to interrupt violacein biosynthesis
- HH01 encodes a QS system homologous to *V. cholerae* and *L. pneumophila*, designated as JqsA/JqsS/JqsR
- The autoinducer synthase genes *jqsA*, *cqsA* and *lqsA* affect violacein biosynthesis in HH01
- Deletion of the AI synthase *jqsA* led to impaired violacein biosynthesis
- The *jqsA* deletion strain HH02 allowed interspecies autoinducer detection

3.2 *Janthinobacterium* sp. HH01 – general characteristics and genome analysis

After chapter 3.1 addressed HH01 as potential AI biosensor, chapters 3.2 and 3.3 are concerned with an analysis of its genome sequence, some general characteristics and investigations regarding secondary metabolite production and defense mechanisms.

3.2.1 Morphology and physiology

Morphology

HH01 is a Gram-negative rod-shaped bacterium. To learn more about the HH01 morphology scanning electron microscope (SEM) and transmission electron microscope (TEM) images were taken (Figure 19). Thereby the rod-shaped form was confirmed and the size estimated to 2-4 µm. Moreover, small remarkable pimple-like structures coating the whole cell surface were detected. They probably function as vesicles, *e.g.*, for the export of secondary metabolites. To exclude the occurrence of a preparation artifact, images were prepared several times. Furthermore as a control images from a closely related strain (*Duganella violaceinigra*) were taken in the same way. In contrast to HH01, *D. violaceinigra* showed no vesicle covering on its cell surface. Based on these results, it can be assumed that the vesicles are a HH01 inherent property.

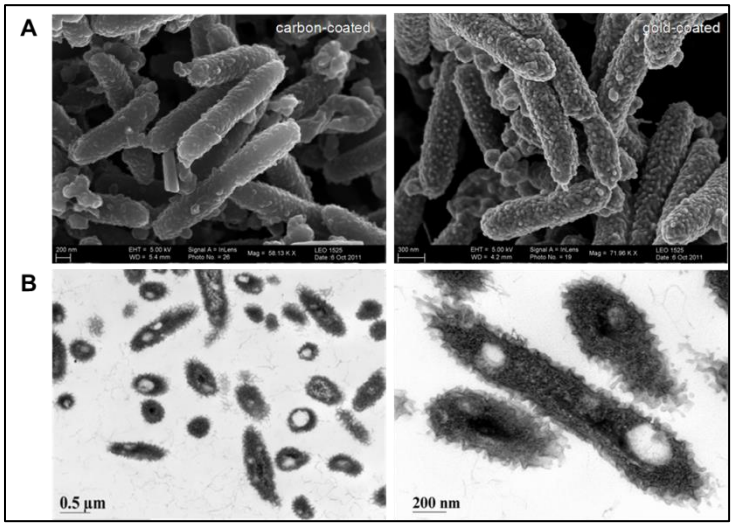

Figure 19. SEM and TEM images of HH01. (A) SEM, left: carbon-coated; right: gold-coated **(B)** TEM.

Physiology

HH01 grew within a wide temperature range between 4 and 28 °C. As a typical feature of the genus *Janthinobacterium* HH01 showed no ability to grow at a temperature of 37 °C. At standard conditions (liquid R2A medium, agitation, 22 °C) a doubling time of about 70 min was found. Interestingly, HH01 was not only able to grow at 4 °C, it also reached the highest optical density at this temperature (Figure 20A).

Analysis of further temperature ranges (17 °C, 22 °C, 28 °C; Figure 20B) revealed a correlation between increased temperature and early cell death as well as a short stationary growth phase.

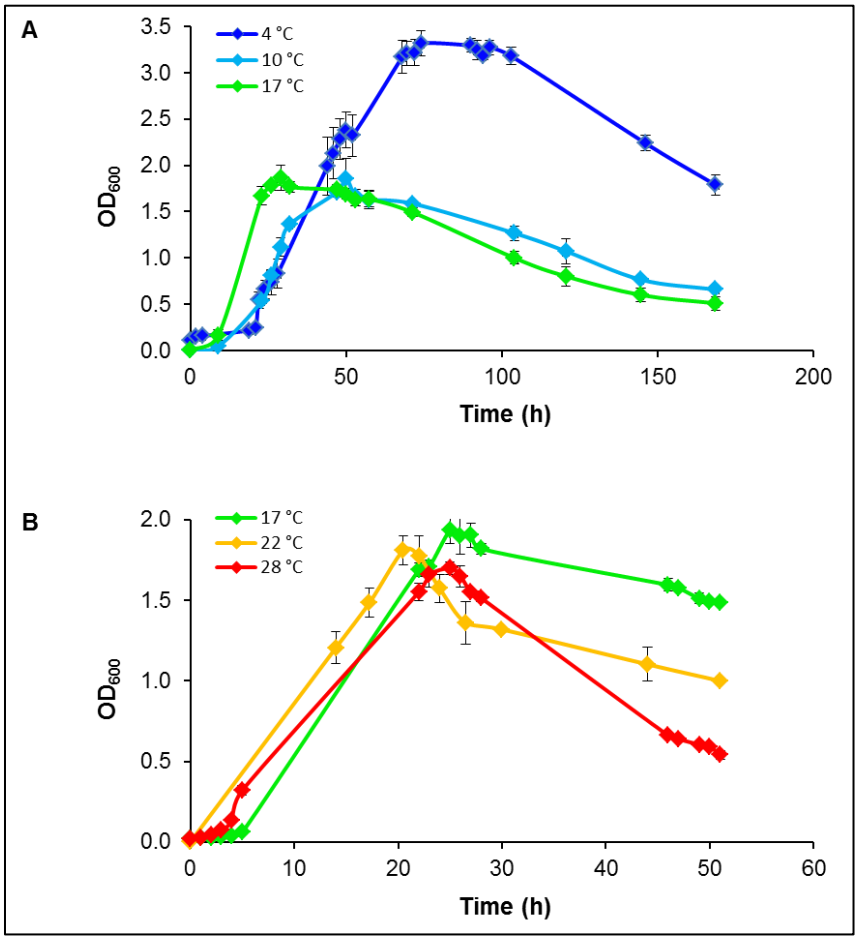

Figure 20. HH01 growth curves. (A) Growth curves recorded at temperatures of 4 °C, 10 °C and 17 °C. **(B)** Growth curves recorded at temperatures of 17 °C, 22 °C and 28 °C. Measurements were performed at least in triplicate.

3.2.2 Phylogenetic analysis

For the phylogenetic classification of HH01 the common 16S rRNA gene sequence analysis (Clarridge 2004; Woese 1987) was applied using primers 616V and 1492R. At the time of determination (May 2012) *Janthinobacterium lividum* strain EU275366 was found as the closest relative of HH01 (Figure 21). For that reason, HH01 was grouped within the genus *Janthinobacterium*.

Accordingly, HH01 is affiliated with the Oxalobacteraceae, which are grouped within the order Burkholderiales of the β-proteobacteria. Thus HH01 expands the group of violacein-producing janthinobacterial strains. Even though, the ability to produce violacein is neither a typical property within the family Oxalobacteraceae nor of the genus *Janthinobacterium* (as mentioned above).

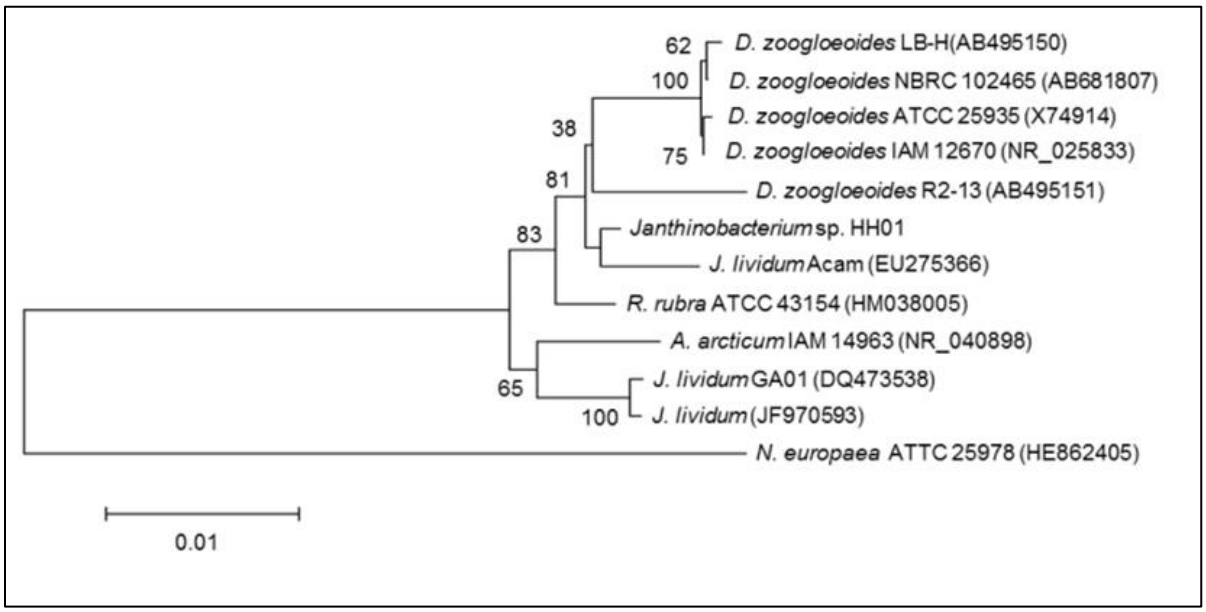

Figure 21. Phylogenetic analysis. The 16S rRNA-based tree was established using the neighbor-joining algorithm in MEGA5 (Tamura *et al.* 2011). Topology was evaluated by bootstrap analysis (1000 repeats, with *N. europaea* as outgroup). Exclusively sequences longer than 1,450 nucleotides of representatives of the next relative (≥97% similarity) species were included. Numbers in parenthesis indicate the corresponding GenBank entries. Bootstrap values are presented as percentages at the branch points. The scale bar represents the expected number of changes per nucleotide position.

3.2.3 Genome sequencing

The sequencing process of the strain *Janthinobacterium* sp. HH01 comprised several steps. Initially, genomic DNA of HH01 was used to generate 454-shotgun and paired-end libraries. By sequencing, more than 1.2 million total reads were obtained and *de novo* assembled to 1,957 contigs. In addition, a large insert fosmid library consisting of about 2,400 fosmid clones was constructed. Ends of 672 recombinant fosmids were sequenced followed by PCR-based techniques to close the remaining gaps. Thereby both genomic DNA and fosmid clones were used as templates. Since gaps still existed, DNA of selected fosmids was used to create small insert plasmid libraries followed by sequencing. The whole-genome shotgun project was deposited at DDBJ/EMBL/ GenBank AMWD00000000; http://www.ncbi.nlm.nih.gov/nuccore/444792393) in two contigs. The entire sequencing project was accomplished in collaboration with the Göttingen Genomics Laboratory (Institute of Microbiology and Genetics, Georg-August University Göttingen, Germany).

The genome sequence revealed a single chromosome with a size of 7,105,753 bp and a mean GC content of 64.19%. A total of 6,098 ORFs was determined. These comprise almost 5,980 protein coding genes and about 104 RNA genes. Currently a function could be assigned to 4,877 protein coding genes, which corresponds to a share of about 80%. The number of RNA genes in turn is composed as follows, there are 20 rRNA genes (6 5S rRNAs, 7 16S rRNAs and 5 23S rRNAs), 84 tRNA genes and 12 are classified as other RNA genes.

After publication of the genome sequence of *Janthinobacterium* sp. Marseille in 2007 (Audic *et al*. 2007; genome size: 4.11 Mbp, GC content: 54.23%), the sequences of HH01 (Poehlein *et al*. 2013), *J.* sp. GC3 (Franklin *et al*. 2012; 6.26 Mbp, 65.54%) and *J. lividum* PAMC 25724 (Kim *et al.* 2012; 4.98 Mbp, 60.60%) followed in 2012. In comparison to the other so far published genome sequences, the HH01 genome size of 7.10 Mbp is remarkably larger and its GC content slightly higher, apart from *J*. sp. GC3, where the base ratio is similar. A detailed tabular comparison of the most important genome features of these microorganisms can be found in Table 11.

Table 11. General genome features of HH01 in comparison to related strains. Data are taken from IMG (Markowitz *et al*. 2012); cited: 2012-01-06.

Characteristics	*J.* sp. HH01	*J.* sp. GC3	*J. lividum* PAMC 25724	*J.* sp. Marseille	*C. violaceum* ATCC 12472
Size (bp)	7,105,753	6,265,216	4,984,958	4,110,251	4,751,080
GC content (%)	64.19	65.54	60.60	54.23	64.83
rRNA genes	20	15	21	6	25
tRNA genes	84	81	80	46	98
Other RNA genes	12	13	13	14	20
Protein coding genes	5,980	5,352	4,432	3,697	4,407
… with function prediction	4,877	4,365	3,538	2,510	2,687
Violacein production	+	-	-	-	+
Temperature range	psychro-tolerant	psychrophil	mesophile	mesophile	mesophile
Temperature optimum	10-17 °C	n.s.	25 °C	30 °C	25 °C
Habitat	Biofilm, aquatic	n.s.	n.s.	Fresh water, host	Fresh water, host, soil, aquatic
Reference	Poehlein *et al*. 2013	Franklin *et al*. 2012	Kim *et al*. 2012	Audic *et al.* 2007	de Vasconcelos *et al.* 2003

+, existent; -, not existent; n.s., not specified.

Following images represent a graphical comparison of HH01 with the other *Janthinobacterium* genomes. In Figure 22 a graphical circular map is shown, giving an overview of the HH01 genome in comparison to other closely related species. The map is based on investigation of the aa identity by blastp analysis.

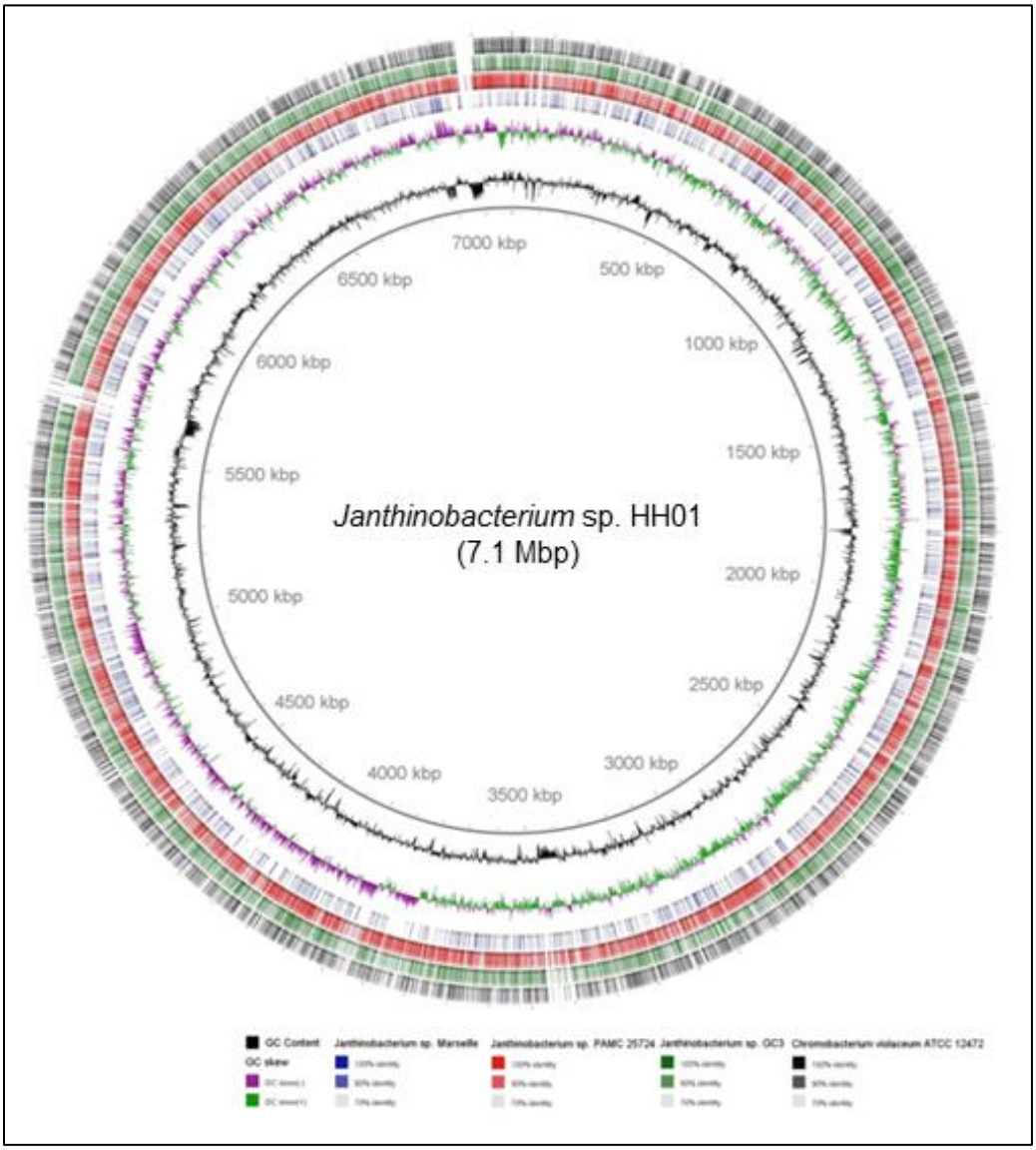

Figure 22. Blastp comparison of the HH01 genome with closely related species. The innermost rings of the genomic map indicate the GC content (black) and GC skew (purple/green). The outer rings show shared identities (according to blastp) with the included genomes. Blastp matches between 70% and 100% amino acid identity are colored from lightest to darkest shade, respectively, according to the key below the diagram. Rings indicate blastp identity, from inside to the outside, between *Janthinobacterium* sp. HH01 and *J.* sp. Marseille, blue; *J.* sp. PAMC 25724, red; *J.* sp. GC3, green; and *C. violaceum* ATCC 12472, black. The image was prepared using BRIG (Blast Ring Image Generator; http://sourceforge.net/projects/brig).

Furthermore, Venn diagrams and synteny dot plots were created. A Venn diagram displaying the fraction of shared genes between the genomes of HH01, *J.* sp. GC3 and *J. lividum* PAMC 25724 is shown in Figure 23A. It revealed that all three genomes share about 3,000 genes, which is referred to as the core genome. *J. lividum* PAMC 25724, of which genome size is significantly smaller than those of HH01 and GC3 represents a percentage share of approximately 70%. HH01 and GC3 share about 12% of its genome (628 genes), which are not present in PAMC, whereas the percentage of matching genes between HH01 and PAMC 25724 is about 6% (249 genes). Moreover, HH01 bears with at least 1,591 protein coding genes the greatest number of unique genes. These genes are associated with a wide range of functions and pathways, including particularly genes associated with signal transduction and regulation as well as genes coding for transport or receptor proteins.

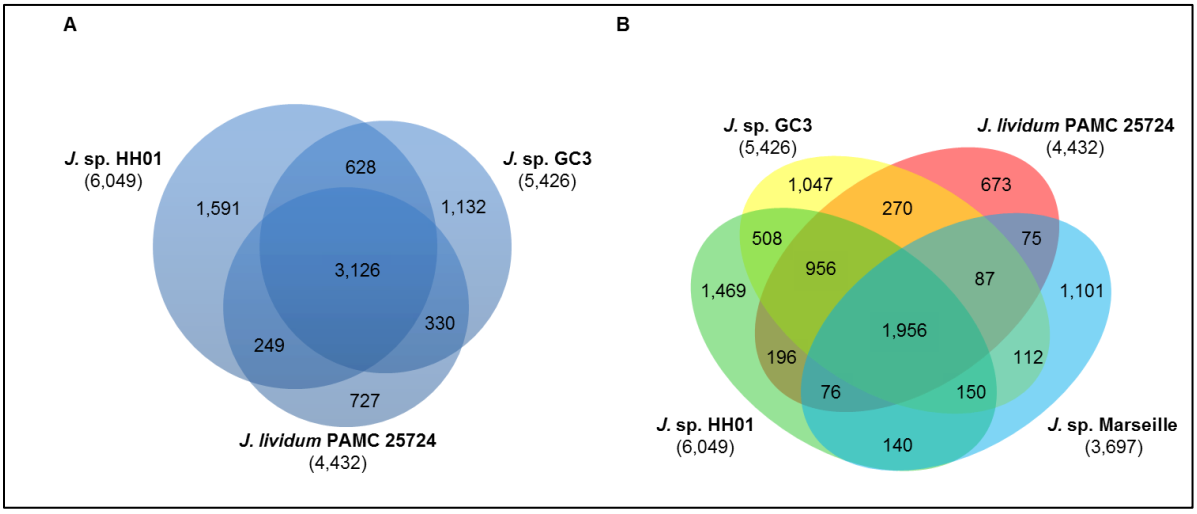

Figure 23. Venn diagram depicting the intersections of protein sets of *J.* sp. HH01, *J.* sp. GC3, *J. lividum* PAMC 25724 and *J.* sp. Marseille. (A) The diagram is based on the gene counts of *J. lividum* PAMC 25724. The remaining intersections between HH01 and GC3 are gene counts in GC3. Due to variable copy numbers of several genes in the three species, the fragments do not add up to the total numbers of genes as indicated in parentheses for HH01 and GC3. **(B)** The diagram is based on the gene counts of *J.* sp. Marseille, the remaining intersection between PAMC, GC3 and HH01 are gene counts in PAMC and finally in GC3. One has to add that due to variable copy numbers of several genes in the four species, the fragments do not add up to the total numbers of genes as indicated in parentheses for HH01, GC3 and PAMC. The numbers of pairwise shared genes were calculated with the phylogenetic profiler function of the IMG/ER platform. Homologous genes within the genomes were detected with a maximum E-value of 10^{-5} and a minimum identity of 30%. Data are taken from the IMG database (Markowitz *et al.* 2012), cited 2013-01-06.

Another Venn diagram shows a comparison of shared genes between the aforesaid genomes and the genome of *J.* sp. Marseille, a somewhat more distant *Janthinobacterium* strain (Figure 23B). The core genome, containing genes present in all strains, is set to a size of 1,956 protein coding genes. This reflects just a share of 53% of the *J.* sp. Marseille genome that represents the smallest genome of the four.

Synteny dot plots are a way of comparing whole genomes based on a nucleotide sequence alignment. A conserved synteny approach can be utilized to identify preserved co-localization of genes on the chromosomes of different species in order to identify orthologous genes and sequence regions. Moreover, genes within a conserved syntenic region in two closely related species are expected to be in the same order and orientation. The dot blot diagrams depicted here were generated by the appropriate tool within the IMG server which uses Nucmer (NUCleotide MUMmer) for genome comparison; each dot represents a region of similarity or orthologous gene in the compared genome. A synteny plot displaying a sequence alignment of the two *Janthinobacterium* strains GC3 (on the x-axis) and HH01 (on the y-axis) is shown in Figure 24A. Here, a certain tendency for synteny was found, because synteny blocks viewed as diagonals on the dot blot were detected. Nevertheless, a number of similar genes seemed not to be located in such a homologous order. The dot plot in Figure 24B representing the chromosomal alignment between the strains HH01 and PAMC 25724, revealed an almost similar result. While a variety of genes was localized in syntenic regions a comparable number of genes tended to translocations or inversions. This comparative analysis of the genome structure of different janthinobacterial strains showed the highest co-linearity between the genomes of GC3 and PAMC25724 (Figure 24C). While in this synteny plot also translocations, duplications, deletions as well as inversions are present, it does nonetheless represent the best comparison of all. In comparison, a fourth sequence alignment was performed between the genomes of HH01 and *J.* sp. Marseille (Figure 24D). Here, only in some parts a relatively low degree of synteny between the similar genes was visible. In summary, it can be concluded that the synteny analysis of the *Janthinobacterium* genomes revealed no striking conservation of gene order. In comparison to the other janthinobacterial strains, HH01 seemed to have the largest similarity to *J.* sp. GC3

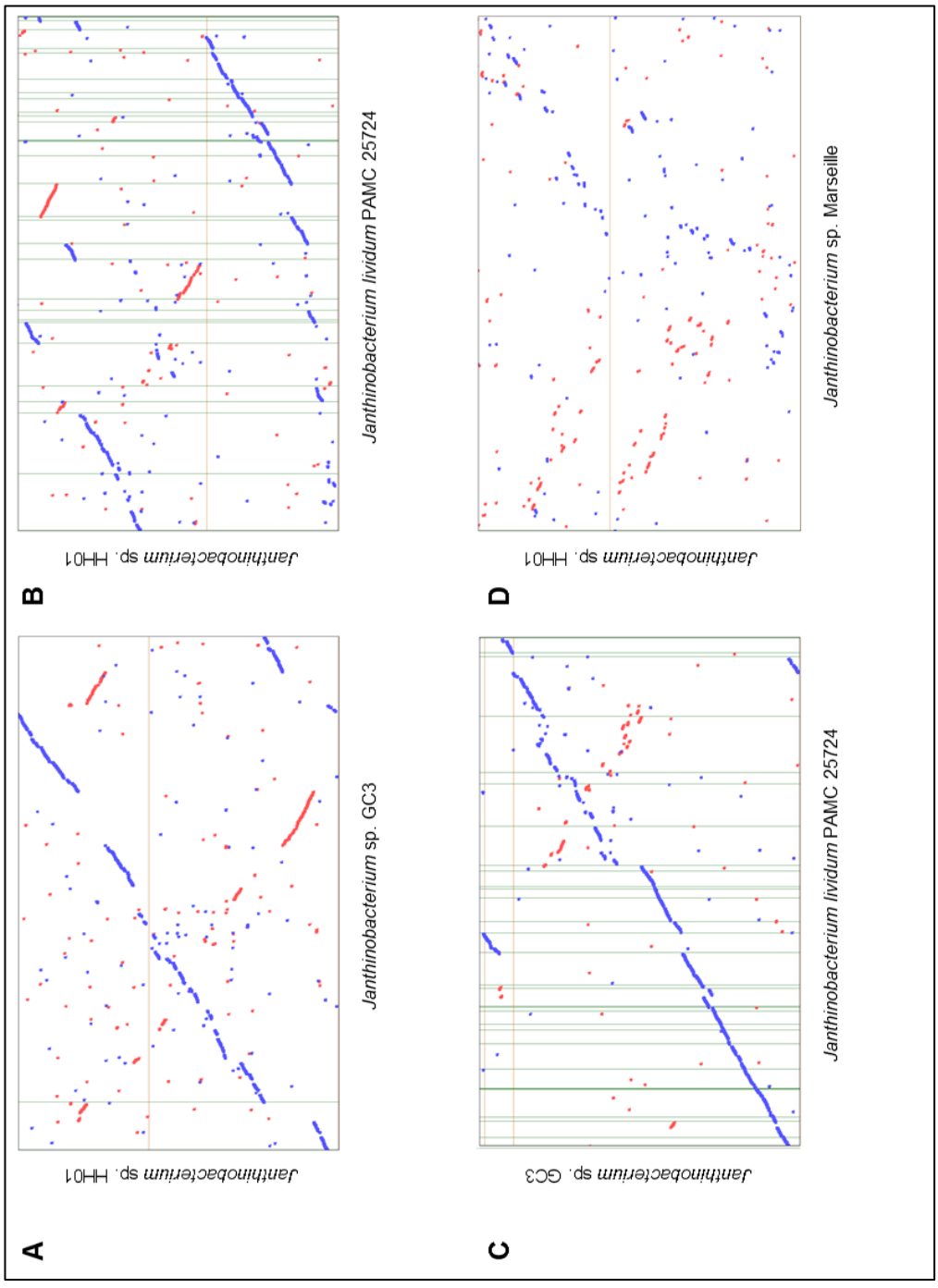

Figure 24. Synteny dot plots between *J.* sp. HH01 and chromosomes of other *Janthinobacterium* strains. **(A)** Synteny dot plot between the chromosomes of *J.* sp. HH01 (y-axis) and *J.* sp. GC3 (x-axis). **(B)** Synteny dot plot between the chromosomes of *J.* sp. HH01 (y-axis) and *J. lividum* PAMC 25724 (x-axis). **(C)** Synteny dot plot between the chromosomes of *J.* sp. GC3 (y-axis) and *J. lividum* PAMC 25724 (x-axis). **(D)** Synteny dot plot between the chromosomes of *J.* sp. HH01 (y-axis) and *J.* sp. Marseille (x- axis). The graphs represent X-Y plots of dots forming syntenic regions between the chromosomes. Data are taken from IMG database (Markowitz *et al.* 2012), cited 2013-01-05.

3.3 *Janthinobacterium* sp. HH01 – secondary metabolites and defense mechanisms

Analysis of the HH01 genome sequence revealed several putative defense mechanisms. This includes the violacein operon, numerous genes transferring resistance towards antibiotics and heavy metals as well as the presence of NRPS/PKS clusters. The most noticeable of these was certainly its ability to produce violacein.

3.3.1 Effect of violacein on *C. elegans* survival and development

Violacein is known for its various properties and biological activities. However, no direct link between violacein and its effect on the survival and development of *C. elegans* was shown so far. Thus, corresponding experiments were performed within this study.

For survival experiments *C. elegans* was exposed to the HH01 WT strain. In the presence of HH01 all tested worms were dead after four days of incubation. This effect was not observed in the presence of non-violacein producing control strains (HH5-1 and *E. coli* strain OP50); here about three quarts of the nematodes were still alive after four days (Figure 25A). The mutant strain HH5-1 (Tn5::*aroC*; Table 2) obtained by transposon mutagenesis (2.6.11; 3.1.4) is due to an EZ-Tn5 insertion in gene *aroC* encoding chorismate synthase AroC disabled in producing tryptophan, the inevitable precursor in violacein biosynthesis. For this reason, the mutant is also incapable of synthesizing violacein.

Since the mutant HH5-1 is not a real violacein knockout mutant another survival experiment was performed to exclude that no other substance produced by HH01 was the trigger for the effect on *C. elegans*. For this, *C. elegans* larvae were exposed to *E. coli* DH5α cells heterologously expressing violacein (pDrive-*vioABCDE,* Table 4) (Figure 25B). About 40% of nematodes were still alive after five days of incubation. The analyzed negative control (*E. coli* expressing empty pDrive vector) did not show this effect; here the survival rate was about 90%. This shows that violacein is toxic for the nematodes.

Beside the nematode´s survival their development was examined. Within these developmental assays the tryptophan- and violacein-negative mutant strain HH5-1 and the *E. coli* strain OP50 served as negative controls. Both control strains had no effect on the worm´s development. The nematodes were able to develop normally in the presence of HH5-1 (Figure 25D) as well as in the presence of *E. coli* OP50 (Figure 25E). However, in the presence of HH01 the nematodes were unable to develop over the larval stage (Figure 25C). Moreover, they exhibited a decreased locomotion and increased avoidance behavior, evident from the fact that most worms were found outside the bacterial lawn (data not shown). Based on these results it was concluded that violacein itself exert impact on *C. elegan*'s survival and development. Nevertheless, it cannot be excluded that other substances, which may be produced by HH01, exert a similar effect.

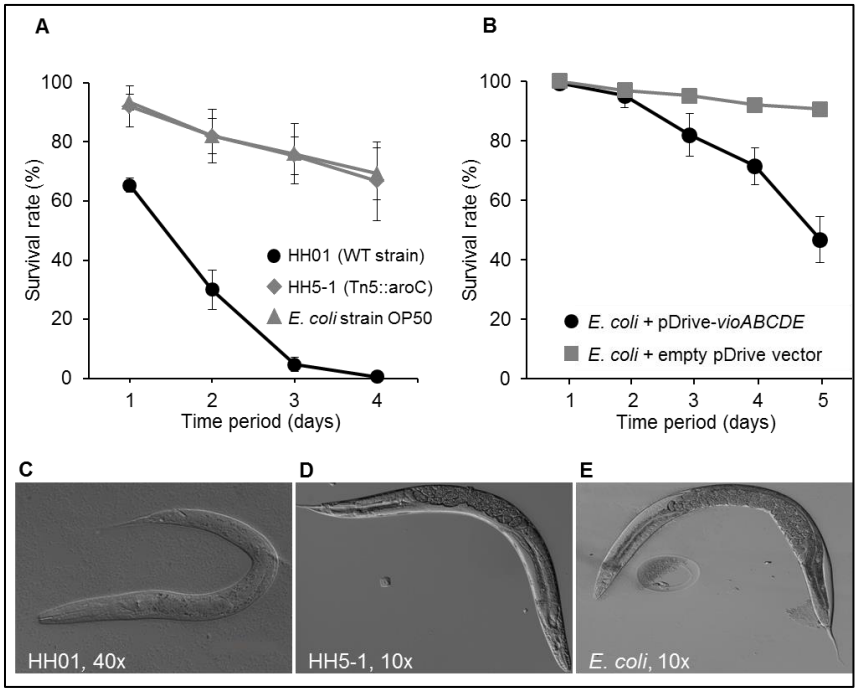

Figure 25. Effect of violacein on *C. elegans* survival and development. (A) Survival rate of *C. elegans* exposed to the HH01 WT strain (black curve). As negative controls the non-violacein producing strains HH5-1 and *E. coli* strain OP50 were used (grey curves). Bars represent the mean±SD. The number of samples was n=5. **(B)** Survival rate of *C. elegans* exposed to *E. coli* DH5α expressing extra copies of HH01 *vioABCDE* genes (black curve). As negative control *E. coli* + empty pDrive vector (grey curve) was used. Bars represent the mean±SD. The number of samples was n=5. **(C - E)** Images showing worms during the developmental assays. (C) HH01 WT strain. (D) Tryptophan- and violacein-negative mutant strain HH5-1. (E) Negative control strain *E. coli* OP50.

3.3.2 Investigations regarding antibiotic and heavy metal resistance

Due to various tests HH01 was found to be resistant to a relatively wide range of various antibiotics - most notably the β-lactam antibiotic ampicillin, an inhibitor of cell wall synthesis. In addition, HH01 grew in the presence of the protein synthesis inhibitors chloramphenicol and tetracycline and the DNA synthesis inhibitor nalidixic acid. HH01 also appeared insensitive to the cell wall synthesis inhibitor cycloserine. In contrast, it was sensitive towards the aminoglycoside antibiotics gentamicin, kanamycin, spectinomycin and streptomycin. The tested antibiotics are listed in Table 13. Since the HH01 genome sequence was available, the underlying genes mediating the antibiotic resistance were analyzed (Table 12). Nevertheless, not all findings could be verified. Whereas the genome sequence confirmed the presence of genes mediating ampicillin, chloramphenicol, and tetracycline resistance, no appropriate genes facilitating the observed resistance to nalidixic acid and cycloserine were found. However, the findings of susceptibility towards gentamicin, kanamycin, spectinomycin, and streptomycin were supported by the lack of corresponding genes in the HH01 genome sequence.

Table 12. Resistance to antibiotics. Experimentally tested antibiotics, as well as the corresponding genes found by sequence comparison in the HH01 genome. n.d., not detectable.

Antibiotics	Susceptibility	Corresponding locus tag
Ampicillin	-	Jab_1c06490, Jab_1c21610, Jab_2c14380
Chloramphenicol	-	Jab_2c12410
Tetracycline	-	Jab_1c02970, Jab_1c09990, Jab_2c01640
Nalidixic acid	-	n.d.
Cycloserine	-	n.d.
Gentamicin	+	-
Kanamycin	+	-
Spectinomycin	+	-
Streptomycin	+	-

Analysis of the HH01 genome sequence revealed several β-lactamases; the genes cited in Table 12 most probably degrade the β-lactam antibiotic ampicillin. The enzyme found to provide resistance towards chloramphenicol (Jab_2c12410) is a chloramphenicol acetyltransferase. The HH01 inherent tetracycline resistance seems to be facilitated by tetracycline efflux. The appropriate MFS transporters mediating the tetracycline resistance in HH01 (Table 12), belong to the drug:H+ antiporter-1 family (DHA1 family)

and are classified as TetA. A detailed summary of the tested antibiotics can be found in Table 13. Here, also information regarding the different effects of the antibiotics on the violacein expression is given.

Table 13. Detailed information about the tested antibiotics and observations regarding the respective violacein expression. This test was carried out on agar plates containing the respective antibiotic concentration. +, growth not affected; (+), impaired growth; -, no growth observed.

Tested antibiotic concentration	Growth	Observed violacein phenotype
Ampicillin (final conc.: 100 µg/mL)	+	purple phenotype
Chloramphenicol (12.5)	+	moderate purple
Chloramphenicol (25)	(+)	moderate purple
Tetracycline (4.5, 9, 13.5, 18, 36, 54)	+	normal to moderate purple
Nalidixic acid (10)	+	purple
Nalidixic acid (20, 50)	(+)/+	not purple
Nalidixic acid (100)	-	-
Cycloserine (10)	+	not purple
Cycloserine (50)	(+)	not purple
Cycloserine (100, 200)	-	-
Gentamicin (5, 10, 25)	+/-	moderate purple
Kanamycin (25, 50)	-	-
Spectinomycin (5)	+	moderate purple
Spectinomycin (10)	(+)	moderate purple
Spectinomycin (25, 50)	-	-
Streptomycin (6.25, 12.5, 25, 50)	-	-

Beside the above presented findings, the HH01 genome sequence encodes a relatively large number of genes correlating with resistance mechanisms both resistance to antibiotics and resistance to heavy metals. About 2% of the protein coding genes are associated with defense mechanisms (Figure A4). Among genes encoding heavy metal resistance are the *ars* operon and *cop* operon, as well as genes encoding chromate ion transporters (Figure 26). Arsenic detoxification is mediated by the *ars* operon, which consists of the genes *arsR*, *arsC*, *arsB* and *arsH* (Figure 26A). Furthermore, HH01 seems to be equipped with the possibility of an active efflux of chromate, which is mediated by the membrane-bound protein ChrA that was found in the HH01 genome at least at four sites (Figure 26B). The third example of a heavy metal transport mechanism encoded by the HH01 genome covers a putative copper operon. The corresponding genes *copB*, *copA*, *copC* and *copD* are shown in Figure 26C.

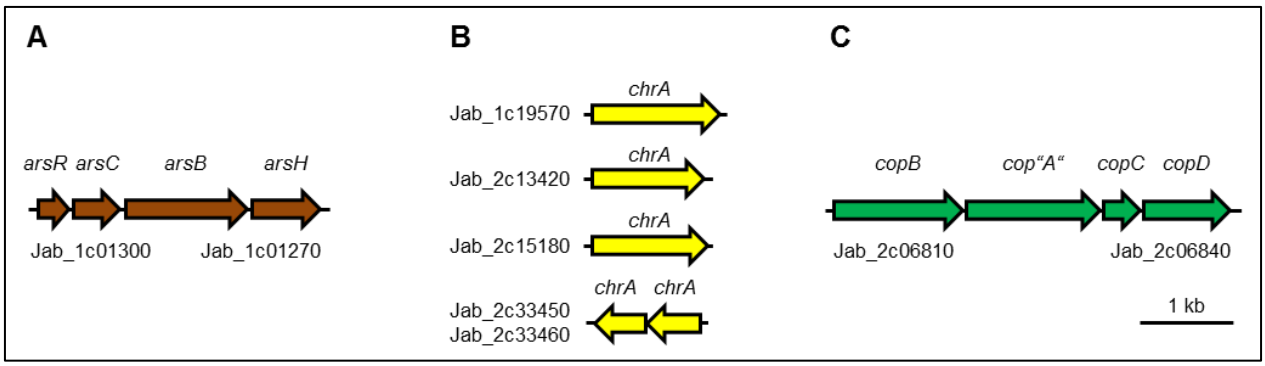

Figure 26. Genes mediating heavy metal resistance encoded by the HH01 genome. (A) The *ars* operon. *arsR*, transcriptional regulator; *arsC*, arsenate reductase; *arsB*, arsenical pump membrane protein; *arsH*, arsenical resistance protein. **(B)** Chromate transporter. HH01 may encode three long-chain CHR (LCHR) and one pair of short-chain (SCHR) chromate ion transporter. **(C)** The *cop* operon. *cop* genes that may be involved in the copper homeostasis of HH01: *copB*, outer membrane protein; *cop"A"*, multicopper oxidase; *copC*, copper resistance protein; *copD*, copper export protein. The indication of the locus tag is related to the first and last ORF of the described operon. The data are taken from the IMG database (Markowitz *et al.* 2012), cited 2013-01-18.

In addition, a larger gene cluster consisting of about 40 ORFs was found in the sequence region from locus tag Jab_2c03840 to Jab_2c04220 (Figure 27). Within a ~50 kb spanning region several specialized gene arrangements were identified; including a CusCBA heavy-metal efflux complex (Jab_2c03840- Jab_2c03860) that may function for the efflux of biocidal copper/Cu(I) and silver/Ag(I) ions. Moreover, an operon encompassing typical lead resistance genes (Jab_2c03910-Jab_2c03940) was identified. The genes *pbrB*, *pbrT*, *pbrR*, and *pbrA* were assigned accordingly. In another part of this sequence region genes encoding cobalt-zinc-cadmium resistance proteins were found (Jab_2c03950-Jab_2c04050). The last noticeable gene arrangement within this cluster contained genes that be may be necessary for copper transport and homeostasis of HH01 (Jab_2c04100-Jab_2c04160). Moreover, due to the finding of at least two transposases and the here not shown up-and downstream sequence region the cluster can probably be considered as a "genomic island".

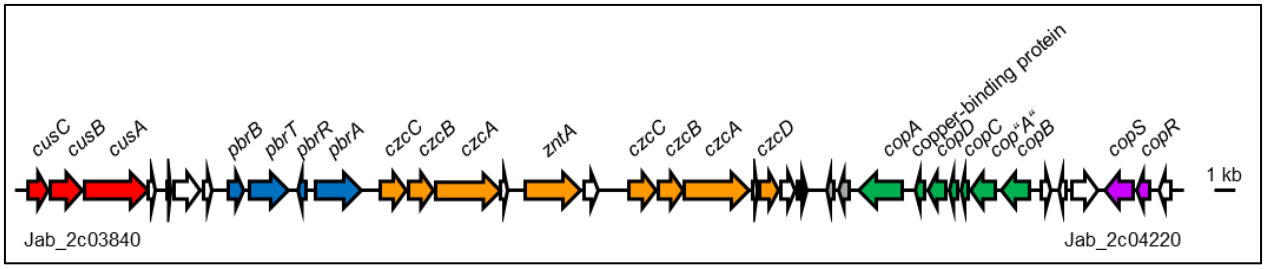

Figure 27. Putative heavy metal transport genes in HH01. 38 ORFs spanning genomic region consisting of a variety of possible genes connected with heavy metal transport. Below the respective genes and the encoded proteins are listed. Red arrows, *cusCBA* encoding a heavy-metal efflux complex (Jab_2c03840- Jab_2c03860). *cusA*, HME-RND inner membrane efflux transporter conferring resistance to Ag(I) and Cu(I) ions; *cusB*, periplasmic component belonging to the membrane fusion protein (MFP) family; *cusC*, outer membrane channel (OMC). A small periplasmic protein, referred to as CusF, normally located between CusC and CusB, was identified as a protein domain within CusB. Blue arrows symbolize a possible lead resistance operon (Jab_2c03910-Jab_2c03940). *pbrB*, C_{55}-PP phosphatase (undecaprenyl pyro-phosphatase); *pbrT*, Pb(II) uptake protein; *pbrR*, transcriptional activator of the MerR family of metal ion-sensing regulatory proteins; *pbrA*, P-type Pb(II) efflux ATPase. Orange arrows, putative cobalt-zinc-cadmium-mediating resistance genes (Jab_2c03950-Jab_2c04050). *czcC*, cobalt-zinc-cadmium resistance protein CzcC (outer membrane efflux protein OEP); *czcB*, cobalt-zinc-cadmium resistance protein CzcB (RND family efflux transporter, MFP (membrane fusion protein) subunit); *czcA*, cobalt-zinc-cadmium resistance protein CzcA (RND superfamily); *zntA*, zinc-cadmium-exporting P-type (transporting) ATPase (HAD superfamily, subfamily IC); *czcD*, cobalt-zinc-cadmium resistance protein CzcD (CDF family). Green arrows, genes connected with copper resistance (Jab_2c04100-Jab_2c04160). *copA*, copper/Cu(II)-exporting P-type ATPase; copper-binding protein; *copD*, copper resistance protein D; *copC*, copper resistance protein CopC; *cusF*, copper-binding periplasmic protein CusF (not shown); *cop"A"*, copper oxidase; *copB*, outer membrane efflux protein (OEP)/copper resistance-related protein. Purple arrows (Jab_2c04200-Jab_2c04210), heavy metal sensor kinase and a heavy metal response regulator (owing to their spatial proximity to the putative copper operon referred as *copS* and *copR*). Grey arrows (Jab_2c04080-Jab_2c04090), transposases (IS66 family). White arrows, hypothetical proteins. Black arrows, not here mentioned proteins. Abbreviations: RND, Resistance-Nodulation-Cell Division; CDF, cation diffusion facilitator. The indication of the locus tag is related to the first and last ORF of the described operon. Sequence data are taken from IMG database (Markowitz *et al.* 2012), cited 2013-01-18.

3.3.3 NRPS/PKS-cluster

Analysis of the HH01 genome revealed seven gene clusters responsible for the biosynthesis of nonribosomal peptide synthetases (NRPS) and one gene cluster for a NRPS-polyketide synthase (PKS) hybrid. A schematic representation of these clusters is depicted in Figure 28. The clusters found in the HH01 genome show the typical gene organization of this megasynthases forming modules. These modules are composed of three specialized domains, each responsible for a specific reaction of the accomplished elongation process. In NRPS these are condensation, adenylation and thiolation (PP-binding) domains. In addition, accessory domains that allow various modifications such as formyltransferases, methyltrasferases, monooxygenases and reductases were identified. Prediction of the structure showing the presumably arising molecules from the NRPS/PKS clusters is given in Figure 29. Especially cluster 4 and 5 may be of particular interest. They can be regarded as one single cluster, since they comprise the continuous sequence region from Jab_2c07140 to Jab_2c07500 and therefore have a size of more than 105 kb. Because of the occurrence of typical NRPS and PKS domains, they can be considered as a NRPS-PKS hybrid. Cluster 5 seems to be a siderophore since it contains siderophore-like domains.

Another enzyme found in HH01 that is involved in a nonribosomal biosynthesis process is the cyanophycin synthetase CphA. This enzyme catalyzes the nonribosomal biosynthesis of cyanophycin, a polymer that is naturally produced by several cyanobacteria, where it serves as a temporary nitrogen reserve material. The responsible genes encoding the CphA for this polymerization reaction in HH01 are *cphA1* (Jab_2c02000), *cphA2* (Jab_2c02030), *cphA3* (Jab_2c20190), and *cphA4* (Jab_2c20200).

Figure 28 (page 73). NRPS/PKS cluster. For the secondary metabolite analysis the antiSMASH program (Medema *et al.* 2011) was used. This figure illustrates the gene organization of cluster 1-8, showing the necessary domains and genes for the NRPS/PKS biosynthesis. Abbreviations: PP-binding, phosphopantetheine attachment site; PPT transferase, 4'-phosphopantetheinyl transferase; NRPS, nonribosomal peptide synthetase; PKS, polyketide synthase; AT, acyltransferase domain; PKS_PP, phosphopantetheine attachment site (phosphopantetheine or pantetheine 4'phosphate) is the prosthetic group of acyl carrier proteins (ACP); FAD, flavin adenine dinucleotide; SDR, short-chain dehydrogenase/reductase; TauD dioxygenase, this family consists of taurine catabolism dioxygenases of the TauD, TfdA family.

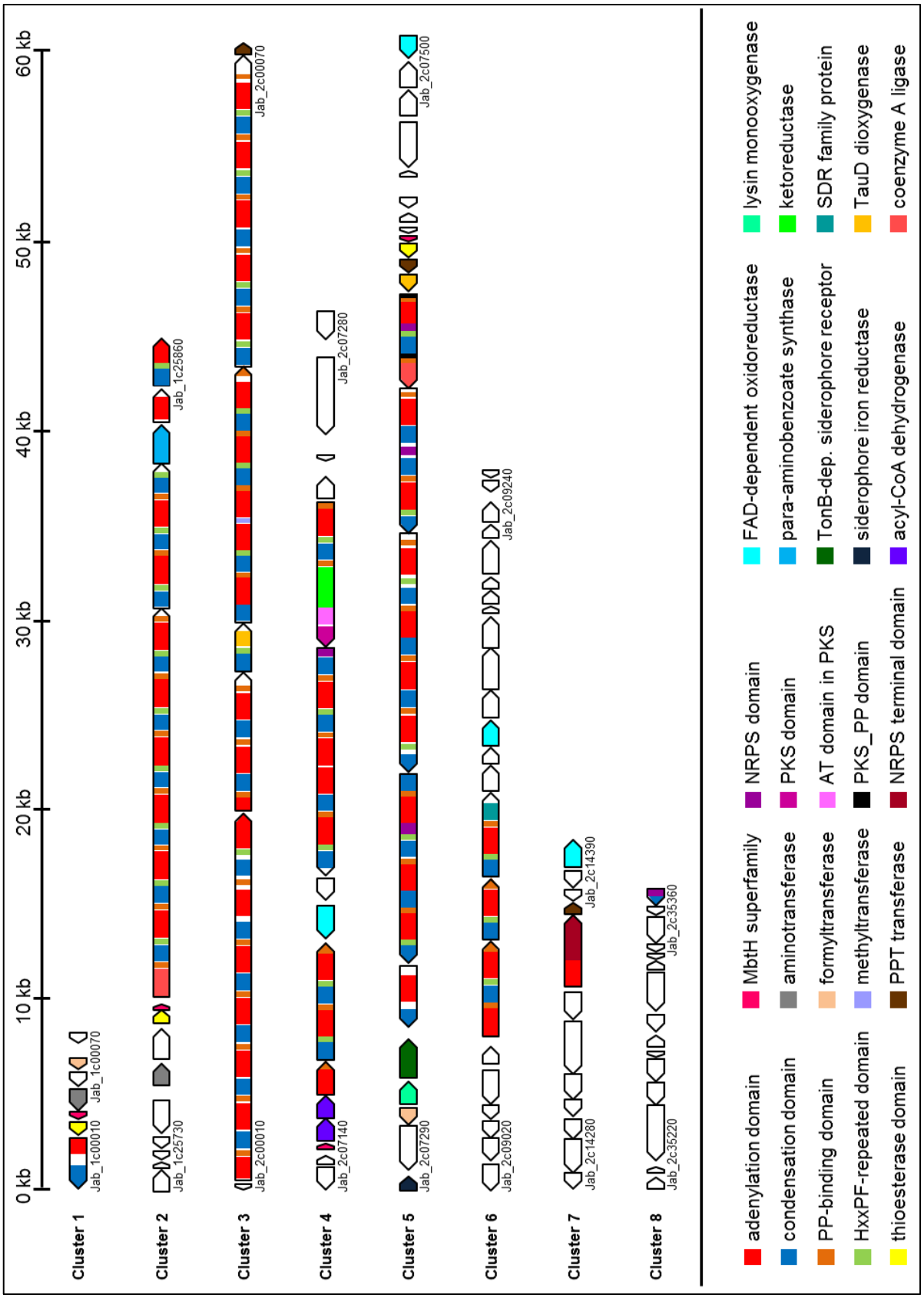
0 kb
10 kb
20 kb
30 kb
40 kb
50 kb
60 kb
Cluster 1
Jab_1c00010
Jab_1c00070
Cluster 2
Jab_1c25730
Jab_1c25860
Cluster 3
Jab_2c00010
Jab_2c00070
Cluster 4
Jab_2c07140
Jab_2c07280
Cluster 5
Jab_2c07290
Jab_2c07500
Cluster 6
Jab_2c09020
Jab_2c09240
Cluster 7
Jab_2c14280
Jab_2c14390
Cluster 8
Jab_2c35220
Jab_2c35360
adenylation domain
condensation domain
PP-binding domain
HxxPF-repeated domain
thioesterase domain
MbtH superfamily
aminotransferase
formyltransferase
methyltransferase
PPT transferase
NRPS domain
PKS domain
AT domain in PKS
PKS_PP domain
NRPS terminal domain
FAD-dependent oxidoreductase
para-aminobenzoate synthase
TonB-dep. siderophore receptor
siderophore iron reductase
acyl-CoA dehydrogenase
lysin monooxygenase
ketoreductase
SDR family protein
TauD dioxygenase
coenzyme A ligase

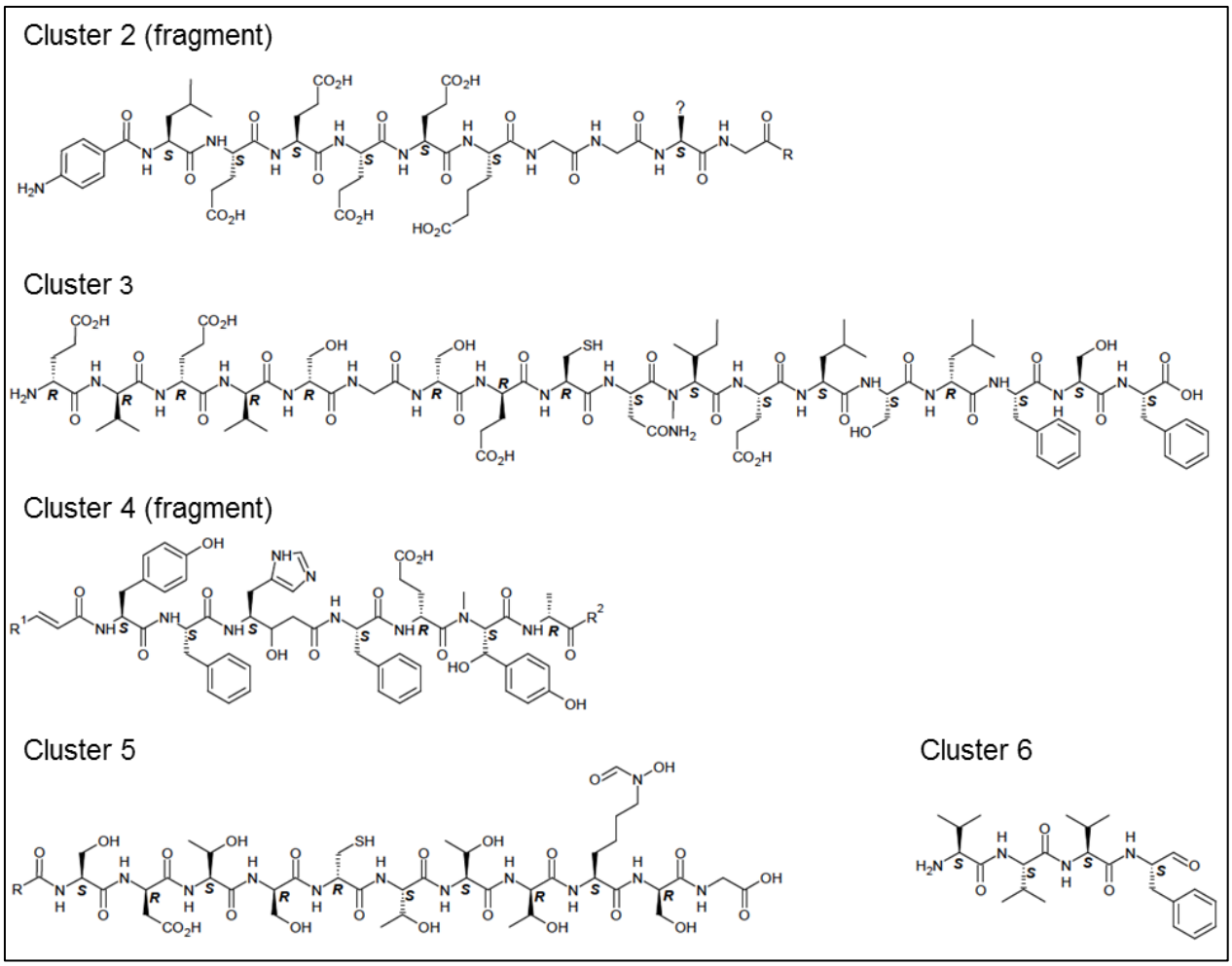

Figure 29. Predicted chemical structures encoded by cluster 2-6.

To predict the chemical structures encoded by the clusters 2-6 the antiSMASH program was used (Medema *et al*. 2011). The compound encoded by **cluster 2** is a peptide consisting of L-amino acids, many amino acids with carboxylic acid side chains and very likely a 4-aminobenzoyl starting unit. Since in this cluster one para-aminobenzoate-synthase Pab is located (Jab_1c25840). The compound encoded by **cluster 3** is a peptide consisting of 18 amino acids. At the N-terminus are almost only D-amino acids and L-amino acids at the C-terminus. The compound encoded by **cluster 4** was difficult to predict, it could be a lipoheptapeptide with a central γ-amino acid resulting from a PKS module (Jab_2c07240), which is part of the NRPS-PKS hybrid. The compound encoded by **cluster 5** is composed of 11 amino acids, a lipoundecapeptide that contains in addition a siderophore-iron reductase (Jab_2c07290) and a TonB-dependent siderophore receptor (Jab_2c07330), suggesting that it may function as a siderophore. The compound encoded by **cluster 6** is a tetrapeptide reduced by the SDR domain at the C-terminus (Jab_2c09100). The predicted structures are shown here in a linear form, but they can also be cyclic. Prediction of the chemical structures was performed with the help of Helge Bode (Molecular Biotechnology, Institute for Molecular Bioscience, Goethe University, Frankfurt, Germany).

3.4 *Janthinobacterium* sp. HH01 – concluding remarks

Analysis of the HH01 genome (AMWD00000000) revealed some interesting features. Figure 30 provides insight into special characteristics that have been identified in HH01.

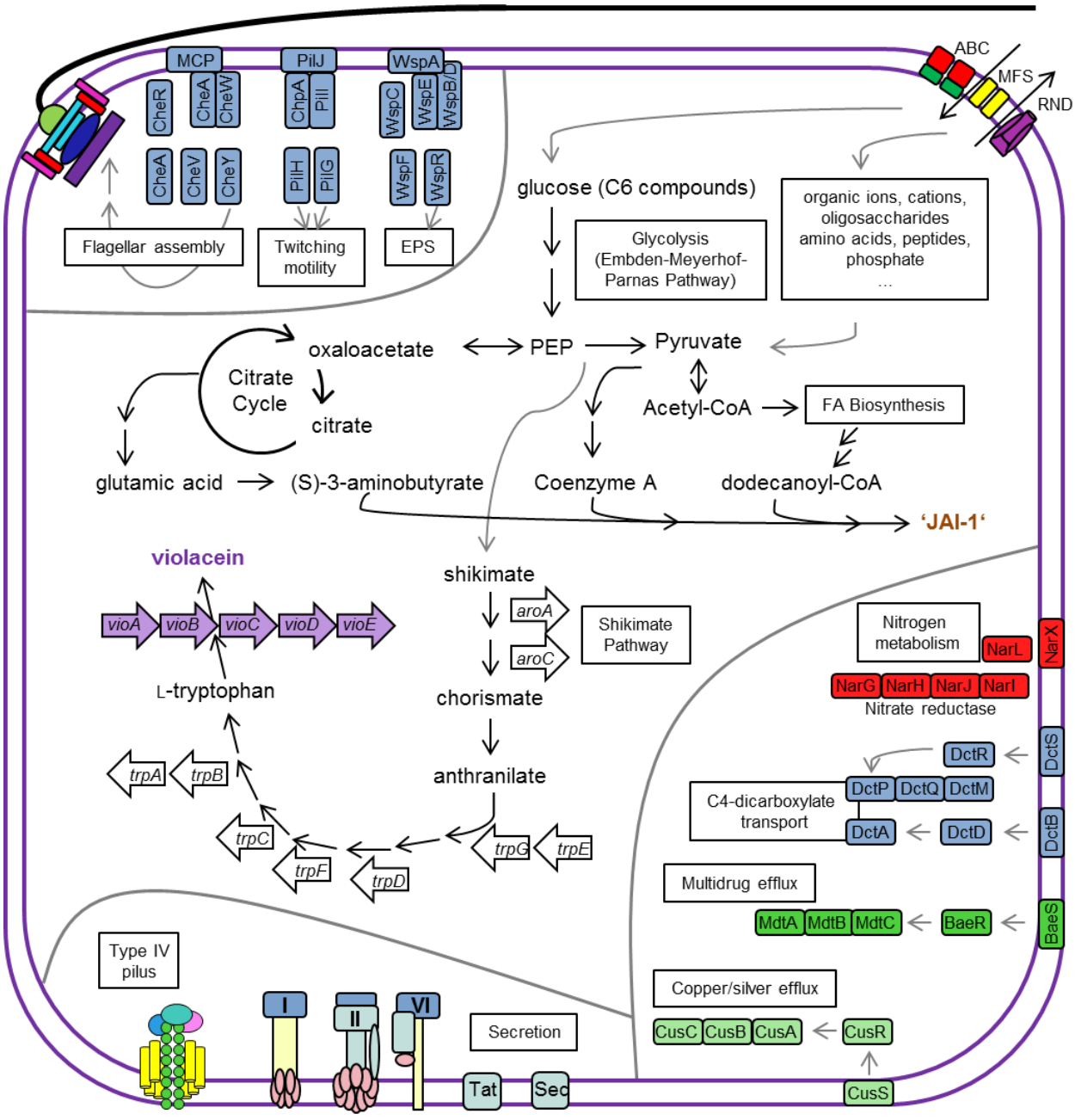

Figure 30. Schematic representation of major components and characteristics encoded in the HH01 genome.

Some parts are in a modified way adapted by KEGG (http://www.genome.jp/kegg/). Data are taken from IMG database (Markowitz *et al.* 2012).

Growth of HH01 is possibly dependent on different carbon and energy sources because corresponding genes are encoded by the HH01 genome sequence. The carbon metabolism presumably depends on the Embden-Meyerhof-Parnas pathway whose genes are entirely present. Beside C6 also C3 and C4 compounds are probably meaningful for HH01 metabolism, since two C4-dicarboxylate transport systems (Dct) were found. These are needed for the absorption and utilization of C4-dicarboxylates such as malate, fumarate and succinate. Furthermore relevant for the HH01 metabolism may be the identified respiratory nitrate reductase (Figure 30; Nar). Important components of the HH01 metabolism including phosphoenolpyruvate (PEP) and fatty acid (FA) biosynthesis are in simplified terms shown in Figure 30 with a special focus the two main findings - the violacein operon (*vioABCDE*) and the novel QS system (shown here as the putative AI molecule 'JAI-1'). Genes associated with the violacein production (*aroA*, *aroC*, *trpA* to *trpG*), which in turn depends on L-tryptophan are shown in Figure 30 and are explained in more detail in 1.1.3.

Maintaining of the entire HH01 homeostasis is provided by a variety of transporter proteins, particularly ABC-type uptake and efflux permeases (ATP-binding cassette (ABC) transporter) as well as transporter of the major facilitator superfamily (MFS) and resistance-nodulation-cell division superfamily (RND). In addition further efflux systems are present, based on two-component systems, such as the multidrug efflux system (BaeRS, MdtABC) and copper/silver efflux system (CusRS, CusCBA).

Concerning secretion systems on one side two major pathways for protein secretion were found: the general secretion (Sec) pathway and the twin arginine translocation (Tat)-pathway. On the other hand genes related to type I, II and VI secretion systems were found. Moreover, type IV pilus assembly proteins encoding genes and two flagellar assembly gene clusters were identified. Relating to flagellar assembly Figure 30 shows associated proteins belonging to the chemotaxis family (Che). These proteins are important for sensing environmental signals, sensory excitation and flagellar motor switch adaption. Further components involved in HH01 chemotaxis are the Pil-Chp operon controlling twitching motility and the Wsp operon regulating extracellular polysaccharide (EPS) production.

3.5 Summary of chapters 3.2 to 3.4

In summary, chapters 3.2 to 3.4 revealed the following most important findings:

- HH01 can grow within a temperature range of 4-28 °C
- HH01 cells are rod-shaped with a pimple-like surface coating
- HH01 whole genome sequencing revealed a genome size of 7.1 Mbp
- Violacein produced by HH01 affects *C. elegans* survival and development
- HH01 possesses several NRPS/PKS-clusters

4 DISCUSSION

Quorum sensing - the microbial means of communication - is a signal transduction mechanism widespread among bacteria. It enables a specific type of gene regulation depending on external triggers, or so called autoinducers. In search of further QS systems or rather the associated bacteria, reporter strains are an indispensable tool.

The aim of this study was to establish a novel reporter strain for the detection of AI-1 molecules. Thereby, the recently isolated violacein producer *Janthinobacterium* sp. HH01 offered a promising target since its violacein production was found to be growth phase-dependent, indicating a QS-regulated mechanism. Analysis of the HH01 genome sequence revealed a gene cluster related to the *Legionella lqs* and *Vibrio cqs* gene clusters. Thus, a major finding of the present study was the identification of a QS system previously unknown in janthinobacterial strains. Moreover, a correlation between this novel QS system *jqs* and the violacein production of HH01 was verified functionally. It was found that the HH01 AI synthase gene *jqsA* but also homologous genes of *L. pneumophila* and *Vibrio* spp. were able to trigger violacein biosynthesis in HH01. Since the latter are known to produce α-hydroxyketone (AHK) molecules, it was further investigated if both the wild-type strain HH01 and the *jqsA* deletion strain HH02 generated here may function as AHK-sensing reporter strains.

4.1 HH01 and HH02 – exploitation of violacein production for the detection of α-hydroxyketone family autoinducers

Production of a distinct phenotype such as an easily quantifiable dye is an excellent feature of a putative biosensor. In search of microbes with this characteristic, the violacein producing strain *Janthinobacterium* sp. HH01 was recently isolated from an aquatic environment. Within this study, its whole genome sequence was deciphered and analyzed. This unveiled several interesting traits such as a number of NRPS/PKS clusters. In addition, it was shown that HH01 is genetically accessible and grows well in

a low to moderate temperature range and may therefore serve as a possible expression strain.

4.1.1 HH01 – so far the largest of all known *Janthinobacterium* genomes

Actually, there are only four sequenced janthinobacterial genomes including HH01. The key data for these are summarized in Table 11. In comparison with the other genomes, HH01 is the largest, with a size of 7.10 Mbp. The GC content was also found to be rather high. The factors influencing the GC content have been discussed for more than 50 years to date (Foerstner *et al.* 2005). In the meantime, there is consensus that several factors are involved (Hildebrand *et al.* 2010) including natural selection (Raghavan *et al*. 2012; Hildebrand *et al.* 2010) and mutational processes (Wu *et al*. 2012). Wu and colleagues (2012) for instance examined the relationship between GC content and mutational mechanisms, and suggested replication and DNA repair mechanisms as the main influencing factors. According to these considerations, other environmental or bacteriological factors such as genome size, temperature, oxygen requirement and habitat are of subsidiary importance or have only an indirect influence. The authors revealed a correlation between GC content variations and the presence of certain DNA polymerase III alpha subunit isoforms. At this HH01 was identified as a member of the dnaE1|dnaE2 group. This correlates very well with its higher GC content, oxygen and temperature requirements, as well as its genome size.

The large genome of HH01 does not only correlate positively with its GC content, but also with its likewise large number of proteins that are encoded by its genome sequence. In comparison with other janthinobacterial strains, *e.g.*, as depicted by synteny dot plots (Figure 24) or Venn diagrams (Figure 23), HH01 differs significantly in some parts from the other analyzed genome sequences. Investigation of proteins frequently found in HH01 revealed that they are particularly involved in signal transduction/ regulation, transport, or serve as receptor proteins (Table 15).

Moreover, HH01 was found to encode a functional violacein operon. This is worth mentioning because none of the other aforesaid janthinobacterial genomes has corresponding genes, although the ability to produce violacein is not uncommon for the genus *Janthinobacterium* (Schloss *et al.* 2010; Pantanella *et al.* 2007).

4.1.2 HH01 expands the group of violacein-producing strains

Analysis of the HH01 genome sequence confirmed the presence of a violacein encoding gene cluster. Comparison of the violacein operons found in various bacterial strains revealed that they are highly conserved. Accordingly, the violacein biosynthesis genes of HH01 can also be similarly found in different strains. This includes, beside the typical violacein producer *Chromobacterium violaceum*, also the *Collimonas* and *Duganella* strains of the family Oxalobacteraceae, and bacteria of the genus *Pseudoalteromonas*.

To identify similarities, the violacein gene clusters of five strains were compared with that of HH01. Thereby phylogenetic analysis of the amino acid (aa) sequence of VioA (Figure 31A) revealed the highest similarity (76%) between HH01 and *Collimonas* sp. MPS11E8. A high identity was also found for *J. lividum* and *Duganella* sp. B2. In contrast, the sequence similarity to *C. violaceum* ATCC 12472 and *Pseudoalteromonas tunicata* D2 was less pronounced. HH01 and *C. violaceum* or *Pseudoalteromonas* share just 52% and 39% of identical aa, respectively. Additionally, an investigation of the further violacein biosynthesis enzymes, VioB to VioE, was carried out. The results thus obtained, which are shown in Figure A3, did not differ significantly for each protein. In line with the phylogenetic analysis of the aa sequences of VioA to VioE a schematic representation of the gene arrangement of the violacein operon including surrounding ORFs was accomplished (Figure 31B). It turned out that despite the high similarity of the violacein operon between the studied strains, the surrounding area differed vastly. Just one ORF present in HH01 was similarly found in the genome of *J. lividum* (aa identity of 76%), annotated as a putative sugar transporter.

The close relatedness of the violacein biosynthetic gene clusters in the analyzed strains might be caused by horizontal gene transfer, a typical approach of bacteria to exchange virulence or antibiotic resistance genes (Eisen 2000; Ochman *et al.* 2000). This gene “jumping” is actually restricted to the operon, but does not affect surrounding genes up- and downstream the violacein operon (Figure 31B). Moreover, the phylogenetic analysis performed here confirmed a previously shown high similarity between *Janthinobacterium* sp., *Duganella* sp, and *Collimonas* sp. on the one hand (Hakvag *et al*. 2009), and between *C. violaceum* and *Pseudoalteromonas* sp. (Thomas *et al.* 2008) on the other hand.

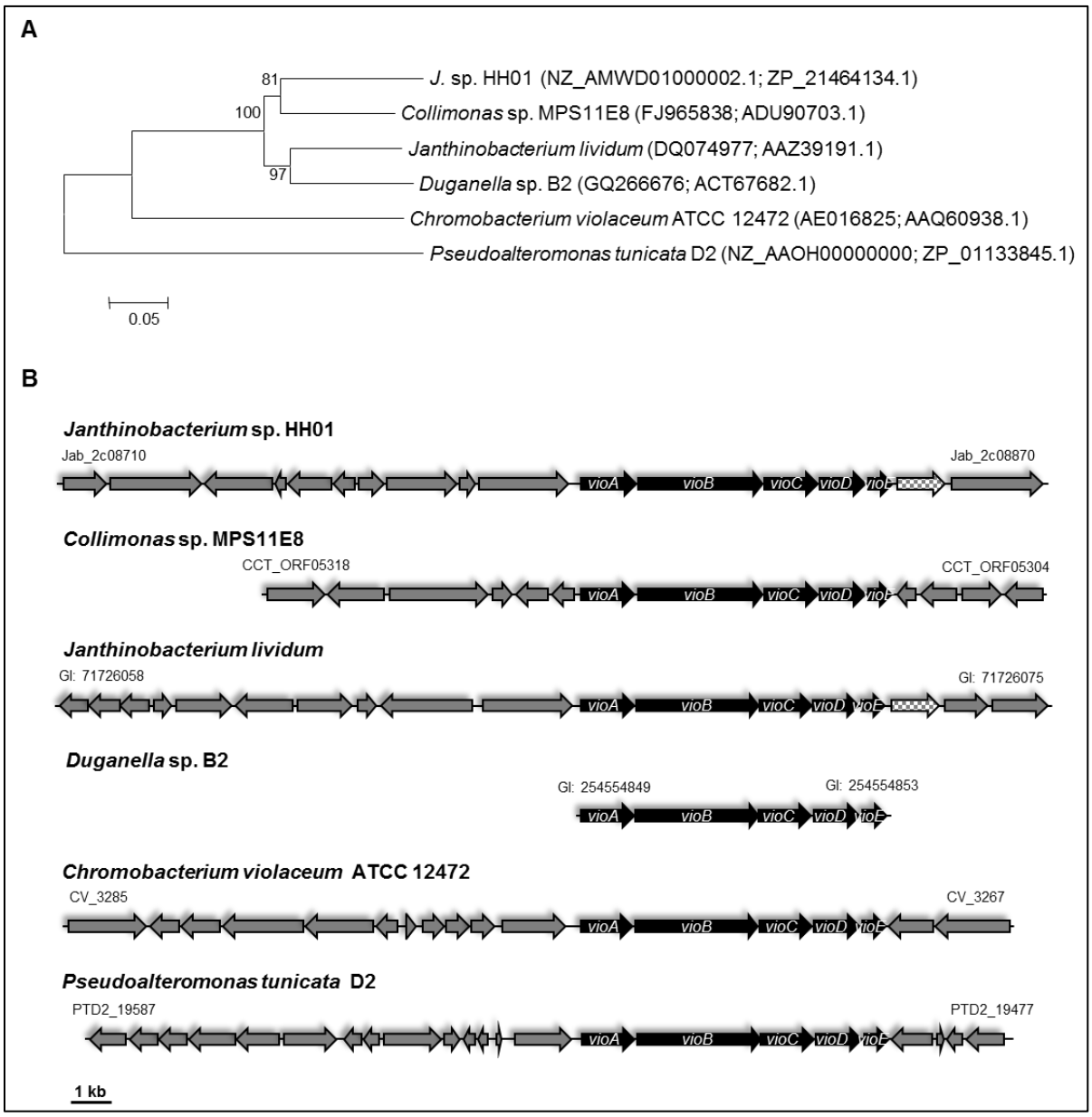

Figure 31. Comparative analysis of the amino acid sequence of VioA. (A) The amino acid sequence of HH01 VioA was compared with similar sequences found in various violacein producers. The sequences used for comparison are shown in brackets. After ClustalW alignment depiction in form of a phylogenetic tree was achieved by applying the maximum likelihood estimation in MEGA5 (Tamura *et al.* 2011). Bootstrap values are shown as percentages at the branch points. The scale bar represents the expected number of substitutions per amino acid. **(B)** Schematic representation of the HH01 violacein operon in comparison to other violacein producing strains. Only one ORF outside the violacein operon was found in two different strains. This matching ORF located in HH01 and *J. lividum* directly downstream the violacein operon is indicated by hatching. For reasons of clarity, alignment of the violacein operon and surrounding ORFs was accomplished based on the 5'-3' orientation in HH01 independently of the original chromosomal orientation. For more details see Table 14. For *Duganella* sp. B2 no upstream or downstream sequence data are available.

4.1.3 HH01 has neither an *N*-AHL- nor an AI-2-QS mechanism

The search for further QS systems in HH01, which are typically found in Gram-negative bacteria, revealed no evidence for *N*-AHL- nor for AI-2-based mechanisms (Table 10). Similarly, in the other investigated *Janthinobacteria* strains no indication of these systems was found except for *J.* sp. GC3. Here, weak evidence for the existence of an AHL-based mechanism was detected. As some bacteria are known to produce specific AIs, but not the cognate receptor (Brito *et al.* 2013) and *vice versa* (Ahmer 2004; Oinuma and Greenberg 2011), this analysis considered both the presence of possible AI synthases as well as that of corresponding receptors. One example of an orphan receptor without corresponding AI synthase, known as the concept of “eavesdropping” (Smith *et al.* 2011), is the LuxR-like receptor SdiA, which was found, for instance in *E. coli* and *Salmonella enterica* (Smith *et al*. 2001). However, not even in this search was a hint of such orphan receptors or emitters identified.

The point that in all strains sequence similarities - albeit weak ones- with respect to the proteins LuxN and LuxQ were found, is probably due to the fact that certain protein domains are common in this protein class (Cheung and Hendrickson 2010). Additionally this reveals a disadvantage of the sequence-based approach. This also became evident while investigating the QS mechanism of *C. violaceum*, whose signaling mechanism is based on AHL molecules (Stauff and Bassler 2011). Here, no similarity to the aa sequences of the AHL synthases LuxI, LasI, and RhlI was found, and only blastp analysis with the *C. violaceum*-inherent protein CviI revealed the expected analogy. This demonstrates that a search based on sequence comparisons may sometimes be insufficient to find similar QS mechanisms. Also, PCR-based approaches are only a limited alternative, since they rely on sequence similarities as well (Spirig *et al*. 2008). This underlines the importance of reporter strains and the necessity of using them as an equivalent or additional method since they allow screening for functional homologous molecules (provided that they have wide receptor sensitivity). Thus, investigations with the AHL-sensing reporter strain *A. tumefaciens* NTL4 were performed in parallel. This strain, which is especially suitable for the detection of C8-3-oxo-HSL molecules but further also for AHL molecules with carbon chain length ranging between C6 and C14

(Zhu *et al.* 1998; Fuqua and Winans 1996), gave no evidence for a possible AHL-based QS mechanism in HH01.

4.1.4 Different regulation of violacein biosynthesis in HH01 and *C. violaceum*

On the one hand, analysis of the violacein operon from different strains revealed that these five genes comprising operon are highly conserved. On the other hand, it was found that this neither applies to surrounding genes up- and downstream from the operon nor to the underlying regulation of gene expression. Both examination of the nucleotide sequence of the 5' flanking region of four of these violacein producers (data not shown) and the aforementioned investigation of the surrounding sequence region (Figure 31B) revealed that this high consistency is actually limited merely to the violacein operon. Interestingly, a detailed look at the HH01 upstream region unveiled plenty of possible signaling genes (Figure 7), a connection with a potential temperature sensitivity, but no similarity to the specific promoter region (*cvi* box) as it was found in *C. violaceum* (Morohoshi *et al*. 2010).

In *C. violaceum* and meanwhile also in another bacterium, *i.e.*, *Pseudoalteromonas* sp. 520P1, a QS-regulated expression of the violacein operon was elucidated (Morohoshi *et al*. 2008; Wang *et al*. 2008; McClean *et al*. 1997). Particularly well-studied is the transcriptional regulation of the violacein gene cluster in *C. violaceum* ATCC 12472, whose complete genome sequence was published in 2003 (de Vasconcelos *et al.* 2003). The QS circuit identified here includes the *cviI* gene, encoding an *N*-AHL synthase and the adjacent gene *cviR*, encoding the related response regulator (Morohoshi *et al*. 2008). Moreover, a 20-bp *lux* box-like palindromic sequence (*cvi* box) was found in the *vioA* promoter region (Morohoshi *et al.* 2010). It is assumed that the CviR/AHL complex binds to the promoter region of the violacein gene cluster and thus activates its transcription (Morohoshi *et al*. 2010).

In contrast, neither bioinformatic studies nor a functional approach with the AHL-sensing reporter strain *A. tumefaciens* NTL4 indicated any AHL-based regulatory mechanisms in HH01. Even though this provides valid evidence, the lack of this widespread QS system cannot be entirely excluded as a possibility. As the sensor strain NTL4 is sensitive to certain but not all AHL molecules, and the possible genes related to

AHL synthases and receptor proteins could also differ from those previously investigated, it thus remained so far undetected.

However, since the genome analysis of HH01 revealed at least one QS system, whose correlation with the violacein production was demonstrated in this study, these results probably indicate a novel means of QS-regulated violacein expression. In addition, both the results of further experiments as well as the variety of sensing-related genes upstream from the violacein operon suggest an apparently more extensive regulation mechanism in HH01. Likewise, this has been speculated in the case of *C. violaceum*, where in addition to the carbon source other yet unknown factors seem to be involved (Antonio and Creczynski-Pasa 2004). Moreover, it was reported that in *J. lividum* glucose, glycerol, and ampicillin exert an influence on the violacein production (Pantanella *et al*. 2007). Similar observations were made when analyzing HH01. Here, the influence of glucose or glycerol was not studied, but it was found that ampicillin and particularly a lower incubation temperature had a positive effect on the amount of violacein. To approach this more extensively, transposon mutagenesis was accomplished in order to get HH01 violacein-impaired transposon mutants.

4.1.5 HH01 is genetically accessible and was subjected to transposon mutagenesis

Analysis regarding the function of certain genes still depends on the usage of strains harboring a gene deletion or mutation within the examined gene. This can be achieved either by a direct gene deletion approach or by random transposon mutagenesis. In order to study the HH01 QS system both methods were applied.

Although investigation of the *jqs* gene cluster revealed a correlation with the violacein biosynthesis of HH01, this approach was used to generate other mutant strains with impaired violacein production, in order to obtain further insights into the HH01 QS system. To create such a violacein-deficient strain, random transposon mutagenesis was utilized. Subsequently, about 35 white or slightly violet clones of this mutant library were examined in detail (3.1.4). However, during this analysis, no transposon insertion

within the violacein operon was detected. This can be due to various reasons. On the one hand, it was assumed if a higher GC content in the violacein encoding genes might have prevented a transposon insertion. Nonetheless, this was not confirmed by investigation of the corresponding sequence region. On the other hand, it was assumed whether a lack of violacein might result in a lethal phenotype, although this assumption is rather unlikely since violacein-impaired mutant strains were obtained. Therefore, the aim was to construct a mutant without functional violacein operon by homologous recombination. However, this attempt failed for unknown reasons while cloning the required vector construct. Instead, transposon mutants which were unable to form violacein due to a transposon insertion in the tryptophan biosynthesis genes were found. Moreover, mutants showing hyperpigmentation were obtained but not further investigated. This supports previous studies reporting on a violacein mutant strain that resulted in hyperpigmentation (Matz *et al*. 2004). The same authors also reported on a *vioA* mutant, defective in violacein biosynthesis (Matz *et al.* 2008). While the first mutant strain was a gene mutation in *C. violaceum* the latter was a mutant of *P. tunicata*.

Another point regarding the transposon mutagenesis screening was the observation that no *jqsA*-deficient mutant was detected. Although the AI synthase JqsA influences the violacein biosynthesis, none of the examined violacein-negative mutant strains revealed its deletion in this gene. Possible explanations for the absence might be that the lacking gene was restored by a paralogous gene or by other yet unknown regulatory mechanisms. This is further supported by identification of one gene in HH01 that might function similarly to JqsA. This gene (Jab_2c30540) is alike the gene *jqsA* annotated as an 8-amino-7-oxononanoate synthase and is also surrounded by sensor histidine kinases and response regulators comparable to the *jqs* cluster (Jab_2c24330 – Jab_2c24350). Thus, the resulting gene product might exhibit a structure similar to the proposed AI JAI-1. Further investigations are needed to unveil the function of this possible second AI synthase gene and whether if might rescue the violacein-impaired phenotype of *jqsA* deletion strain HH02. However, this was not performed as part of this study.

Instead, at least two independent sensor histidine kinase/response regulator gene clusters were affected by transposon insertion (Jab_1c01080/Jab_1c01090 and

Jab_2c00660/Jab_2c00670). All these mutants represented a complete or nearly complete violacein-negative phenotype. Therefore, an interruption of the violacein-regulating pathway was proposed. For Jab_1c01080/Jab_1c01090 an association with the synthesis of certain amino acids can be assumed, since the interrupted genes are adjacent to a conserved gene arrangement encoding, *i.a.*, enzymes for the synthesis of glutamate and histidine. The other transposon insertions located in Jab_2c00660 and Jab_2c00670, a signal transduction histidine kinase and a sensor histidine kinase, hit a less conserved region and it is thus unnecessary to speculate about a possible involvement in specific regulatory pathways.

At least ten transposon insertions were found in genes of the tryptophan biosynthesis pathway. This is actually self-explanatory as tryptophan is the direct substrate of the violacein synthesis. However, more surprising in the analysis of non-violacein producing transposon mutant clones was the discovery of a group of RNA-related genes (Table 9). These were gene *rhlE*, encoding ATP-dependent RNA helicase RhlE (DEAD-type), gene *rne*, encoding ribonuclease E, and a gene encoding 23S ribosomal RNA. These proteins might be part of the HH01 “RNA degradosome”, which appears to be similar to that found in the psychrotrophic bacterium *Pseudomonas syringae* (Purusharth *et al*. 2005). Here and presumably also in HH01 it is beside other proteins composed of RNA helicase RhlE, endoribonuclease E (RNase E) and exoribonuclease R (RNase R). However, this does not explain the observed temperature dependence of the violacein biosynthesis of HH01 with a shift to lower temperatures apparently inducing gene expression. A possible explanation for this observed phenomenon might be the distinct/specific structure that was identified in the sequence region upstream the *vioA* start codon (Figure A1). This hairpin-like structure located in the 5´untranslated region (5´UTR) of the violacein operon might function as post-transcriptional intracellular thermosensor. Such temperature-responsive RNAs, or rather RNA thermometers, are RNA control elements of bacterial genes (Klinkert and Narberhaus 2009), and are known to function, *i.a.*, in the control of virulence factor expression (Papenfort and Vogel 2010). The here identified structure of a possible RNA thermosensor is apparently not affected by a temperature shift, as it was tested by *in silico* analysis (http://rna.urmc.rochesteredu/ RNAstructure Web/) in a temperature range

between 10 and 37 °C. It is therefore proposed that it might be targeted by RNA helicases such as the DEAD-box helicase RhlE, whose deletion resulted in a violacein-impaired phenotype. RNA helicases can unwind or resolve RNA duplexes using ATP hydrolysis (Kaberdin and Bläsi 2013; Phadtare and Severinov 2010; Bizebard *et al*. 2004). This activity of RNA helicases was found to be particularly important in cold-adapted organisms. Here, these enzymes accelerate structural RNA rearrangements such as the unwinding reaction that proceed rapidly at high temperatures, but needs the assistance of enzymes such as the RNA helicase RhlE at low temperatures (Iost *et al*. 2013; Cartier *et al*. 2010). A similar function or involvement was found for RNase E and RNase R (Tamura *et al.* 2012; Awano *et al*. 2010). Therefore, it can be summarized that the specific RNA structure upstream from the *vioABCDE* gene cluster together with the here described RNA-related transposon mutants provide a possible explanation for their impaired violacein production. Nevertheless, a correlation with the tryptophan biosynthesis pathway cannot be excluded since here also RNA-based regulatory mechanisms are known to control gene expression (Merino *et al.* 2008; Yanofsky 2007).

Finally, analysis of mutant clones impaired in violacein production also revealed frequent transposon insertions in the gene encoding Lon protease. Although Lon proteases are known to be involved in protein quality control by degrading misfolded and denatured proteins (Gottesman 2003; Jenal and Hengge-Aronis 2003; Dougan *et al.* 2002), this was not expected since there appears to be no direct link between this indeed important factor for maintaining cellular homeostasis and violacein biosynthesis. However, recently published studies have shown that Lon is also involved in the regulation of AHL-mediated QS signaling systems, *e.g.*, in *B. cenocepacia*, *P. putida*, and *P. aeruginosa* (Takaya *et al.* 2008; Bertani *et al.* 2007). Thereby it was found that the Lon protease acts, *e.g.*, in *P. aeruginosa,* as a negative regulator of its key QS systems, LasI/LasR and RhlI/RhlR, *i.a.*, by posttranslational control of LasI (Takaya *et al.* 2008). The failure of this essential QS system explains, why *lon*-disrupted cells revealed an increased pyocyanine production, since this virulence factor is in *P. aeruginosa* regulated by the affected QS systems (Whiteley *et al*. 1999). Moreover, this suggests that Lon is also involved in the regulation of the violacein operon. However, the findings obtained so far for HH01 merely unveiled that lacking Lon is associated with a reduced

violacein production. Nevertheless, it can be speculated that in this regulatory pathway also the *jqs* system or other factors are involved. Therefore, it seems worthwhile to investigate the existing transposon mutants defective in the gene *lon* in more detail; especially, since it was reported that in addition to the mentioned QS system other regulatory factors such as sigma factors, *e.g.*, RpoN and RpoS are affected indirectly by Lon protease (Takaya *et al.* 2008).

4.1.6 HH01 owns a QS system homologous to *V. cholerae* and *L. pneumophila*

One of the major findings when examining the HH01 genome sequence was the identification of a QS system well-known from *Legionella pneumophila* and *Vibrio* spp. The *Legionella lqs* gene cluster includes the AI synthase LqsA, the sensor kinase LqsS and the response regulator LqsR (Sprig *et al*. 2008; Tiaden *et al*. 2007). The related *cqs* system of *V. cholerae* and *V. harveyi* comprises the genes *cqsA* and *cqsS* (Henke and Bassler 2004; Miller *et al.* 2002). Accordingly, the homologous system of HH01 was designated *Janthinobacterium* quorum sensing (*jqs*), and the corresponding genes *jqsA*, *jqsS* and *jqsR*. The AI synthases CqsA and LqsA, catalyze the production of similar diffusible signaling molecules, belonging to the novel class of α-hydroxyketone (AHK) AIs. The *Legionella* AI molecule (LAI-1) was identified as 3-hydroxypentadecan-4-one (Spirig *et al.* 2008), and the related molecule from *V. cholerae*, cholera autoinducer-1 (CAI-1) as 3-hydroxytridecan-4-one (Higgins *et al.* 2007). Therefore, the still putative HH01 signaling molecule presumably synthesized by the enzyme JqsA was designated JAI-1.

A recently published study (Tiaden *et al.* 2010a) as well as analyses performed in this thesis (Figure 11) revealed a distribution of these QS gene clusters in several strains among environmental bacteria. Beside *V. cholerae*, *V. harveyi* and *L. pneumophila* it was also found in further microbes belonging to α-, β, and γ-proteobacteria, as well as Chlorobi. Thus, identification of the *jqs* cluster of HH01 extended the group of microbes using a QS system that was so far experimentally studied only in *Vibrio* and *Legionella*. These studies proved that the AHK-based QS systems of *L. pneumophila* and *V. cholerae* are similar both at the sequence and

functional level. This was for instance demonstrated by the fact that *lqsA* partially restores the deletion of *cqsA* in *V. cholerae* (Spirig *et al*. 2008). Analogous experiments conducted in this thesis showed that not only the HH01 gene *jqsA* but also the homologous gene from *L. pneumophila* (*lqsA*) as well as the slightly less similar genes from *V. cholerae* (*cqsA*$_{Vch}$) and *V. harveyi* (*cqsA*$_{Vh}$) affected the violacein synthesis of HH01 (3.1.6). This suggests that this type of cell-cell communication has an inter-species character.

4.1.7 QS in HH01, *L. pneumophila* and *V. cholerae* – similar and yet so different

The *cqs*/*lqs* gene cluster regulates in *V. cholerae* and *L. pneumophila* genes responsible for pathogen-host cell interactions, bacterial virulence, formation of biofilms or extracellular filaments as well as a genomic island and competence (Suckow *et al*. 2011; Tiaden *et al.* 2010b; Henke and Bassler 2004; Miller *et al.* 2002). Moreover, a first hint towards regulation of violacein production by the homologous gene cluster *jqs* was found in the context of this study. So far, QS-regulated violacein biosynthesis has been elucidated only in *C. violaceum* (Morohoshi *et al.* 2008) and *Pseudoalteromonas* (Wang *et al*. 2008). In these strains, regulation of the purple pigment is based on signaling molecules of the AHL family. Moreover, it was found that in *C. violaceum* a variety of other factors are subjected to QS regulation, including expression of antibiotics, hydrogen cyanide, protease, and chitinase (de Vasconcelos *et al.* 2003; Chernin *et al.* 1998).

However, while the influence of the *jqs* system on HH01 violacein biosynthesis was reproducible during the performed tests, no effect on other phenotypes was observed. Therefore, further experiments are needed to detect those genes that are controlled by the HH01 *jqs* system. Here the focus should not only be directed on the AI synthase JqsA, as achieved within this study, but also on the response regulator JqsR and the sensor kinase JqsS. This is since these proteins might be the more critical components of the signal transduction mechanism and probably exert an even greater impact on the downstream regulated target genes. This was shown at least in the analysis of *L. pneumophila* mutant strains lacking the individual components - *lqsA*, *lqsS*, and *lqsR* - or even the entire *lqs* gene cluster (Tiaden *et al.* 2010b; 2008; 2007).

Comparison of the gene expression of *lqsR* and *lqsS* mutants with wild-type *L. pneumophila* revealed that in stationary growth phase approximately 80 to 100 genes were up- or downregulated in the mutant strains (Tiaden *et al.* 2010b; 2007). In the absence of *lqsA*, however, only a few genes were affected (Tiaden *et al.* 2010b). The most pronounced outcome was caused as expected by deletion of the complete *lqs* gene cluster, here more than 300 genes were differentially regulated (at least 2-fold) in stationary growth phase (Tiaden *et al.* 2008). The majority of altered genes were associated with virulence, motility and cell division (Tiaden *et al*. 2010b; 2008; 2007). Interestingly, a genomic island, which encodes multiple metal ion efflux pumps, was also affected (Tiaden and Hilbi 2012).

Since a comparable gene arrangement was found in HH01, it would be interesting to examine whether this is also subjected to QS regulation. In addition, it would be worthwhile to identify other target genes of the *jqs* system. Beside the mentioned genomic island, the identified NRPS/PKS-clusters (3.3.3), further resistance genes, genes responsible for flagellar formation and competence genes might be presumably regulated by the *jqs* system. To investigate this in more detail, the absence of the homologous genes in HH01 should be studied in analogy to the *Legionella* mutants. Since a *jqsA* deletion strain is already available, generation of the other mutant strains, Δ*jqsS*, Δ*jqsR*, and even a complete *jqs* deletion should be achieved. Subsequently performed transcriptome analysis might then be a conceivable approach to elucidate the phenotypes regulated by the HH01 QS system.

The only observation in HH01 in the context of *jqs* regulation so far is an altered expression of the violacein operon. On the one hand, overexpression of the AI synthase genes *jqsA*, *lqsA*, and *cqsA* induced violacein production (3.1.6). On the other hand, lack of the AI synthase *jqsA* resulted in a reduced violacein biosynthesis as shown by data obtained in *jqsA* deletion strain HH02 (3.1.7). This indicates a general relationship between the HH01 QS system and the expression of the violacein synthase genes. A more detailed examination was achieved by comparing the growth curves of HH01 and HH02 as well as the corresponding violacein quantity (3.1.8; Figure 16). It was found that lack of the *jqsA* gene had only minor influence on the growth behavior, proving that an absent AI synthase had no vital effect on the cell *per se*. In contrast, the impact on

the violacein amount was quite pronounced, since the *jqsA* deletion strain HH02 produced significantly less violacein compared to the HH01 wild-type strain. Moreover, it was observed that after an increase of the violacein amount in the log phase, which was correlated with a decreasing number of cells, no decrease but rather a continuous increase of the violacein quantity occurred (Figure 16). Therefore, the violacein operon appears to be induced in the stationary growth phase. Although this seems initially surprising or could be attributed to stress that the cells were exposed to, similar results are likewise recognized in *L. pneumophila* and *V. cholerae* (Bolitho *et al*. 2011; Tiaden *et al.* 2010b; 2008; 2007).

Even though it is commonly assumed that virulence factors are upregulated at high cell density, the converse is known from *V. cholerae*. Here, at low cell density and hence absence of its AI CAI-1, genes necessary for biofilm formation and virulence factor production are expressed. In contrast, the corresponding genes are attenuated at high cell density (Bolitho *et al*. 2011). However, further genes in *V. cholerae* are regulated the other way around; *e.g.*, bioluminescence and protease production are induced at high cell density by the CAI-1-mediated QS circuit and are repressed without this trigger. A similar but not identical link is also existent in *L. pneumophila*. Here, it is not the cell density that is the decisive factor, but rather the stage of the growth phase (Tiaden and Hilbi 2012). Thus, when analyzing the expression levels of the different mutant strains, pronounced changes were observed in stationary growth phase, while in the replicative growth phase almost no differences in gene regulation patterns were observed (Tiaden *et al.* 2007). Here, particularly the response regulator LqsR acts as a crucial component of the *lqs* cluster and its role in the transition from the replicative to the transmissive (virulent) phase was proposed (Tiaden *et al*. 2007).

In addition, the authors suggested also for the further components of the cluster functions beyond the *lqsA*/*lqsR*/*lqsS* system. They assumed that the sensor kinase LqsS might signal to other yet unknown response regulators, whereby other target genes besides the LqsR-regulated ones could be controlled. They also suggested that the AHK signaling molecule(s) produced by the AI synthase LqsA could trigger more receptor kinases than LqsS (Tiaden *et al.* 2010b; 2008). Furthermore, analysis of the QS systems of *V. cholerae* and *L. pneumophila* showed that in addition to the *cqs*/*lqs* gene cluster

other components including alternative sigma factors RpoS (σ^S/σ^{38}) and FliA (σ^{28}), conserved RNA binding proteins, such as Hfq and CsrA (RsmA), and the GTP-binding protein Hflx are involved (Tiaden *et al*. 2008; 2007). For this reason, it would be interesting to consider which components of the well-studied regulatory circuits of *L. pneumophila* and *V. cholerae* can additionally be found in HH01. Although in the investigation of HH01 so far no experimentally evidence for such a complex regulatory network was provided, this was nevertheless included in the attempt to outline the putative regulatory circuit of HH01 (4.1.8).

4.1.8 First attempt to outline a possible QS regulatory network of HH01

Based on the tests so far conducted as well as the available genome sequence, an attempt was made to try to develop an assumption of a possible regulatory network in HH01 (Figure 32).

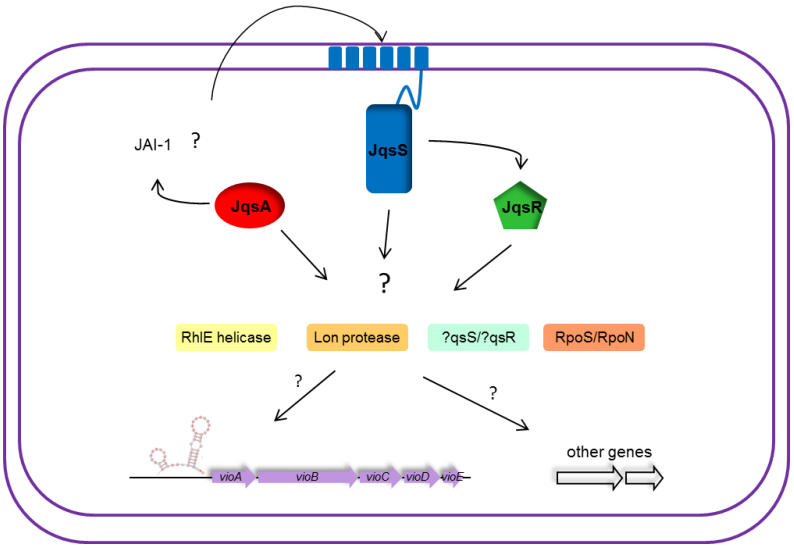

Figure 32. Putative QS regulation in HH01. The HH01 JqsA/JqsS/JqsR system seems to have influence on the expression of the violacein operon. But it is still unknown which components are involved in this process. Violacein-impaired transposon mutants were found in RNA-related genes such as the RhlE helicase and in genes encoding lon protease. In addition, further genes encoding sensor histidine kinases and response regulators (shown as ?qsS/?qsR) were detected in the analysis of violacein-impaired transposon mutants. Whether these proteins have a direct or indirect impact is not yet known. It remained also unclear if further regulatory mechanisms, *e.g.*, sigma factors RpoS/RpoN, which are part of *Vibrio* and *Legionella* gene regulation, are involved in HH01 QS. Moreover, it was not determined if further genes might be controlled by QS in HH01.

4.1.9 *jqsA* deletion strain HH02 – a novel α-hydroxyketone-sensing biosensor

While transposon mutagenesis failed to generate a knock-out of the HH01 AI synthase gene *jqsA*, a homologous recombination approach succeeded (3.1.7). As expected, this deletion strain, designated as HH02, showed impaired violacein biosynthesis confirming the influence of the *jqs* system on HH01 violacein production. Further experiments revealed that the impaired violacein biosynthesis of HH02 was functionally restored; both by exogenous addition of the proposed AI molecule JAI-1 and by internal expression of the gene *jqsA*. These results provided initial evidence that HH02 might serve as appropriate reporter strain for AI molecules. Moreover, it was found within this study that the HH02 phenotype can be rescued by homologous genes of *V. cholerae* (*cqsA*) and *L. pneumophila* (*lqsA*). In addition, complementation of HH02 was achieved with related strains encoding an AI synthase gene with similarity to that found in HH01 (3.1.9). Due to this fact, it can be concluded that with HH02 a new AI biosensor strain for the detection of α-hydroxyketone-like AIs was developed. By this means, HH02 is comparable to the AHL-sensing reporter strain *C. violaceum* CV026 (McClean *et al.* 1997).

Like HH02, the strain CV026 is unable to produce its own AI molecule and thus resulting in a violacein-negative phenotype. In CV026, this autoinducer deficiency is a result of a mini-Tn5 insertion in the *cviI* gene, encoding the C6-HSL synthase (McClean *et al.* 1997). Consequently, there is a missing QS-regulated induction of violacein synthesis, which can be used for a straightforward application to detect exogenous AHL molecules. Here, CV026 proved suitable to recognize AHLs having acyl chains from C4 to C8 in length (Steindler and Venturi 2007; McClean *et al.* 1997); with its natural AI, *N*-hexanoyl-L-homoserine lactone (C6-HSL), triggering the strongest effect. This bioassay strain CV026 is based on a mutation in *C. violaceum* ATCC 31532 (McClean *et al.* 1997). In contrast, analysis of the QS circuit of *C. violaceum* ATCC 12472 revealed 3-hydroxy-C10-HSL as its major AHL (Morohoshi *et al.* 2008). Similar to HH01 disruption of its AI synthase gene was obtained by single recombination, resulting in the *cviI*-deleted mutant VIR07 (Morohoshi *et al.* 2008). Unlike CV026, violacein production of VIR07 was induced in response to long-chain AHLs with *N*-acyl side chains from C10 to C16 in length. This different use of AHL molecules can be attributed to the particular

structure of the AHL synthases CviI and the corresponding receptor protein CviR. Thereby the AHL synthases (AAQ61751.2; AAP32920.1) of both *C. violaceum* strains, ATCC 12472 and ATCC 31532, have only moderate similarity with a maximum identity over the whole protein of 59%. In contrast, comparison of the two receptor proteins (AAQ61750.2; AAP32919.1) based on blastp analysis revealed a surprisingly high maximum identity of 77% over the whole protein. This is caused by the fact that both sequences are in large parts almost 100% identical. However, a range of 32 amino acids is only present in ATCC 12472 (AAQ61750.2), but not on ATCC 31532 (AAP32919.1). This shows clearly, how different structures of receptor proteins cause individual sensitivity for certain AI molecules. Considering this, it would be interesting to examine the sensitivity of the here presented reporter strain HH02 compared with similar mutant strains of *V. cholerae* and *V. harveyi*.

4.1.10 HH02 – complementation by *V. cholerae cqsA*, but not *vice versa*

Whereas HH02 was at least partially restored by its own AI synthase gene *jqsA* as well as by the homologous genes *cqsA* and *lqsA*, this was not shown the other way around. Meaning that both a *V. harveyi* and a *V. cholerae cqsA* mutant could not be complemented by *jqsA* overexpression (3.1.10). For this reason, it would be interesting to have a closer look at the CAI-1/LAI-1 signaling molecules as well as their signal perception sensor kinases CqsS/LqsS. A recent publication identified that the CAI-1 receptor CqsS and the potential LAI-1 receptor LqsS belong to the class of six transmembrane helix two-component sensor histidine kinases (Tiaden *et al*. 2010a). Even though the process of signal reception and sensor kinase interaction has not yet been worked out in all of its details, there are already deep insights into sensitivity and specificity determinants of CqsS sensor kinases (Ng *et al.* 2010). Particularly, motifs located within the six transmembrane sensor domain near the N-terminus of the protein are crucial for ligand binding and signal transduction (Tiaden and Hilbi 2012; Ng *et al.* 2010). Comprehensive analyses have shown that within these six transmembrane α-helices both conserved as well as variable amino acids affect the binding capacity/specificity towards the AHK signaling molecules.

Thereby, within the first three transmembrane helices (TM1 to TM3) some rather conserved motifs were identified, which are supposed to be essential for AHK binding and signal transduction. Sequence comparison revealed that these motifs are conserved not only in *Vibrio* CqsS homologues and in *L. pneumophila* LqsS (Tiaden and Hilbi 2012), but also in HH01 JqsS (Figure 33). Because of the widespread distribution of these conserved amino acids (with regard to HH01 JqsS/Figure 33, these are in TM1, *e.g.*, G44, P46, Y49, I51, W52, etc.), it can be assumed that these motifs constitute a common ligand-binding domain; displaying a tendency for interaction with chemical properties that equally exist in all AHK molecules (Tiaden and Hilbi 2012).

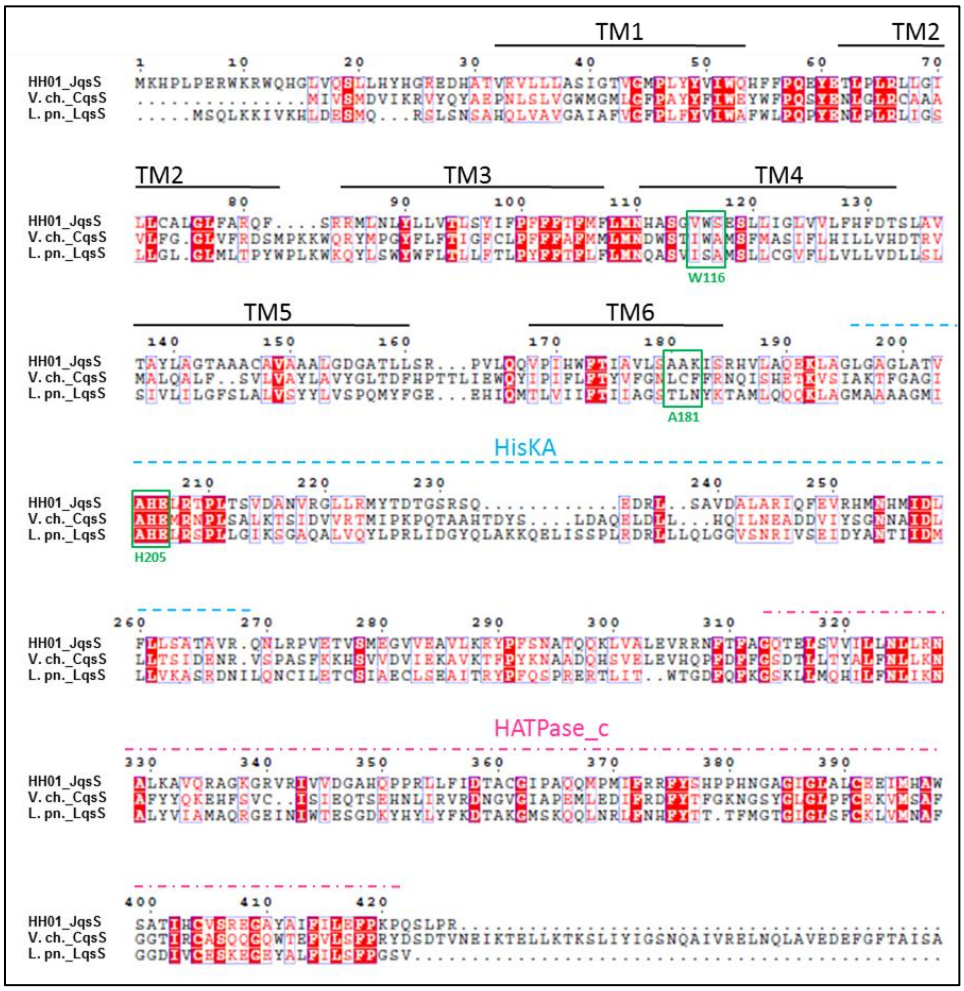

Figure 33. Amino acid alignment of the similar autoinducer signal perception sensor kinases JqsS, CqsS and LqsS. The aa alignment was based on the sequences of HH01 JqsS (ZP_21465659), *V. cholerae* CqsS (NP_232913) and *L. pneumophila* LqsS (YP_006506866). Designated domains: TM, transmembrane helices; HisKA; histidine kinase A; HATPase_c, catalytic ATP binding and transferase domain. Numbering refers to the amino acid sequence of JqsS. The CqsS sequence spans 686 amino acids, these are not entirely shown.

In contrast, the second half of the receptor domain (TM4 to TM6) was found to be more variable, suggesting that important components of ligand-binding specificity for distinct AHK analogues are located here. At this point, mainly two regions with a decisive influence on the structure of the favored molecule were detected. Since an AHK molecule can be divided into a head and a tail group, there are also two different areas in the receptor protein which are involved.

On the one hand specific aa in TM4 decide on the preference towards the AI head group (Tiaden and Hilbi 2012). It was found that the corresponding aa which are located in this area in the *V. cholerae* CqsS receptor favor an amino modification at position C3 of the AI molecule over the hydroxyl modification (Ng *et al*. 2010). Interestingly, exactly the same aa were identified in the HH01 JqsS receptor at this position (W116 and S119, Figure 33). Moreover, these observations are in line with the first assumed molecule structure of the proposed JAI-1 molecule (Figure A2). These observations suggest an amino group at position C3 of the JqsS receptor, and therefore an amino-modified AI-1 derivative ("*Am-JAI-1*"). However, since the first experiment was not confirmed, this assumption remains speculative.

On the other hand, certain aa residues within the protein domain TM6 are *i.a.*, crucial for the length of the acyl tail of the bound AHK ligand (Tiaden and Hilbi 2012). Based on the HH01 JqsS aa sequence, comparison of this region revealed neither a special similarity to the CqsS nor the LqsS sequence. Here, in particular the region around position A181 in HH01 (Figure 33) seems to be associated with a preferred length of the bound acyl chain. In *V. cholerae* this position is corresponding to CqsS C170; here a preference for a C10 acyl tail (and a lower affinity to C8) was found. This ligand specificity towards a shorter chain length is accompanied by observations regarding substrate selection of *V. cholerae* CqsA, employing C10-CoA as well as C8-CoA (Wei *et al*. 2011). In addition, studies have shown that LAI-1 with a C12 acyl tail is not detected by *V. cholerae* CqsS (Spirig *et al.* 2008). A similar preference for shorter acyl tails was also observed in *V. harveyi*. Its CqsS receptor appears to bind only CAI-1 derivates with a C8 acyl tail (Ng *et al*. 2011). Furthermore, it was found that *V. harveyi* CqsS is even more selective concerning the bound AI molecule, because it preferentially binds Ea-C8-CAI-1 (Tiaden and Hilbi 2012). Summarized this explains the results of the

complementation assays performed with the *jqsA* gene and *V. harveyi* as well as *V. cholerae cqsA* mutants (3.1.10). This is since the predicted aforementioned JAI-1 molecule structure exhibits a C12 acyl tail (Figure 33), and would due to its size not fit in the CqsS receptors of *V. harveyi* and *V. cholerae*. Moreover, these results are verified by observations demonstrated for the *L. pneumophila* LqsA/LqsS system (Tiaden and Hilbi 2012), whose LqsS receptor protein has on this determining position (in HH01 A181; Figure 33), the small aa T175 and L176, explaining its ligand binding specificity towards LAI-1 derivates with a C10 or C12 acyl tail. In analogy, this can also be stated for HH01; because the JqsS receptor harbors at these positions small aa, *i.e.*, A180 and A181, as well.

Although this may confirm the correctness of the predicted JAI-1 structure (Figure A2), further analyses did not confirm the prediction of the first structure. Instead, subsequently performed analytics revealed a completely different molecular structure. The thus obtained predicted structure shows on one side indeed similarity to known AI molecules, but is otherwise not in line with the above described observations revealed by sequence comparison. Therefore, further measurements are needed to obtain the exact JAI-1 molecule structure.

Nevertheless, based on the analyses performed within this thesis it can be stated that the putative HH01 AI receptor protein JqsS does not only detect its own signaling molecule JAI-1, but also the AI molecules CAI-1 derived from *V. cholerae* and *V. harveyi* as well as LAI-1 from *L. pneumophila*. Moreover, additional results obtained with further JAI-1-like-bearing bacteria, providing first evidence of an HH02 complementation (3.1.9). Therefore, it can be stated that HH01 as well as HH02 can serve as reporter strains for the detection of AHK molecules. Accordingly, to establish primarily HH02 as a suitable biosensor, supporting results are needed to verify the findings obtained so far. In addition, it should be investigated, why *V. harveyi* and *V. cholerae* Δ*cqsA* mutant strains were not rescued by the proposed JAI-1 molecule. This could be achieved by the final elucidation of the JAI-1 molecular structure. Concerning that point, it would also be interesting to examine how the proposed JAI-1 molecule would match with the *L. pneumophila* LqsS receptor protein, and thus a Δ*lqsA* mutant strain.

4.2 Conclusion and outlook

In conclusion, this study provides evidence that the genome sequence of *J.* sp. HH01 encodes a QS system, which triggers its violacein production. The here investigated strains HH01 and Δ*jqsA* HH02 can be considered as applicable biosensors for the detection of autoinducers of the AHK family.

Future experiments should be directed to confirm the feasibility of these reporter strains (i) by analysis of further strains harboring similar QS systems and (ii) by investigating further habitats and other environmental samples where homologous AIs might be present. In addition, both *jqsS* and *jqsR* should be studied concerning their function within the HH01 QS circuit to unveil for instance their involvement in the regulation of further genes.

5 Summary

Bacteria have evolved a mechanism of cell-cell communication, which is known as quorum sensing (QS) and relies on the synthesis, detection and response to diffusible signal molecules. By now several types of QS signals, referred to as autoinducers (AI), are known. Of these, the *N*-acyl-L-homoserine lactone family is the best characterized group. Other later identified molecules, such as the α-hydroxyketones (AHK) have been studied less extensively. Therefore, it is imperative to analyze further compounds with autoinducer activity and also the associated strains and phenotypes. This is particularly since it was found that mainly virulence-related genes are regulated by QS pathways. Thus, the search for further QS systems and in particular their interruption is of promising scope within microbial research. Here, beside sequencing and other molecular biological techniques reporter strains are of great importance. These are susceptible to a specific AI class and allow a qualitative and/or quantitative analysis of existing AI molecules.

In the present study the recently isolated violacein producer *Janthinobacterium* sp. HH01 was analyzed by whole genome sequencing and with regard to its functionality as reporter strain. Investigations revealed an obviously measurable phenotype, genetic accessibility and a QS system homologous to *V. cholerae* and *L. pneumophila* (that relies on AHK signaling molecules). By analogy this novel *Janthinobacterium* QS system was referred to as *jqs*. Further investigations revealed a correlation of the AI synthase JqsA and HH01 violacein production. It was also found that violacein production in HH01 can be triggered by overexpressing the *Vibrio* and *Legionella* AI synthase genes *cqsA* and *lqsA*. These results were furthermore confirmed by the here established *jqsA* deletion strain HH02. This strain revealed an impaired violacein phenotype that was rescued by overexpression of the *jqsA* gene and moreover by the homologous AI synthase genes *cqsA* and *lqsA*. In conclusion, the obtained data provides the first proof-of-concept that both HH01 and HH02 can serve as reporter strains to detect AHK-like AIs. This is further supported by the fact that both strains feature the following most important characteristics of such detection systems: (i) the production of an easily quantifiable phenotype, (ii) they are undemanding in terms of cultivation, (iii) non-pathogen, and (iv) sensitive to different structures of a certain AI class.

6 Zusammenfassung

Bakterien haben eine Form der Zell-Zell-Kommunikation entwickelt, die als Quorum sensing (QS) bezeichnet wird und die von der Synthese, Detektion und Reaktion diffundierender Signalmoleküle abhängt. Mittlerweile sind verschiedene Arten dieser QS-Signalmoleküle, die auch als Autoinducer (AI) bezeichnet werden, bekannt. Von diesen ist die Familie der *N*-Acylhomoserinlactone die am besten charakterisierte Gruppe. Andere später identifizierte Moleküle, wie zum Beispiel die α-Hydroxyketone (AHK), sind dagegen bislang weniger intensiv erforscht. Daher ist es unerlässlich, weitere Molekülstrukturen mit Autoinducer-Aktivität als auch die damit assoziierten Bakterien und deren QS-regulierte Phänotypen zu untersuchen. Insbesondere da im Rahmen der QS-Forschung herausgefunden wurde, dass speziell Virulenz-Eigenschaften durch QS-Wege reguliert werden. Aus diesem Grund ist die Suche nach weiteren QS-Systemen und ihre Inhibierung ein vielversprechendes Feld innerhalb der mikrobiellen Forschung. Hier sind neben der Sequenzierung und anderen molekularbiologischen Techniken Reporterstämme von großer Bedeutung. Diese erkennen jeweils eine bestimmte AI-Klasse und erlauben so eine qualitative und/oder quantitative Analyse vorhandener AI-Moleküle.

Die vorliegende Arbeit widmete sich der Untersuchung des kürzlich isolierten Violacein-Produzenten *Janthinobacterium* sp. HH01 durch Etablierung seiner Genomsequenz und Analysen bezüglich seiner Funktionalität als Reportersystem. Die Untersuchungen zeigten, dass HH01 mit der Violacein-Synthese nicht nur einen offensichtlich gut messbaren Phänotyp aufweist, sondern auch genetisch zugänglich ist und ein QS-System besitzt, welches Ähnlichkeit zu entsprechenden Systemen in *V. cholerae* und *L. pneumophila* (die auf AHK-Signalmolekülen beruhen) hat. In Analogie wurde dieses neue *Janthinobacterium* QS-System als *jqs* bezeichnet. Weitere Untersuchungen zeigten einen Zusammenhang zwischen der HH01-AI-Synthase JqsA und der HH01-Violacein-Produktion. Des Weiteren wurde herausgefunden, dass eine erhöhte Violacein-Produktion in HH01 durch die Überexpression der *Vibrio* und *Legionella* AI-Synthase-Gene *cqsA* und *lqsA* ausgelöst werden kann. Diese Ergebnisse konnten außerdem durch die in dieser Arbeit etablierte *jqsA*-Deletionsmutante HH02 bestätigt werden. HH02 wies eine gestörte Violacein-Produktion auf, welche durch die

Überexpression der Gene *jqsA* und der homologen AI-Synthase-Gene *cqsA* und *lqsA* wiederhergestellt werden konnte. Abschließend erbringen die erhaltenen Daten somit einen ersten Nachweis, dass beide Stämme, HH01 und HH02, als Reportersysteme zur Detektion von AHK-ähnlichen Autoinducern verwendet werden können. Denn beide Stämme weisen die folgenden wichtigsten Charakteristika solcher Detektionssysteme auf: (i) Ausprägung eines einfach quantifizierbaren Phänotyps, (ii) geringe Ansprüche in Bezug auf Nährstoffbedarf und Inkubationstemperatur, (iii) nicht-pathogen und (iv) sensitiv gegenüber verschiedenen Molekülstrukturen einer bestimmten AI-Klasse.

7 References

Agematu, H., K. Suzuki, *et al*. (2011). "*Massilia* sp. BS-1, a novel violacein-producing bacterium isolated from soil." Biosci Biotechnol Biochem **75**(10):2008-10.

Ahmer, B. M. (2004). "Cell-to-cell signalling in *Escherichia coli* and *Salmonella enterica*." Mol Microbiol **52**(4):933-45.

Albuquerque, P. and A. Casadevall (2012). "Quorum sensing in fungi-a review." Med Mycol **50**(4):337-45.

Ambrozic Avgustin, J., D. Zgur Bertok, *et al*. (2013). "Isolation and characterization of a novel violacein-like pigment producing psychrotrophic bacterial species *Janthinobacterium svalbardensis* sp. nov." Antonie Van Leeuwenhoek **103**(4):763-9.

Antonio, R. V. and T. B. Creczynski-Pasa (2004). "Genetic analysis of violacein biosynthesis by *Chromobacterium violaceum*." Genet Mol Res **3**(1):85-91.

Antunes, L. C., R. B. Ferreira, *et al*. (2010). "Quorum sensing in bacterial virulence." Microbiology **156**(Pt 8):2271-82.

Aranda, S., M. Montes-Borrego, *et al.* (2011). "Purple-pigmented violacein-producing *Duganella* spp. inhabit the rhizosphere of wild and cultivated olives in southern Spain." Microb Ecol **62**(2):446-59.

Atkinson, S., C. Y. Chang, *et al.* (2006). "Quorum sensing in *Yersinia enterocolitica* controls swimming and swarming motility." J Bacteriol **188**(4):1451-61.

Atkinson, S., J. P. Throup, *et al*. (1999). "A hierarchical quorum-sensing system in *Yersinia pseudotuberculosis* is involved in the regulation of motility and clumping." Mol Microbiol **33**(6):1267-77.

Audic, S., C. Robert, *et al.* (2007). "Genome analysis of *Minibacterium massiliensis* highlights the convergent evolution of water-living bacteria." PLoS Genet **3**(8):e138.

August, P. R., T. H. Grossman, *et al*. (2000). "Sequence analysis and functional characterization of the violacein biosynthetic pathway from *Chromobacterium violaceum*." J Mol Microbiol Biotechnol **2**(4):513-9.

Awano, N., V. Rajagopal, *et al*. (2010). "*Escherichia coli* RNase R has dual activities, helicase and RNase." J Bacteriol **192**(5):1344-52.

Balibar, C. J. and C. T. Walsh (2006). "In vitro biosynthesis of violacein from L-tryptophan by the enzymes VioA-E from *Chromobacterium violaceum*." Biochemistry **45**(51):15444-57.

Barber, C. E., J. L. Tang, *et al*. (1997). "A novel regulatory system required for pathogenicity of *Xanthomonas campestris* is mediated by a small diffusible signal molecule." Mol Microbiol **24**(3):555-66.

Bassler, B. L. (1999). "How bacteria talk to each other: regulation of gene expression by quorum sensing." Curr Opin Microbiol **2**(6):582-7.

Bassler, B. L., E. P. Greenberg, *et al.* (1997). "Cross-species induction of luminescence in the quorum-sensing bacterium *Vibrio harveyi*." J Bacteriol **179**(12):4043-5.

Bassler, B. L., M. Wright, *et al.* (1993). "Intercellular signalling in *Vibrio harveyi*: sequence and function of genes regulating expression of luminescence." Mol Microbiol **9**(4):773-86.

Bassler, B. L., M. Wright, *et al*. (1994). "Multiple signalling systems controlling expression of luminescence in *Vibrio harveyi*: sequence and function of genes

encoding a second sensory pathway." Mol Microbiol **13**(2):273-86.
Becker, M. H., R. M. Brucker, *et al.* (2009). "The bacterially produced metabolite violacein is associated with survival of amphibians infected with a lethal fungus." Appl Environ Microbiol **75**(21):6635-8.
Belin, P., M. Moutiez, *et al.* (2012). "The nonribosomal synthesis of diketopiperazines in tRNA-dependent cyclodipeptide synthase pathways." Nat Prod Rep **29**(9):961-79.
Bertani, I., G. Rampioni, *et al*. (2007). "The *Pseudomonas putida* Lon protease is involved in *N*-acyl homoserine lactone quorum sensing regulation." BMC Microbiol **7**:71.
Birnboim, H. C. and J. Doly (1979). “A rapid alkaline extraction procedure for screening recombinant plasmid DNA.” Nucleic Acids Res **7** (6):1513-1523.
Biswa, P. and M. Doble (2013). "Production of acylated homoserine lactone by Gram-positive bacteria isolated from marine water." FEMS Microbiol Lett **343**(1):34-41.
Bizebard, T., I. Ferlenghi, *et al*. (2004). "Studies on three *E. coli* DEAD-box helicases point to an unwinding mechanism different from that of model DNA helicases." Biochemistry **43**(24):7857-66.
Blosser, R. S. and K. M. Gray (2000). "Extraction of violacein from *Chromobacterium violaceum* provides a new quantitative bioassay for *N*-acyl homoserine lactone autoinducers." J Microbiol Methods **40**(1):47-55.
Bolitho, M. E., L. J. Perez, *et al*. (2011). "Small molecule probes of the receptor binding site in the *Vibrio cholerae* CAI-1 quorum sensing circuit." Bioorg Med Chem **19**(22):6906-18.
Brenner, S. (1974). "The genetics of *Caenorhabditis elegans*." Genetics **77**(1):71-94.
Brito, P. H., E. P. Rocha, *et al*. (2013). "Natural genome diversity of AI-2 quorum sensing in *Escherichia coli*: conserved signal production but labile signal reception." Genome Biol Evol **5**(1):16-30.
Brosius, J., A. Ullrich, *et al*. (1981). "Construction and fine mapping of recombinant plasmids containing the rrnB ribosomal RNA operon of *E. coli*." Plasmid **6**(1):112-8.
Brucker, R. M., R. N. Harris, *et al.* (2008). "Amphibian chemical defense: antifungal metabolites of the microsymbiont *Janthinobacterium lividum* on the salamander Plethodon cinereus." J Chem Ecol **34**(11):1422-9.
Camara, M., A. Hardman, *et al.* (2002b). "Quorum sensing in *Vibrio cholerae*." Nat Genet **32**(2):217-8.
Camara, M., P. Williams, *et al*. (2002a). "Controlling infection by tuning in and turning down the volume of bacterial small-talk." Lancet Infect Dis **2**(11):667-76.
Campbell, J., Q. Lin, *et al.* (2009). "New and unexpected insights into the modulation of LuxR-type quorum sensing by cyclic dipeptides." ACS Chem Biol **4**(12):1051-9.
Cartier, G., F. Lorieux, *et al*. (2010). "Cold adaptation in DEAD-box proteins." Biochemistry **49**(12):2636-46.
Carver, T., N. Thomson, *et al*. (2009). "DNAPlotter: circular and linear interactive genome visualization." Bioinformatics **25**(1):119-20.
Carver, T. J., K. M. Rutherford, *et al*. (2005). "ACT: the Artemis Comparison Tool." Bioinformatics **21**(16):3422-3.
Chen, X., S. Schauder, *et al*. (2002). "Structural identification of a bacterial quorum-sensing signal containing boron." Nature **415**(6871):545-9.
Chernin, L. S., M. K. Winson, *et al*. (1998). "Chitinolytic activity in *Chromobacterium violaceum*: substrate analysis and regulation by quorum sensing." J Bacteriol

180(17):4435-41.
Cheung, J. and W. A. Hendrickson (2010). "Sensor domains of two-component regulatory systems." Curr Opin Microbiol **13**(2):116-23.
Churchill, M. E. and L. Chen (2011). "Structural basis of acyl-homoserine lactone-dependent signaling." Chem Rev **111**(1):68-85.
Clarridge, J. E., 3rd (2004). "Impact of 16S rRNA gene sequence analysis for identification of bacteria on clinical microbiology and infectious diseases." Clin Microbiol Rev **17**(4):840-62, table of contents.
de Carvalho, M. P. and W. R. Abraham (2012). "Antimicrobial and biofilm inhibiting diketopiperazines." Curr Med Chem **19**(21):3564-77.
de Kievit, T. R. and B. H. Iglewski (2000). "Bacterial quorum sensing in pathogenic relationships." Infect Immun **68**(9):4839-49.
de Vasconcelos, A.T., D. F. de Almeida *et al*. (2003). "The complete genome sequence of *Chromobacterium violaceum* reveals remarkable and exploitable bacterial adaptability." Proc Natl Acad Sci U S A **100**(20):11660-5.
Defoirdt, T., N. Boon, *et al*. (2008). "Quorum sensing and quorum quenching in *Vibrio harveyi*: lessons learned from in vivo work." Isme J **2**(1):19-26.
Degrassi, G., C. Aguilar, *et al*. (2002). "Plant growth-promoting *Pseudomonas putida* WCS358 produces and secretes four cyclic dipeptides: cross-talk with quorum sensing bacterial sensors." Curr Microbiol **45**(4):250-4.
Deng, Y., J. Wu, *et al.* (2010). "Structural and functional characterization of diffusible signal factor family quorum-sensing signals produced by members of the *Burkholderia cepacia* complex." Appl Environ Microbiol **76**(14):4675-83.
Deng, Y., J. Wu, *et al*. (2011). "Listening to a new language: DSF-based quorum sensing in Gram-negative bacteria." Chem Rev **111**(1):160-73.
Dias Jr, L. C., J. D. Da Motta Neto, *et al*. (2002). "Semiempirical INDO/S study on the absorption spectrum of violacein." J Mol Struct (Theocem) 580(1-3):85-90.
Diggle, S. P., P. Cornelis, *et al.* (2006). "4-quinolone signalling in *Pseudomonas aeruginosa*: old molecules, new perspectives." Int J Med Microbiol **296**(2-3):83-91.
Docquier, J. D., T. Lopizzo, *et al*. (2004). "Biochemical characterization of the THIN-B metallo-beta-lactamase of *Janthinobacterium lividum*." Antimicrob Agents Chemother **48**(12):4778-83.
Dong, Y. H., J. L. Xu, *et al*. (2000). "AiiA, an enzyme that inactivates the acylhomoserine lactone quorum-sensing signal and attenuates the virulence of *Erwinia carotovora*." Proc Natl Acad Sci U S A **97**(7):3526-31.
Dougan, D. A., A. Mogk, *et al.* (2002). "AAA+ proteins and substrate recognition, it all depends on their partner in crime." FEBS Lett **529**(1):6-10.
Du, G., L. Liu, *et al.* (2007). "Production of polyvinyl alcohol-degrading enzyme with *Janthinobacterium* sp. and its application in cotton fabric desizing." Biotechnol J **2**(6):752-8.
Dubern, J. F. and S. P. Diggle (2008). "Quorum sensing by 2-alkyl-4-quinolones in *Pseudomonas aeruginosa* and other bacterial species." Mol Biosyst **4**(9):882-8.
Ducey TF, Dyer DW (2002) TN™ Transposon insertion sites in the genome of *Neisseria gonorrhoeae*. Epicentre Forum 9:6-7.
Durán, N., G. Z. Justo, *et al.* (2007). "Violacein: properties and biological activities." Biotechnol Appl Biochem **48**(Pt 3):127-33.
Eberhard, A., A. L. Burlingame, *et al*. (1981). "Structural identification of autoinducer of

Photobacterium fischeri luciferase." Biochemistry **20**(9):2444-9.
Eberl, L. (2006). "Quorum sensing in the genus Burkholderia." Int J Med Microbiol **296**(2-3):103-10.
Eisen, J. A. (2000). "Horizontal gene transfer among microbial genomes: new insights from complete genome analysis." Curr Opin Genet Dev **10**(6):606-11.
Engebrecht, J., K. Nealson, *et al.* (1983). "Bacterial bioluminescence: isolation and genetic analysis of functions from *Vibrio fischeri*." Cell **32**(3):773-81.
Engebrecht, J. and M. Silverman (1984). "Identification of genes and gene products necessary for bacterial bioluminescence." Proc Natl Acad Sci U S A **81**(13):4154-8.
Federle, M. J. (2009). "Autoinducer-2-based chemical communication in bacteria: complexities of interspecies signaling." Contrib Microbiol **16**:18-32.
Federle, M. J. and B. L. Bassler (2003). "Interspecies communication in bacteria." J Clin Invest **112**(9):1291-9.
Foerstner, K. U., C. von Mering, *et al*. (2005). "Environments shape the nucleotide composition of genomes." EMBO Rep **6**(12):1208-13.
Franklin *et al*. 2012. http://www.ncbi.nlm.nih.gov/nuccore/459354782
Fuqua, C. and E. P. Greenberg (1998). "Self perception in bacteria: quorum sensing with acylated homoserine lactones." Curr Opin Microbiol **1**(2):183-9.
Fuqua, C. and S. C. Winans (1996). "Conserved cis-acting promoter elements are required for density-dependent transcription of *Agrobacterium tumefaciens* conjugal transfer genes." J Bacteriol **178**(2):435-40.
Fuqua, W. C. and S. C. Winans (1994). "A LuxR-LuxI type regulatory system activates *Agrobacterium* Ti plasmid conjugal transfer in the presence of a plant tumor metabolite." J Bacteriol **176**(10):2796-806.
Fuqua, W. C., S. C. Winans, *et al*. (1994). "Quorum sensing in bacteria: the LuxR-LuxI family of cell density-responsive transcriptional regulators." J Bacteriol **176**(2):269-75.
Gleave, A. P., R. K. Taylor, *et al*. (1995). "Cloning and sequencing of a gene encoding the 69-kDa extracellular chitinase of *Janthinobacterium lividum*." FEMS Microbiol Lett **131**(3):279-88.
Gomes, J., A. Grunau, *et al.* (2013). "Bioinspired, releasable quorum sensing modulators." Chem Commun (Camb) **49**(2):155-7.
Gottesman, S. (2003). "Proteolysis in bacterial regulatory circuits." Annu Rev Cell Dev Biol **19**:565-87.
Graupner, K., K. Scherlach, *et al.* (2012). "Imaging mass spectrometry and genome mining reveal highly antifungal virulence factor of mushroom soft rot pathogen." Angew Chem Int Ed Engl **51**(52):13173-7.
Grice, E. A., H. H. Kong, *et al*. (2008). "A diversity profile of the human skin microbiota." Genome Res **18**(7):1043-50.
Hakvag, S., E. Fjaervik, *et al.* (2009). "Violacein-producing *Collimonas* sp. from the sea surface microlayer of costal waters in Trondelag, Norway." Mar Drugs **7**(4):576-88.
Hanahan, D. (1983). "Studies on transformation of *Escherichia coli* with plasmids." J Mol Biol **166**(4):557-80.
Haudecoeur, E. and D. Faure (2010). "A fine control of quorum-sensing communication in *Agrobacterium tumefaciens*." Commun Integr Biol **3**(2):84-8.
He, Y. W. and L. H. Zhang (2008). "Quorum sensing and virulence regulation in

Xanthomonas campestris." FEMS Microbiol Rev **32**(5):842-57.
Heeb, S., M. P. Fletcher, *et al*. (2011). "Quinolones: from antibiotics to autoinducers." FEMS Microbiol Rev **35**(2):247-74.
Henke, J. M. and B. L. Bassler (2004). "Three parallel quorum-sensing systems regulate gene expression in *Vibrio harveyi*." J Bacteriol **186**(20):6902-14.
Higgins, D. A., M. E. Pomianek, *et al.* (2007). "The major *Vibrio cholerae* autoinducer and its role in virulence factor production." Nature **450**(7171):883-6.
Hildebrand, F., A. Meyer, *et al*. (2010). "Evidence of selection upon genomic GC-content in bacteria." PLoS Genet **6**(9):e1001107.
Hirano, S., S. Asamizu, *et al.* (2008). "Crystal structure of VioE, a key player in the construction of the molecular skeleton of violacein." J Biol Chem **283**(10):6459-66.
Holden, M. T., S. Ram Chhabra, *et al*. (1999). "Quorum-sensing cross talk: isolation and chemical characterization of cyclic dipeptides from *Pseudomonas aeruginosa* and other gram-negative bacteria." Mol Microbiol **33**(6):1254-66.
Holloway, B. W., V. Krishnapillai, *et al*. (1979). "Chromosomal genetics of Pseudomonas." Microbiol Rev **43**(1):73-102.
Hong, K. W., C. L. Koh, *et al.* (2012). "Quorum quenching revisited--from signal decays to signalling confusion." Sensors (Basel) **12**(4):4661-96.
Hornung, C., A. Poehlein, *et al.* (2013). "The *Janthinobacterium* sp. HH01 Genome Encodes a Homologue of the *V. cholerae* CqsA and *L. pneumophila* LqsA Autoinducer Synthases." PLoS One **8**(2):e55045.
Hoshino, T. (2011). "Violacein and related tryptophan metabolites produced by *Chromobacterium violaceum*: biosynthetic mechanism and pathway for construction of violacein core." Appl Microbiol Biotechnol **91**(6):1463-75.
Hwang, I., P. L. Li, *et al*. (1994). "TraI, a LuxI homologue, is responsible for production of conjugation factor, the Ti plasmid N-acylhomoserine lactone autoinducer." Proc Natl Acad Sci U S A **91**(11):4639-43.
Iost, I., T. Bizebard, *et al.* (2013). "Functions of DEAD-box proteins in bacteria: Current knowledge and pending questions." Biochim Biophys Acta **1829**(8):866-877.
Jahan, N., J. A. Potter, *et al*. (2009). "Insights into the biosynthesis of the *Vibrio cholerae* major autoinducer CAI-1 from the crystal structure of the PLP-dependent enzyme CqsA." J Mol Biol **392**(3):763-73.
Jenal, U. and R. Hengge-Aronis (2003). "Regulation by proteolysis in bacterial cells." Curr Opin Microbiol **6**(2):163-72.
Jiang, P. X., H. S. Wang, *et al*. (2010). "Reconstruction of the violacein biosynthetic pathway from *Duganella* sp. B2 in different heterologous hosts." Appl Microbiol Biotechnol **86**(4):1077-88.
Jimenez, P. N., G. Koch, *et al*. (2012). "The multiple signaling systems regulating virulence in *Pseudomonas aeruginosa*." Microbiol Mol Biol Rev **76**(1):46-65.
Johnsen, M. G., O. C. Hansen, *et al.* (2010). "Isolation, characterization and heterologous expression of a novel chitosanase from *Janthinobacterium* sp. strain 4239." Microb Cell Fact **9**:5.
Johnson, J. H., A. A. Tymiak, *et al*. (1990). "Janthinocins A, B and C, novel peptide lactone antibiotics produced by *Janthinobacterium lividum*. II. Structure elucidation." J Antibiot (Tokyo) **43**(8):920-30.
Kaberdin, V. R. and U. Bläsi (2013). "Bacterial helicases in post-transcriptional control." Biochim Biophys Acta **1829**(8):878-883.

Kämpfer, P., E. Falsen, *et al.* (2008). "Reclassification of *Pseudomonas mephitica* Claydon and Hammer 1939 as a later heterotypic synonym of *Janthinobacterium lividum* (Eisenberg 1891) De Ley *et al*. 1978." Int J Syst Evol Microbiol **58**(Pt 1):136-8.

Kanamaru, K., K. Kanamaru, *et al.* (2000). "SdiA, an *Escherichia coli* homologue of quorum-sensing regulators, controls the expression of virulence factors in enterohaemorrhagic *Escherichia coli* O157:H7." Mol Microbiol **38**(4):805-16.

Kane, M. D., L. K. Poulsen, *et al.* (1993). "Monitoring the enrichment and isolation of sulfate-reducing bacteria by using oligonucleotide hybridization probes designed from environmentally derived 16S rRNA sequences." Appl Environ Microbiol **59**(3):682-6.

Kelly, R. C., M. E. Bolitho, *et al*. (2009). "The *Vibrio cholerae* quorum-sensing autoinducer CAI-1: analysis of the biosynthetic enzyme CqsA." Nat Chem Biol **5**(12):891-5.

Kim, S. J., S. C. Shin, *et al*. (2012). "Genome sequence of *Janthinobacterium* sp. strain PAMC 25724, isolated from alpine glacier cryoconite." J Bacteriol **194**(8):2096.

Kimmel, K. E. and S. Maier (1969). "Effect of cultural conditions on the synthesis of violacein in mesophilic and psychrophilic strains of *Chromobacterium*." Can J Microbiol **15**(1):111-6.

Klinkert, B. and F. Narberhaus (2009). "Microbial thermosensors." Cell Mol Life Sci **66**(16):2661-76.

Kovach, M. E., P. H. Elzer, *et al*. (1995). "Four new derivatives of the broad-host-range cloning vector pBBR1MCS, carrying different antibiotic-resistance cassettes." Gene **166**(1):175-6.

Krysciak, D., C. Schmeisser, *et al.* (2011). "Involvement of multiple loci in quorum quenching of autoinducer I molecules in the nitrogen-fixing symbiont *Rhizobium* (*Sinorhizobium*) sp. strain NGR234." Appl Environ Microbiol **77**(15):5089-99.

LaSarre, B. and M. J. Federle (2013). "Exploiting quorum sensing to confuse bacterial pathogens." Microbiol Mol Biol Rev **77**(1):73-111.

Lassak, J., A. L. Henche, *et al.* (2010). "ArcS, the cognate sensor kinase in an atypical Arc system of *Shewanella oneidensis* MR-1." Appl Environ Microbiol **76**(10):3263-74.

Latifi, A., M. K. Winson, *et al*. (1995). "Multiple homologues of LuxR and LuxI control expression of virulence determinants and secondary metabolites through quorum sensing in *Pseudomonas aeruginosa* PAO1." Mol Microbiol **17**(2):333-43.

Lee, J., J. Wu, *et al*. (2013). "A cell-cell communication signal integrates quorum sensing and stress response." Nat Chem Biol **9**(5):339-43.

Letunic, I., T. Doerks, *et al.* (2012) "SMART 7: recent updates to the protein domain annotation resource." Nucleic Acids Res **40**(Database issue):D 302-5.

Li, Y. H. and X. Tian (2012). "Quorum sensing and bacterial social interactions in biofilms." Sensors (Basel) **12**(3):2519-38.

Lincoln, S. P., T. R. Fermor, *et al*. (1999). "*Janthinobacterium agaricidamnosum* sp. nov., a soft rot pathogen of *Agaricus bisporus*." Int J Syst Bacteriol **49 Pt 4**:1577-89.

Lo Scrudato, M. and M. Blokesch (2012). "The regulatory network of natural competence and transformation of *Vibrio cholerae*." PLoS Genet **8**(6):e1002778.

Lowery, C. A., T. J. Dickerson, *et al*. (2008). "Interspecies and interkingdom communication mediated by bacterial quorum sensing." Chem Soc Rev

37(7):1337-46.
Manefield, M., T. B. Rasmussen, *et al*. (2002). "Halogenated furanones inhibit quorum sensing through accelerated LuxR turnover." Microbiology **148**(Pt 4):1119-27.
Mangwani, N., H. R. Dash, *et al*. (2012). "Bacterial quorum sensing: functional features and potential applications in biotechnology." J Mol Microbiol Biotechnol **22**(4):215-27.
Markowitz, V. M., I. M. Chen, *et al.* (2012). "IMG: the Integrated Microbial Genomes database and comparative analysis system." Nucleic Acids Res **40**(Database issue):D115-22.
Marvig, R. L. and M. Blokesch (2010). "Natural transformation of *Vibrio cholerae* as a tool--optimizing the procedure." BMC Microbiol **10**:155.
Matz, C., P. Deines, *et al.* (2004). "Impact of violacein-producing bacteria on survival and feeding of bacterivorous nanoflagellates." Appl Environ Microbiol **70**(3):1593-9.
Matz, C., J. S. Webb, *et al*. (2008). "Marine biofilm bacteria evade eukaryotic predation by targeted chemical defense." PLoS One **3**(7):e2744.
McClean, K. H., M. K. Winson, *et al*. (1997). "Quorum sensing and *Chromobacterium violaceum*: exploitation of violacein production and inhibition for the detection of N-acylhomoserine lactones." Microbiology **143 (Pt 12)**:3703-11.
Medema, M. H., K. Blin, *et al*. (2011). "antiSMASH: rapid identification, annotation and analysis of secondary metabolite biosynthesis gene clusters in bacterial and fungal genome sequences." Nucleic Acids Res **39**(Web Server issue):W339-46.
Merino, E., R. A. Jensen, *et al*. (2008). "Evolution of bacterial trp operons and their regulation." Curr Opin Microbiol **11**(2):78-86.
Miller, M. B., K. Skorupski, *et al.* (2002). "Parallel quorum sensing systems converge to regulate virulence in *Vibrio cholerae*." Cell **110**(3):303-14.
Mojib, N., R. Philpott, *et al.* (2010). "Antimycobacterial activity in vitro of pigments isolated from Antarctic bacteria." Antonie Van Leeuwenhoek **98**(4):531-40.
Montgomery K., J. Charlesworth, *et al*. (2013) “Quorum sensing in extreme environments”. Life 3:131-48.
Morohoshi, T., K. Fukamachi, *et al.* (2010). "Regulation of the violacein biosynthetic gene cluster by acylhomoserine lactone-mediated quorum sensing in *Chromobacterium violaceum* ATCC 12472." Biosci Biotechnol Biochem **74**(10):2116-9.
Morohoshi, T., M. Kato, *et al*. (2008). "*N*-acylhomoserine lactone regulates violacein production in *Chromobacterium violaceum* type strain ATCC 12472." FEMS Microbiol Lett **279**(1):124-30.
Nealson, K. H., T. Platt, *et al.* (1970). "Cellular control of the synthesis and activity of the bacterial luminescent system." J Bacteriol **104**(1):313-22.
Needleman, S. B. and C. D. Wunsch (1970). "A general method applicable to the search for similarities in the amino acid sequence of two proteins." J Mol Biol **48**(3):443-53.
Ng, W. L. and B. L. Bassler (2009). "Bacterial quorum-sensing network architectures." Annu Rev Genet **43**:197-222.
Ng, W. L., L. J. Perez, *et al.* (2011). "Signal production and detection specificity in *Vibrio* CqsA/CqsS quorum-sensing systems." Mol Microbiol **79**(6):1407-17.
Ng, W. L., Y. Wei, *et al*. (2010). "Probing bacterial transmembrane histidine kinase receptor-ligand interactions with natural and synthetic molecules." Proc Natl Acad

Sci U S A **107**(12):5575-80.
Njoroge, J. and V. Sperandio (2009). "Jamming bacterial communication: new approaches for the treatment of infectious diseases." EMBO Mol Med **1**(4):201-10.
Ochman, H., J. G. Lawrence, *et al*. (2000). "Lateral gene transfer and the nature of bacterial innovation." Nature **405**(6784):299-304.
Oinuma, K. and E. P. Greenberg (2011). "Acyl-homoserine lactone binding to and stability of the orphan *Pseudomonas aeruginosa* quorum-sensing signal receptor QscR." J Bacteriol **193**(2):421-8.
Overbeek, R., N. Larsen, *et al*. (2003). "The ERGO genome analysis and discovery system." Nucleic Acids Res **31**(1):164-71.
Paggi, R. A., C. B. Martone, *et al*. (2003). "Detection of quorum sensing signals in the haloalkaliphilic archaeon *Natronococcus occultus*." FEMS Microbiol Lett **221**(1):49-52.
Pantanella, F., F. Berlutti, *et al*. (2007). "Violacein and biofilm production in *Janthinobacterium lividum*." J Appl Microbiol **102**(4):992-9.
Papenfort, K. and J. Vogel (2010). "Regulatory RNA in bacterial pathogens." Cell Host Microbe **8**(1):116-27.
Pereira, C. S., J. A. Thompson, *et al*. (2013). "AI-2-mediated signalling in bacteria." FEMS Microbiol Rev **37**(2):156-81.
Pesci, E. C., J. B. Milbank, *et al*. (1999). "Quinolone signaling in the cell-to-cell communication system of *Pseudomonas aeruginosa*." Proc Natl Acad Sci U S A **96**(20):11229-34.
Phadtare, S. and K. Severinov (2010). "RNA remodeling and gene regulation by cold shock proteins." RNA Biol **7**(6):788-95.
Poehlein *et al*. 2013. http://www.ncbi.nlm.nih.gov/nuccore/444792393
Poehlein, A., B. Kusian, *et al*. (2011). "Complete genome sequence of the type strain *Cupriavidus necator* N-1." J Bacteriol **193**(18):5017.
Pohlmann, A., W. F. Fricke, *et al*. (2006). "Genome sequence of the bioplastic-producing "Knallgas" bacterium *Ralstonia eutropha* H16." Nat Biotechnol **24**(10):1257-62.
Purusharth, R. I., F. Klein, *et al.* (2005). "Exoribonuclease R interacts with endoribonuclease E and an RNA helicase in the psychrotrophic bacterium *Pseudomonas syringae* Lz4W." J Biol Chem **280**(15):14572-8.
Raghavan, R., Y. D. Kelkar, *et al*. (2012). "A selective force favoring increased G+C content in bacterial genes." Proc Natl Acad Sci U S A **109**(36):14504-7.
Rajamani, S., J. Zhu, *et al*. (2007). "A LuxP-FRET-based reporter for the detection and quantification of AI-2 bacterial quorum-sensing signal compounds." Biochemistry **46**(13):3990-7.
Rasmussen, T. B., M. Manefield, *et al*. (2000). "How *Delisea pulchra* furanones affect quorum sensing and swarming motility in *Serratia liquefaciens* MG1." Microbiology **146 Pt 12**:3237-44.
Reasoner, D. J. and E. E. Geldreich (1985). "A new medium for the enumeration and subculture of bacteria from potable water." Appl Environ Microbiol **49**(1):1-7.
Riedel, K., M. Hentzer, *et al*. (2001). "*N*-acylhomoserine-lactone-mediated communication between *Pseudomonas aeruginosa* and *Burkholderia cepacia* in mixed biofilms." Microbiology **147**(Pt 12):3249-62.
Rossolini, G. M., M. A. Condemi, *et al*. (2001). "Metallo-beta-lactamase producers in environmental microbiota: new molecular class B enzyme in *Janthinobacterium*

lividum." Antimicrob Agents Chemother **45**(3):837-44.
Rumbaugh, K. P. and G. F. Kaufmann (2012). "Exploitation of host signaling pathways by microbial quorum sensing signals." Curr Opin Microbiol **15**(2):162-8.
Rutherford, S. T. and B. L. Bassler (2012). "Bacterial quorum sensing: its role in virulence and possibilities for its control." Cold Spring Harb Perspect Med **2**(11).
Ryan, R. P., Y. Fouhy, *et al.* (2006). "Cell-cell signaling in *Xanthomonas campestris* involves an HD-GYP domain protein that functions in cyclic di-GMP turnover." Proc Natl Acad Sci U S A **103**(17):6712-7.
Sambrook, J., D. W. Russel, Ed. (2001). Molecular cloning, a laboratory manual. New York, USA, Cold Spring Harbor Laboratory Press.
Sanger, F., S. Nicklen, *et al.* (1977). "DNA sequencing with chain-terminating inhibitors." Proc Natl Acad Sci U S A **74**(12):5463-7.
Schiex, T., J. Gouzy, *et al*. (2003). "FrameD: A flexible program for quality check and gene prediction in prokaryotic genomes and noisy matured eukaryotic sequences." Nucleic Acids Res **31**(13):3738-41.
Schloss, P. D., H. K. Allen, *et al*. (2010). "Psychrotrophic strain of *Janthinobacterium lividum* from a cold Alaskan soil produces prodigiosin." DNA Cell Biol **29**(9):533-41.
Shank, E. A. and R. Kolter (2009). "New developments in microbial interspecies signaling." Curr Opin Microbiol **12**(2):205-14.
Sharif, D. I., J. Gallon, *et al*. (2008). "Quorum sensing in Cyanobacteria: *N*-octanoyl-homoserine lactone release and response, by the epilithic colonial cyanobacterium *Gloeothece* PCC6909." Isme J **2**(12):1171-82.
Shaw, P. D., G. Ping, *et al.* (1997). "Detecting and characterizing *N*-acyl-homoserine lactone signal molecules by thin-layer chromatography." Proc Natl Acad Sci U S A **94**(12):6036-41.
Shi, Y.-L., X.-Z. Lu, *et al.* (2008). “A new β-agarase from marine bacterium *Janthinobacterium* sp. SY12.” World J Microbiology and Biotechnology **24**(11):2659-64.
Shirata, A., T. Tsukamoto, *et al.* (2000). “Isolation of bacteria producing bluish-purple pigment and use for dyeing.“ JARQ **34**:131-40.
Simon R., U. Priefer, *et al*. (1983) “A broad host range mobilization system for *in vivo* genetic engineering: Transposon mutagenesis in Gram-negative bacteria.” Bio/technol **1**(9):784-91.
Smith, J. L., P. M. Fratamico, *et al*. (2011). "Eavesdropping by bacteria: the role of SdiA in *Escherichia coli* and *Salmonella enterica* serovar Typhimurium quorum sensing." Foodborne Pathog Dis **8**(2):169-78.
Smith, M. B., J. N. Smith, *et al.* (2001). "SdiA of *Salmonella enterica* is a LuxR homolog that detects mixed microbial communities." J Bacteriol **183**(19):5733-42.
Sneath, P.H.A 1984. Genus *Janthinobacterium*, p. 376-377. In N.R. Krieg and J. G. Holt (ed.), Bergey´s manual of systematic bacteriology. The Williams & Wilkins Co., Baltimore.
Sperandio, V., J. L. Mellies, *et al*. (1999). "Quorum sensing controls expression of the type III secretion gene transcription and protein secretion in enterohemorrhagic and enteropathogenic *Escherichia coli*." Proc Natl Acad Sci U S A **96**(26):15196-201.
Spirig, T., A. Tiaden, *et al.* (2008). "The *Legionella* autoinducer synthase LqsA produces an alpha-hydroxyketone signaling molecule." J Biol Chem **283**(26):18113-23.

Spurr, A. R. (1969). "A low-viscosity epoxy resin embedding medium for electron microscopy." J Ultrastruct Res **26**(1):31-43.
Srivastava, D. and C. M. Waters (2012). "A tangled web: regulatory connections between quorum sensing and cyclic Di-GMP." J Bacteriol **194**(17):4485-93.
Stauff, D. L. and B. L. Bassler (2011). "Quorum sensing in *Chromobacterium violaceum*: DNA recognition and gene regulation by the CviR receptor." J Bacteriol **193**(15):3871-8.
Steindler, L. and V. Venturi (2007). "Detection of quorum-sensing *N*-acyl homoserine lactone signal molecules by bacterial biosensors." FEMS Microbiol Lett **266**(1):1-9.
Steiner, E., J. Scott, *et al*. (2012). "An agr quorum sensing system that regulates granulose formation and sporulation in *Clostridium acetobutylicum*." Appl Environ Microbiol **78**(4):1113-22.
Stiernagle, T. (2006). "Maintenance of *C. elegans*." WormBook:1-11.
Suckow, G., P. Seitz, *et al*. (2011). "Quorum sensing contributes to natural transformation of *Vibrio cholerae* in a species-specific manner." J Bacteriol **193**(18):4914-24.
Surette, M. G., M. B. Miller, *et al*. (1999). "Quorum sensing in *Escherichia coli*, *Salmonella typhimurium*, and *Vibrio harveyi*: a new family of genes responsible for autoinducer production." Proc Natl Acad Sci U S A **96**(4):1639-44.
Syngkon, A., S. Elluri, *et al*. (2010). "Studies on a novel serine protease of a ΔhapAΔprtV *Vibrio cholerae* O1 strain and its role in hemorrhagic response in the rabbit ileal loop model." PLoS One **5**(9):e13122.
Takaya, A., F. Tabuchi, *et al.* (2008). "Negative regulation of quorum-sensing systems in *Pseudomonas aeruginosa* by ATP-dependent Lon protease." J Bacteriol **190**(12):4181-8.
Tamura, K., D. Peterson, *et al.* (2011). "MEGA5: molecular evolutionary genetics analysis using maximum likelihood, evolutionary distance, and maximum parsimony methods." Mol Biol Evol **28**(10):2731-9.
Tamura, M., J. A. Kers, *et al*. (2012). "Second-site suppression of RNase E essentiality by mutation of the deaD RNA helicase in *Escherichia coli*." J Bacteriol **194**(8):1919-26.
Tao, F., Y. W. He, *et al.* (2010). "The cyclic nucleotide monophosphate domain of *Xanthomonas campestris* global regulator Clp defines a new class of cyclic di-GMP effectors." J Bacteriol **192**(4):1020-9.
Tatusov, R. L., E. V. Koonin, *et al*. (1997). "A genomic perspective on protein families." Science **278**(5338):631-7.
Tech, M. and R. Merkl (2003). "YACOP: Enhanced gene prediction obtained by a combination of existing methods." In Silico Biol **3**(4):441-51.
Tempe, J., A. Petit, *et al*. (1977). "Thermosensitive step associated with transfer of the Ti plasmid during conjugation: Possible relation to transformation in crown gall." Proc Natl Acad Sci U S A **74**(7):2848-9.
Thomas, T., F. F. Evans, *et al*. (2008). "Analysis of the *Pseudoalteromonas tunicata* genome reveals properties of a surface-associated life style in the marine environment." PLoS One **3**(9):e3252.
Thomson, N. R., M. A. Crow, *et al.* (2000). "Biosynthesis of carbapenem antibiotic and prodigiosin pigment in *Serratia* is under quorum sensing control." Mol Microbiol **36**(3):539-56.

Tiaden, A. and H. Hilbi (2012). "alpha-Hydroxyketone synthesis and sensing by *Legionella* and *Vibrio*." Sensors (Basel) **12**(3):2899-919.

Tiaden, A., T. Spirig, *et al.* (2008). "Synergistic contribution of the *Legionella pneumophila lqs* genes to pathogen-host interactions." J Bacteriol **190**(22):7532-47.

Tiaden, A., T. Spirig, *et al*. (2010a). "Bacterial gene regulation by alpha-hydroxyketone signaling." Trends Microbiol **18**(7):288-97.

Tiaden, A., T. Spirig, *et al*. (2010b). "The autoinducer synthase LqsA and putative sensor kinase LqsS regulate phagocyte interactions, extracellular filaments and a genomic island of *Legionella pneumophila*." Environ Microbiol **12**(5):1243-59.

Tiaden, A., T. Spirig, *et al*. (2007). "The *Legionella pneumophila* response regulator LqsR promotes host cell interactions as an element of the virulence regulatory network controlled by RpoS and LetA." Cell Microbiol **9**(12):2903-20.

Tommonaro, G., G. R. Abbamondi, *et al*. (2012). "Diketopiperazines produced by the halophilic archaeon, *Haloterrigena hispanica*, activate AHL bioreporters." Microb Ecol **63**(3):490-5.

Venturi, V. (2006). "Regulation of quorum sensing in *Pseudomonas*." FEMS Microbiol Rev **30**(2):274-91.

Wang, L. H., Y. He, *et al*. (2004). "A bacterial cell-cell communication signal with cross-kingdom structural analogues." Mol Microbiol **51**(3):903-12.

Wang, Y., A. Ikawa, *et al.* (2008). "Quorum sensing signaling molecules involved in the production of violacein by *Pseudoalteromonas*." Biosci Biotechnol Biochem **72**(7):1958-61.

Waters, C. M. and B. L. Bassler (2005). "Quorum sensing: cell-to-cell communication in bacteria." Annu Rev Cell Dev Biol **21**:319-46.

Watnick, P. I., C. M. Lauriano, *et al*. (2001). "The absence of a flagellum leads to altered colony morphology, biofilm development and virulence in *Vibrio cholerae* O139." Mol Microbiol **39**(2):223-35.

Wei, Y., L. J. Perez, *et al*. (2011). "Mechanism of *Vibrio cholerae* autoinducer-1 biosynthesis." ACS Chem Biol **6**(4):356-65.

White, C. E. and S. C. Winans (2007). "Cell-cell communication in the plant pathogen *Agrobacterium tumefaciens*." Philos Trans R Soc Lond B Biol Sci **362**(1483):1135-48.

Whiteley, M., K. M. Lee, *et al*. (1999). "Identification of genes controlled by quorum sensing in *Pseudomonas aeruginosa*." Proc Natl Acad Sci U S A **96**(24):13904-9.

Wiggins, P. J., J. M. Smith, *et al*. (2011). “Gut of red-backed salamanders (*Plethodon cinereus*) may serve as a reservoir for an antifungal cutaneous bacterium.” J Herpetology **45**(3):329-32.

Williams, P., K. Winzer, *et al*. (2007). "Look who's talking: communication and quorum sensing in the bacterial world." Philos Trans R Soc Lond B Biol Sci **362**(1483):1119-34.

Winson, M. K., S. Swift, *et al*. (1998). "Construction and analysis of *luxCDABE*-based plasmid sensors for investigating *N*-acyl homoserine lactone-mediated quorum sensing." FEMS Microbiol Lett **163**(2):185-92.

Woese, C. R. (1987). "Bacterial evolution." Microbiol Rev **51**(2):221-71.

Wu, H., Z. Zhang, *et al*. (2012). "On the molecular mechanism of GC content variation among eubacterial genomes." Biol Direct **7**:2.

Yang, L. H., H. Xiong, *et al*. (2007). "Effect of agitation on violacein production in

Pseudoalteromonas luteoviolacea isolated from a marine sponge." Lett Appl Microbiol **44**(6):625-30.

Yang, M., K. Sun, *et al*. (2009). "Functional analysis of three AHL autoinducer synthase genes in *Mesorhizobium loti* reveals the important role of quorum sensing in symbiotic nodulation." Can J Microbiol **55**(2):210-4.

Yanofsky, C. (2007). "RNA-based regulation of genes of tryptophan synthesis and degradation, in bacteria." RNA **13**(8):1141-54.

Yildiz, F. H. and G. K. Schoolnik (1998). "Role of rpoS in stress survival and virulence of *Vibrio cholerae*." J Bacteriol **180**(4):773-84.

Zhang, G., F. Zhang, *et al.* (2012). "Acyl homoserine lactone-based quorum sensing in a methanogenic archaeon." Isme J **6**(7):1336-44.

Zhang, R., P. Yang, *et al.* (2011). "Molecular and biochemical characterization of a new alkaline beta-propeller phytase from the insect symbiotic bacterium *Janthinobacterium* sp. TN115." Appl Microbiol Biotechnol **92**(2):317-25.

Zhu, J., J. W. Beaber, *et al.* (1998). "Analogs of the autoinducer 3-oxooctanoyl-homoserine lactone strongly inhibit activity of the TraR protein of *Agrobacterium tumefaciens*." J Bacteriol **180**(20):5398-405.

Zhu, J. and J. J. Mekalanos (2003). "Quorum sensing-dependent biofilms enhance colonization in *Vibrio cholerae*." Dev Cell **5**(4):647-56.

8 Appendix

8.1 Supporting Figures

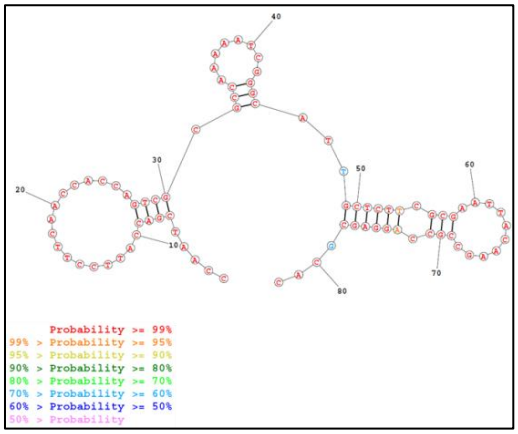

Figure A1. Possible structure of a putative RNA thermosensor located in the *vioA* 5'-UTR (generated using "RNA structure Web Servers for RNA Secondary Structure Prediction"; http://rna.urmc.rochester.edu/RNAstructureWeb/).

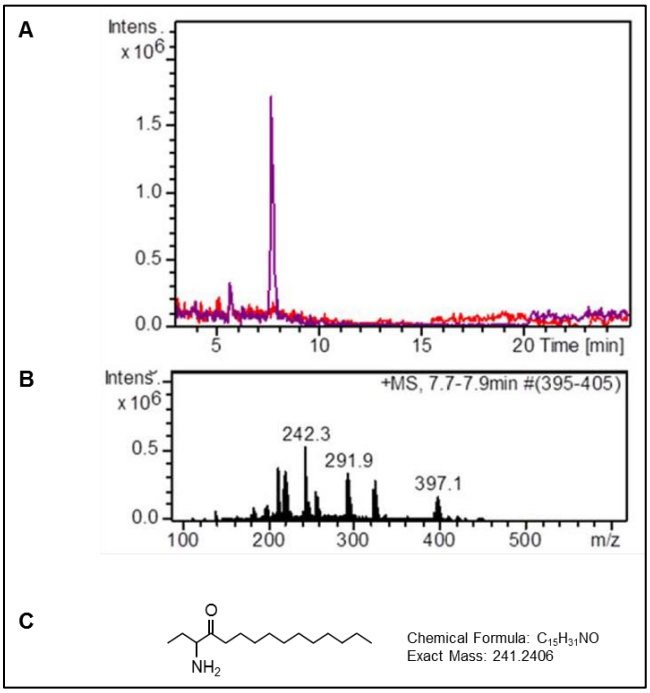

Figure A2. HPLC-ESI-MS analytics to unveil the proposed JAI-1 molecular structure. (A) Spectrum of extracted mass signal $[M+H]^+$ *m/z* = 242.3 (positive ions; *m/z* =242.3 ± 0.3) showing JAI-1 synthase sample (purple) and negative control (red). **(B)** Respective mass spectrum at t_R 7.7 min of the synthase sample. **(C)** The thus predicted but not confirmed molecular structure for JAI-1.

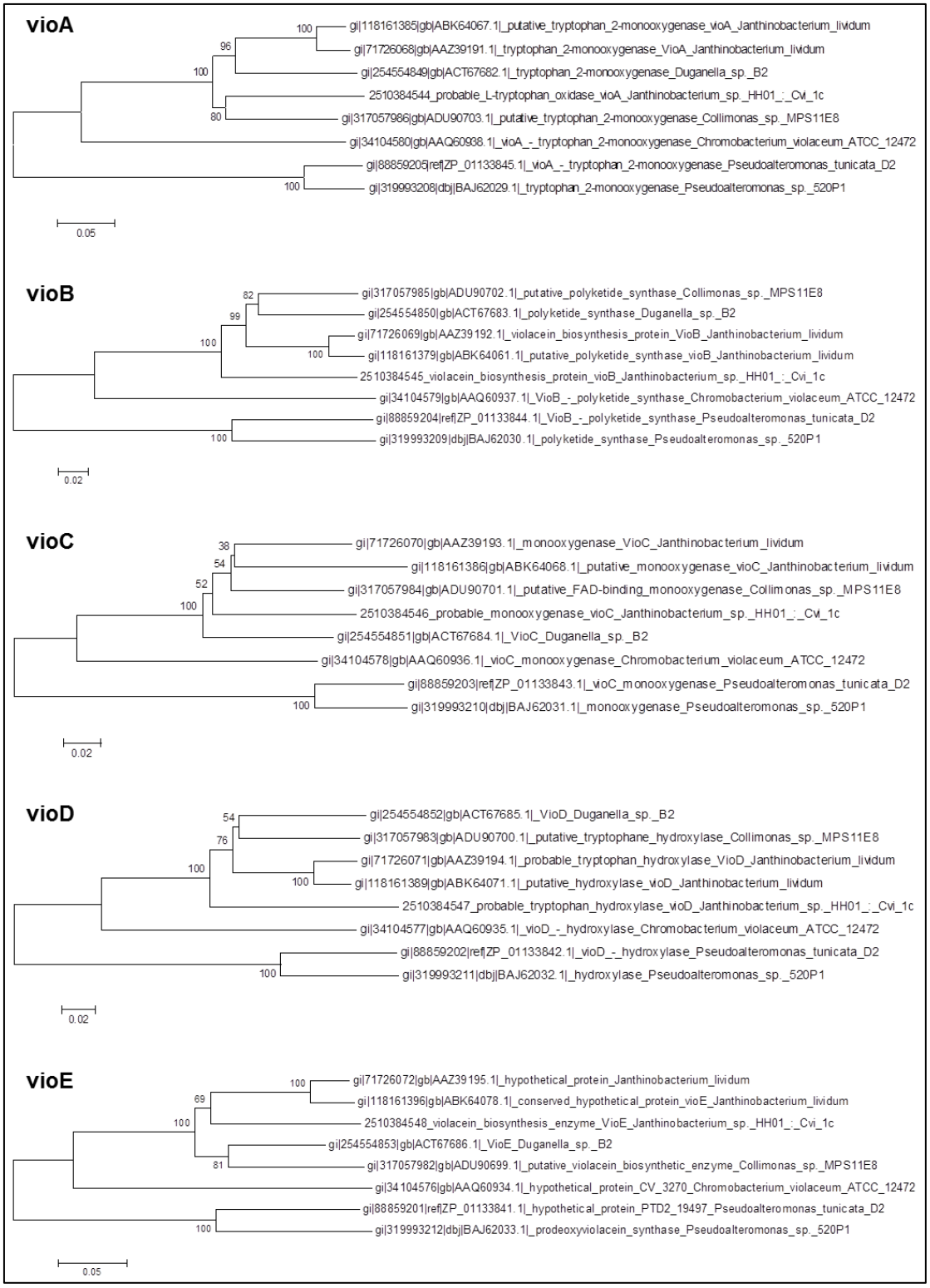

Figure A3. Comparative analysis of the amino acid sequence of VioA to VioE.

.

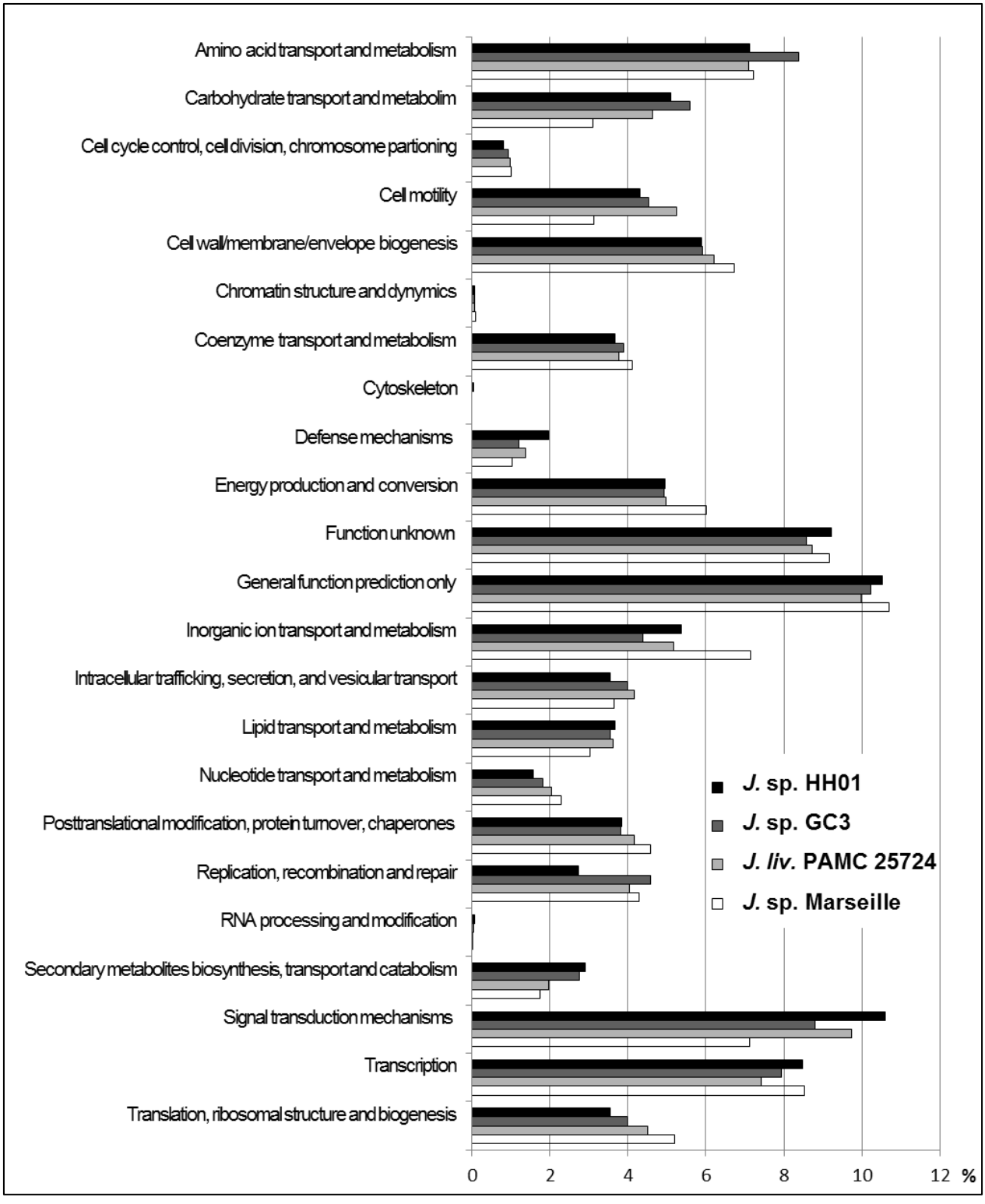

Figure A4. Statistical analysis of janthinobacterial genomes regarding COG categories. Analysis of *J.* sp. HH01, *J.* sp. GC3, *J. lividum* PAMC 25724 and *J.* sp. Marseille based on COG categories. Data are taken from the IMG database (Markowitz *et al.* 2012), cited 2013-01-15.

8.2 Supporting Tables

Table 14. Overview of the genes upstream and downstream the violacein operon in other organisms except *Janthinobacterium* sp. HH01.

Locus tag	Size (bp)	Predicted gene function
Collimonas sp. MPS11E8[1)]		
CCT_ORF05304	918	putative substrate binding transport protein
CCT_ORF05305	957	putative fatty acid desaturase
CCT_ORF05306	882	putative SPFH domain/band 7 family protein
CCT_ORF05307	459	putative acetyltransferase
CCT_ORF05308	576	***vioE*** (violacein biosynthesis protein)
CCT_ORF05309	1,119	***vioD*** (tryptophan hydroxylase)
CCT_ORF05310	1,290	***vioC*** (monooxygenase)
CCT_ORF05311	3,036	***vioB*** (violacein biosynthesis protein)
CCT_ORF05312	1,308	***vioA*** (tryptophan 2-monooxygenase)
CCT_ORF05313	549	putative acetyltransferase
CCT_ORF05314	807	putative amino acid transporter periplasmic ligand binding protein
CCT_ORF05315	474	putative acyl CoA thioester hydrolase
CCT_ORF05316	2,394	putative TonB-dependent receptor
CCT_ORF05317	1,383	putative mercuric reductase pyruvate/2-oxoglutarate dehydrogenase complex
CCT_ORF05318	1,473	putative N-acyl-D-amino-acid deacylase
Janthinobacterium lividum[2)]		
GI: 71726058	693	putative aspartate/glutamate racemase
GI: 71726059	756	short-chain dehydrogenase/reductase family oxidoreductase
GI: 71726060	735	transcriptional regulator GntR family
GI: 71726061	447	putative thioesterase
GI: 71726062	1,365	putative transporter
GI: 71726063	1,485	hypothetical protein
GI: 71726064	1,344	diguanylate cyclase (GGDEF) with PAS/PAC and GAF domain
GI: 71726065	444	hypothetical protein
GI: 71726066	2,232	monomeric isocitrate dehydrogenase
GI: 71726067	2,202	putative TonB-dependent outer membrane receptor
GI: 71726068	1,308	***vioA*** (tryptophan 2-monooxygenase)
GI: 71726069	3,021	***vioB*** (violacein biosynthesis protein)
GI: 71726070	1,290	***vioC*** (monooxygenase)
GI: 71726071	1,119	***vioD*** (tryptophan hydroxylase)
GI: 71726072	582	***vioE*** (violacein biosynthesis enzyme)
GI: 71726073	1,164	putative sugar transporter/AraJ-type arabinose efflux permease
GI: 71726074	1,044	putative transcriptional regulator AraC family
GI: 71726075	1,362	hypothetical protein
***Duganella* sp. B2**[3)]		
GI:254554849	1,308	***vioA*** (tryptophan 2-monooxygenase)
GI:254554850	3,018	***vioB*** (polyketide synthase)
GI:254554851	1,290	***vioC*** (monooxygenase)
GI:254554852	1,119	***vioD*** *(*tryptophan hydroxylase*)*
GI:254554853	576	***vioE*** (violacein biosynthesis enzyme)
***Chromobacterium violaceum* ATCC 12472**[4)]		
CV_3267	1,263	hypothetical protein
CV_3268	1,821	hypothetical protein
CV_3269	1,098	hypothetical protein

CV_3270	576	***vioE*** (violacein biosynthesis protein)
CV_3271	1,122	***vioD*** (tryptophan hydroxylase)
CV_3272	1,290	***vioC*** (monooxygenase)
CV_3273	2,997	***vioB*** (polyketide synthase)
CV_3274	1,257	***vioA*** (tryptophan 2-monooxygenase)
CV_3275	1,533	putative sphingomyelinase/beta-hemolysin
CV_3276	579	hypothetical protein
CV_3277	570	hypothetical protein
CV_3278	543	putative cytochrome b561
CV_3279	222	hypothetical protein
CV_3280	528	hypothetical protein
CV_3281	1,680	acetate permease actP
CV_3282	1,965	acetyl-CoA synthetase acsA
CV_3283	960	hypothetical protein
CV_3284	711	hypothetical protein
CV_3285	1,890	putative methyl-accepting chemotaxis protein

***Pseudoalteromonas tunicata* D2**[5)]		
PTD2_19477	909	putative histone deacetylase family protein
PTD2_19482	360	tryptophanyl-tRNA synthetase
PTD2_19487	186	hypothetical protein
PTD2_19492	999	tryptophanyl-tRNA synthetase
PTD2_19497	600	***vioE*** (violacein biosynthesis protein)
PTD2_19502	1,134	***vioD*** (tryptophan hydroxylase)
PTD2_19507	1,290	***vioC*** (monooxygenase)
PTD2_19512	3,030	***vioB*** (polyketide synthase)
PTD2_19517	1,287	***vioA*** (tryptophan 2-monooxygenase)
PTD2_19522	1,389	MATE efflux family protein
PTD2_19527	129	hypothetical protein
PTD2_19532	240	hypothetical protein
PTD2_19537	288	hypothetical protein
PTD2_19542	387	hypothetical protein
PTD2_19547	1,398	asparaginyl-tRNA synthetase
PTD2_19552	381	hypothetical protein
PTD2_19557	432	hypothetical protein
PTD2_19562	1,308	adenosylmethionine-8-amino-7-oxononanoate aminotransferase (7,8-diaminopelargonic acid synthetase), PLP-dependent
PTD2_19567	1,044	biotin synthase; contains an iron-sulfur cluster and PLP
PTD2_19572	1,137	8-amino-7-oxononanoate synthase (7-keto-8-aminopelargonic acid synthetase)
PTD2_19577	777	desthiobiotin biosynthesis; reaction prior to pimeloyl CoA
PTD2_19582	684	desthiobiotin synthetase
PTD2_19587	888	heat shock protein HtpX

[1)] *Collimonas* sp MPS11E8 (http://www.ncbi.nlm.nih.gov/nuccore/FJ965838; cited: 2013-01-27), GenBank: FJ965838; locus tag CCT_ORF05304 to CCT_ORF05318; corresponding protein ID ADU90695 to ADU90709. [2)] *Janthinobacterium lividum* contig 186 (http://www.ncbi.nlm.nih.gov/nuccore/DQ074977; cited: 2013-01-31); GenBank: DQ074977; locus tag GI: 71726058 to GI: 71726075; corresponding protein ID AAZ39181 to AAZ39198. [3)] *Duganella* sp. B2 (http://www.ncbi.nlm.nih.gov/nuccore/GQ266676; cited: 2013-02-01); GenBank: GQ266676; locus tag GI:254554849 to GI:254554853; corresponding protein ID ACT67682 to ACT67686. [4)] *C. violaceum* ATCC 12472 (http://www.ncbi.nlm.nih.gov/nuccore/34105712; cited: 2013-02-01); GenBank: AE016825; locus tag CV_3267 to CV_3285; corresponding protein ID AAQ60931 to AAQ60949. [5)] *Pseudoalteromonas tunicata* D2 (http://www.ncbi.nlm.nih.gov/nuccore/AAOH00000000; cited: 2013-02-01); GenBank: NZ_AAOH00000000; locus tag PTD2_19477 to PTD2_19587; corresponding protein ID ZP_01133837 to ZP_01133859.

Table 15. Comparative analysis of *J.* sp. HH01 and related strains *J.* sp. GC3 and *J. lividum* PAMC 25724 based on COG categories.

Funtion ID	Name	HH01	GC3	PAMC
Signal transduction/regulation				
COG0583	Transcriptional regulator	**91**	77	50
COG0642	Signal transduction histidine kinase	**76**	64	52
COG0745	Response regulators consisting of a CheY-like receiver domain and a winged-helix DNA-binding domain	**38**	25	21
COG0789	Predicted transcriptional regulator	**12**	6	6
COG0840	Methyl-accepting chemotaxis protein	**49**	32	42
COG1309	Transcriptional regulator	**30**	24	17
COG1846	Transcriptional regulator	**18**	12	8
COG2197	Response regulator containing a CheY-like receiver domain and an HTH DNA-binding domain	**16**	8	9
COG2199	Diguanylate cyclase	**25**	13	14
COG3275	Putative regulator of cell autolysis	**13**	2	5
COG3279	Response regulator of the LytR/AlgR family	**14**	4	8
COG4585	Signal transduction histidine kinase	**14**	9	7
Transport proteins/receptor proteins				
COG0577	ABC-type antimicrobial peptide transport system, permease component	**8**	2	1
COG0834	ABC-type amino acid transport/signal transduction systems, periplasmic component/domain	**38**	22	6
COG0841	Cation/multidrug efflux pump	**14**	8	9
COG0845	RND family efflux transporter, MFP subunit	**20**	10	11
COG1131	ABC-type multidrug transport system, ATPase component	**15**	8	7
COG1538	Outer membrane protein, efflux transporter	**21**	14	14
COG1629	Outer membrane receptor proteins, mostly Fe transport	**49**	16	26
COG2271	Sugar phosphate permease	**12**	2	4
COG2814	Arabinose efflux permease	**37**	29	28
COG4206	Outer membrane cobalamin receptor protein	**12**	6	1
COG4771	Outer membrane receptor for ferrienterochelin and colicins	**26**	9	13
Metabolite enzymes				
COG0596	Predicted hydrolases or acyltransferases	**27**	15	12
COG0654	2-polyprenyl-6-methoxyphenol hydroxylase and related FAD-dependent oxidoreductases	**13**	3	3
COG1020	Nonribosomal peptide synthetase modules and related proteins	**19**	14	1
COG1228	Imidazolonepropionase and related aminohydrolases	**10**	1	1
COG1680	Beta-lactamase class C and other penicillin binding proteins	**16**	4	3
COG1835	Predicted acyltransferases	**13**	4	2
COG3386	Gluconolactonase	**7**	2	2

Table 16. Strains and corresponding accession numbers of JqsA-like AI synthases used for phylogenetic analysis (Figure 11).

Examined strains	Accession number
Ralstonia eutropha H16	YP_728640
Cupriavidus necator N-1	YP_004680649
Cupriavidus taiwanensis LMG19424	YP_001796752
Collimonas fungivorans Ter331	YP_004750816
Janthinobacterium sp. HH01	ZP_21465658
Polaromonas naphthalenivorans CJ2	YP_983733
Ramlibacter tataouinensis TTB310	YP_004617950
Rhodomicrobium vannielii ATCC 17100	YP_004010985
Salinisphaera shabanensis E1L3A	ZP_08550556
Nitrococcus mobilis Nb-231	ZP_01127067
Burkholderia xenovorans LB400	YP_555293
Marinomonas mediterranea MMB-1	YP_004314772
Marinomonas posidonica IVIA-Po-181	YP_004482197
Legionella pneumophila subsp. pneumophila str. Philadelphia-1	YP_096734
Legionella pneumophila str. Paris	YP_125092
Legionella pneumophila str. Lens	YP_127984
Chlorobium phaeobacteroides DSM 266	YP_912394
Chlorobium ferrooxidans DSM 13031	ZP_01385258
Chlorobium limicola DSM 245	YP_001942557
Prosthecochloris aestuarii DSM 271	YP_002015366
Photobacterium sp. SKA34	ZP_01162832
Vibrio cholerae CIRS 101	ZP_05420646
Photobacterium profundum SS9	YP_133409
Vibrio parahaemolyticus RIMD 2210633	NP_800221
Vibrio alginolyticus 12G01	ZP_01260612
Vibrio harveyi ATCC BAA-1116	YP_001448208
Vibrio splendidus 12B01	ZP_00990208

8.3 Abbreviations

aa	Amino acid
ABC	ATP-binding cassette (transporter)
$A._{bidest.}$	Double distilled water
ACP	Acyl carrier protein
AHK	α-hydroxyketone
AHL	Acyl homoserine lactone
AI	Autoinducer
AI-1	Autoinducer 1
AI-2	Autoinducer 2
Amp^R	Ampicillin resistance
AT	*Agrobacterium tumefaciens* (medium)
ATP	Adenosine triphosphate
BLAST	Basic Local Alignment Search Tool
bp	Base pair(s)
C	Carbon
°C	Degree Celsius
CAI-1	Cholera autoinducer-1
CDS	Coding sequence
Che	Chemotaxis
Cm^R	Chloramphenicol resistance
COG	Clusters of orthologous groups
conc.	Concentration
Cyc^R	Cycloserine resistance
d	Day
DCM	Dichloromethane
Dct	Dicarboxylate transport system
DKP	Diketopiperazine
d.l.	Detection limit
DMF	Dimethylformamide
DNA	Deoxyribonucleic acid
dNTP	Deoxynucleoside triphosphate
DPD	Dihydroxypentanedione
DSF	Diffusible signal factor

DSMZ	Deutsche Sammlung von Mikroorganismen
DTT	Dithiothreitol
E	E-value
EDTA	Ethylene diamine tetraacetic acid
e.g.	*exempli gratia* (for example)
EMBL	European Molecular Biology Laboratory
EPS	Extracellular polysaccharide
ESI	Electrospray ionization
et al.	*et alii* (and others)
EtOH	Ethanol
FA	Fatty acid
g	Gram
Gm^R	Gentamicin resistance
h	Hour
Hap	Hemagglutinin/protease activity
HisKA	Histidine kinase A
HPLC	High performance liquid chromatography
HRMS	High-resolution mass spectrometer
HSL	Homoserine lactone
i.a.	*inter alia* (among others)
i.e.	*id est* (that is)
IPTG	Isopropyl β-D-1-thiogalactopyranoside
JAI	*Janthinobacterium* autoinducer
kb	Kilobase(s)
Km^R	Kanamycin resistance
kV	Kilovoltage
L	Liter
LAI-1	*Legionella* autoinducer-1
LB	Lysogenic broth
m	Milli- (1×10^{-3})
M	Molar
Mbp	Mega base pair(s)
MCS	Multiple cloning site
MFS	Major Facilitator Superfamily
mg	Milligram

min	Minutes
mL	Milliliter
mm	Millimeter
mM	Millimolar
MS	Mass spectrometry
MW	Molecular weight
m/z	Mass-to-charge ratio
µ	Micro (1×10^{-6})
µF	Microfarad
µg	Microgram
µL	Microliter
µM	Micromolar
n	Nano (1×10^{-9})
Nal^R	Nalidixic acid resistance
NCBI	National Center for Biotechnolgy Information
n.d.	Not detectable
Neo^R	Neomycin resistance
nm	Nanometer
nov.	Novus
NRPS	Nonribosomal peptide synthetase
n.s.	Not specified
nt	Nucleotide
OD	Optical density
ORF	Open reading frame
PCR	Polymerase chain reaction
PEP	Phosphoenolpyruvate
Pfu	*Pyrococcus furiosus* (polymerase)
pH	Negative logarithm to the base 10 of the concentration of hydrogen ions
PKS	Polyketide synthase
PQS	*Pseudomonas* quinolone signal
pv.	Pathovar
PVP	Purple violet pigment
QQ	Quorum quenching
QS	Quorum sensing
QSI	Quorum sensing inhibitor

R	Resistance
RNA	Ribonucleic acid
RNase	Ribonuclease
RND	Resistance-nodulation-cell division superfamily
rpm	Rotation per minute
rRNA	Ribosomal ribonucleic acid
RT	Room temperature
SD	Standard deviation
SDS	Sodium dodecyl sulfate
sec	Seconds
SEM	Scanning electron microscopy
SMART	Simple Modular Architecture Research Tool
sp.	Species
Sp^R	Spectinomycin resistance
TAE	Tris-acetate EDTA
T_{ann}	Annealing temperature
Taq	*Thermus aquaticus* (polymerase)
TAT	Twin arginine translocation
Tc^R	Tetracycline resistance
T_m	Melting temperature
TEM	Transmission electron microscopy
TM	Transmembrane
t_R	Retention time
tRNA	Transfer ribonucleic acid
Tris	Tris-(hydroxymethyl)-aminoethane
U	Unit (enzyme activity)
UTR	Untranslated region
UV	Ultraviolet
V	Voltage
VAI	*Vibrio* autoinducer
vol.	Volume
v/v	Volume per volume
WT	Wild type
w/v	Weight per volume
X-Gal	5-Bromo-4-chloro-3-indolyl-β-D-galactopyranoside

Nucleotide bases

A	Adenine	G	Guanine
C	Cytosine	T	Thymine
U	Uracil		

Amino acids

A	Ala	Alanine	M	Met	Methionine
C	Cys	Cysteine	N	Asn	Asparagine
D	Asp	Aspartic acid	P	Pro	Proline
E	Glu	Glutamic acid	Q	Gln	Glutamine
F	Phe	Phenylalanine	R	Arg	Arginine
G	Gly	Glycine	S	Ser	Serine
H	His	Histidine	T	Thr	Threonine
I	Ile	Isoleucine	V	Val	Valine
K	Lys	Lysine	W	Trp	Tryptophan
L	Leu	Leucine	Y	Tyr	Tyrosine

8.4 Acknowledgement

First of all I want to thank Prof. Dr. Wolfgang Streit, who gave me the opportunity to perform my Ph.D. research in his lab. I am thankful that he provided me a project, which was both challenging and suspenseful. Furthermore, I thank Prof. Dr. Peter Heisig for accepting the supervision of my Ph.D. thesis.

I am very thankful to Christel Schmeisser, Dagmar Krysciak and Christina Hornung for proofreading my thesis from the scientific aspect and their helpful improvement suggestions. I am also very grateful to Warren Greig, who corrected this thesis from the viewpoint of a native speaker.

Thanks to all those, who were involved in the comprehensive publication resulting from this work: I thank Frederike Haack, Martina Schmidt, Gabi Timmermann, Eva Spieck, Ines Krohn-Molt, Andreas Bonge, Christian Utpatel, Andreas Pommerening-Röser and particularly Anja Poehlein and her sequencing team in Göttingen, Christel Schmeisser and Wolfgang Streit. Furthermore I thank all participating cooperation partners: Hinrich Schulenburg and his team in Kiel, Melanie Blokesch and participating group members in Lausanne, the kindly cooperation of Kirsten Jung and her working group in Martinsried and the support of Edna and Helge Bode in Frankfurt.

Furthermore, I thank Nicolas Rychlik for the support concerning knockout mutant generation, Matthias Szesny for HPLC analyses and Hubert Hilbi for the pTS21 vector.

Moreover, I thank all current and previous members of the entire research group, with whom I worked together: Andreas, Angela, Arek, Boris, Christel, Christian, Christiane, Dagmar, Ebrahim, Frederike, Gabi, Gao, Gesche, Ines, Jenny, Julia, Katja, Mariita, Martina, Mirjam, Moritz, Nele, Nico, Nine, Patrick, Regina, Sabine K., Sabine Z., Sascha, Steffi, Ulrich and Uschi.

And to put it a little more private at the end: I thank heartily my family and friends for tolerating my lack of time and stressed-out behavior, particularly in the recent months and weeks. Especially I am grateful to Tini and Stefan, for their never ending support, patience, keeping my numerous doubts and who regularly had a hot meal for me. “WoMan does not live by biscuit alone…!”

8.5 Eidesstattliche Versicherung

Hiermit erkläre ich an Eides statt, dass ich die vorliegende Dissertationsschrift selbst verfasst und keine anderen als die angegebenen Quellen und Hilfsmittel verwendet habe.

Hamburg, 02. 05. 2013

Claudia K. Hornung